

The spatial distribution of zooplankton production in the western Tasman Sea: A size-spectra approach



Photos courtesy of A. Slotwinski, CSIRO

Zoe White

A thesis in fulfilment of the requirements for the degree of
Master of Philosophy at the University of New South Wales

School of Biological, Earth and Environmental Sciences

Faculty of Science

August 2018



Australia's
Global
University

Thesis/Dissertation Sheet

Surname/Family Name	:	White
Given Name/s	:	Zoe
Abbreviation for degree as give in the University calendar	:	M.Phil
Faculty	:	Science
School	:	BEES
Thesis Title	:	The spatial distribution of zooplankton production in the western Tasman Sea: A size-spectra approach

Abstract 350 words maximum:

My thesis explores the relationships of zooplankton community size spectra with their physical environment using data from voyages into the western Tasman Sea, off south-eastern Australia. This economically important region is under the influence of the strengthening East Australian Current, which is warming and changing the Tasman Sea marine ecosystems. Using 39 tows of an Optical Plankton Counter (OPC) from 2004-2016, statistical relationships are developed to model zooplankton biomass and community size structure for the region. Four characteristics of the zooplankton size spectra were examined – total biomass, abundance, geometric mean size (300-1200 µm equivalent spherical diameter) and slope of the normalised biomass size spectrum. My results show that the patterns in the zooplankton size spectra are driven by the environmental variables - sea surface temperature (SST), Chlorophyll-a biomass, sea level anomaly (SLA) and bathymetry. SST and SLA showed negative relationships with all response variables and Chlorophyll-a showed a positive relationship with all response variables. Bathymetry was retained in two models, for abundance and NBSS intercept, of which the relationships were negative. The models were all significant, with 18-46% of the variability explained.

These linear models were then used to model zooplankton biomass and community size structure for the region over the period 2003-2016. The hindcast maps of zooplankton community size structure indicate spatially dynamic distributions of zooplankton production which revealed a significant decrease in abundance and biomass over the study period.

Assessment of the model results with corresponding data from the Continuous Plankton Recorder (CPR) found a significantly positive relationship between zooplankton abundance from the CPR and the OPC ($p<0.05$).

The output further extends insights into the changes in spatial distribution of zooplankton in the western Tasman Sea as the ocean environment changes. Zooplankton productivity could more clearly define spatial patterns in fish abundance and biomass, which is often represented by satellite chlorophyll-a relationships. This is applicable to defining the seascape ecology of the western Tasman Sea zooplankton community size structure, which underpins existing dynamic ocean management of the long line industry.

Declaration relating to disposition of project thesis/dissertation

I hereby grant to the University of New South Wales or its agents the right to archive and to make available my thesis or dissertation in whole or in part in the University libraries in all forms of media, now or here after known, subject to the provisions of the Copyright Act 1968. I retain all property rights, such as patent rights. I also retain the right to use in future works (such as articles or books) all or part of this thesis or dissertation.

I also authorise University Microfilms to use the 350 word abstract of my thesis in Dissertation Abstracts International (this is applicable to doctoral theses only).

.....
Signature

.....
Date

The University recognises that there may be exceptional circumstances requiring restrictions on copying or conditions on use. Requests for restriction for a period of up to 2 years must be made in writing. Requests for a longer period of restriction may be considered in exceptional circumstances and require the approval of the Dean of Graduate Research.

ORIGINALITY STATEMENT

'I hereby declare that this submission is my own work and to the best of my knowledge it contains no materials previously published or written by another person, or substantial proportions of material which have been accepted for the award of any other degree or diploma at UNSW or any other educational institution, except where due acknowledgement is made in the thesis. Any contribution made to the research by others, with whom I have worked at UNSW or elsewhere, is explicitly acknowledged in the thesis. I also declare that the intellectual content of this thesis is the product of my own work, except to the extent that assistance from others in the project's design and conception or in style, presentation and linguistic expression is acknowledged.'

Signed

Date

COPYRIGHT STATEMENT

'I hereby grant the University of New South Wales or its agents the right to archive and to make available my thesis or dissertation in whole or part in the University libraries in all forms of media, now or here after known, subject to the provisions of the Copyright Act 1968. I retain all proprietary rights, such as patent rights. I also retain the right to use in future works (such as articles or books) all or part of this thesis or dissertation.'

I also authorise University Microfilms to use the 350 word abstract of my thesis in Dissertation Abstract International (this is applicable to doctoral theses only).

I have either used no substantial portions of copyright material in my thesis or I have obtained permission to use copyright material; where permission has not been granted I have applied/will apply for a partial restriction of the digital copy of my thesis or dissertation.'

Signed

Date

AUTHENTICITY STATEMENT

'I certify that the Library deposit digital copy is a direct equivalent of the final officially approved version of my thesis. No emendation of content has occurred and if there are any minor variations in formatting, they are the result of the conversion to digital format.'

Signed

Date

Abstract

My thesis explores the relationships of zooplankton community size spectra with the physical environment using data from voyages into the western Tasman Sea, off south-eastern Australia. This economically important region is under the influence of the strengthening East Australian Current, which is warming and changing marine ecosystems. Using 39 tows of an Optical Plankton Counter (OPC) from 2004 - 2016, statistical relationships are developed to model zooplankton biomass and community size structure for the region. Five characteristics of the zooplankton size spectra were examined – total biomass, abundance, geometric mean size and the normalised biomass size spectrum (NBSS) slope and intercept. My results show that the patterns in the zooplankton size spectra are driven by the environmental variables - sea surface temperature (SST), Chlorophyll- α biomass, sea level anomaly (SLA) and bathymetry. SST and SLA showed negative relationships with all response variables and Chlorophyll- α showed a positive relationship with all response variables. Bathymetry was negatively related to abundance and NBSS intercept, and positively related to GMS. The models were all significant, with 18 - 46% of the variability explained.

These linear models were then used to model zooplankton biomass and community size structure for the region over the period 2003 - 2016. The hindcast maps of zooplankton community size structure indicate spatially dynamic distributions of zooplankton production and a significant decrease in abundance and biomass over the study period. Assessment of the model results with corresponding data from the Continuous Plankton Recorder (CPR) found a significantly positive relationship between zooplankton abundance from the CPR and the OPC ($p < 0.05$).

The output further extends insights into the changes in spatial distribution of zooplankton in the western Tasman Sea as the ocean environment changes. Zooplankton productivity could more clearly define spatial patterns in fish abundance and biomass, which is often represented by satellite chlorophyll- α relationships. This will contribute to seascape ecology of the western Tasman Sea zooplankton size

structure, and underpins existing dynamic ocean management of the long line industry.

Acknowledgements

I wish to thank my supervisors Iain Suthers, Jason Everett and Anthony Richardson, for all their encouragement, time spent helping me with this project, good humour and patience. I wish to also thank Ryan Heneghan for sharing his knowledge and passion for modelling and zooplankton. I have enjoyed attending the meetings with you all and being in such great company.

I wish to also thank the FAMER team at USNW. Iain knows how to pick a good colourful bunch! I am grateful for all the laughs and times you have all helped me out.

Talia Stelling-Wood, aka 'Superwoman', and Matt Holland, it's great to have been able to share this journey right through from the MMarScMgt with you both. It's nice to know I'm not the only crazy one leaving fortunes and all possibility of saving for a house in Sydney, to come and study again at such an old age. Catharina Vendl, thanks for all the fun and waffles. I really appreciate all your endless energy for adventure, social get togethers and your studies. Thanks for all your encouragement and positivity!

Thanks to everyone in the Marine lab on level 4, for your smiles and help when I needed it.

I wish to thank the scientists and crew of the R/V Southern Surveyor and R/V Investigator, especially Lindsay Pender and Brett Muir (CSIRO) who were instrumental in the SeaSoar and Triaxus deployments. I loved the two voyages on the R.V. Investigator, everyone is so friendly and the food is so good! Thank you for looking after all our research needs, as well as going beyond the call of duty and looking after us as well!

Probably most importantly of all I wish to thank my parents Sue and Harry White. I don't know what you think I am doing with my life coming back to uni, but thanks for supporting me regardless.

And finally, thanks to my one true love, the Ocean herself. You are my teacher and greatest source of inspiration. I strive to give back to you all you have given to me.

This research was funded by ARC Discovery Projects DP150102656 held by Iain M. Suthers, Anthony J. Richardson, Dr Mark Baird (CSIRO) and Evgeny Pakhomov (UBC). Satellite Data was sourced from the NASA Goddard Space Flight Centre, Ocean Ecology Laboratory, Ocean Biology Processing Group and the Integrated Marine Observing System (IMOS), an initiative of the Australian Government being conducted as part of the National Collaborative Research Infrastructure Strategy and the Super Science Initiative.

Table of Contents

Abstract.....	iii
Acknowledgements.....	v
Table of Contents.....	vii
List of Acronyms.....	ix
Table of Figures.....	x
List of Tables	xiii
Chapter 1 General Introduction.....	1
1.1 Zooplankton diversity and ecology	1
1.2. Zooplankton size-structure	3
1.3. Metrics of the size spectrum.....	6
1.4 Measuring particle size with an optical plankton counter (OPC)	9
1.5 Study Area and the western Tasman Sea	15
1.6 Aims of this research.....	18
Chapter 2 : Quantifying the link between the size-distribution of zooplankton and satellite-derived oceanographic variables	22
2.1 Abstract.....	22
2.2 Introduction	23
2.3 Methods.....	27
2.3.1 Study Region	27
2.3.2 In-situ Data Collection.....	27
2.3.3 Remotely Sensed Observations	30
2.3.4 Zooplankton Size Spectra.....	30
2.3.5 Determining watermasses	31
2.3.6 Statistical Analysis.....	33
2.4 Results.....	34
2.4.1 Water-mass specific differences	34
2.4.2 Environmental drivers of zooplankton size spectra.....	36
2.5 Discussion:	39
2.5.1 Zooplankton Biomass and Abundance in the western Tasman Sea	39
2.5.2 Zooplankton size-spectra and its implications for trophic ecology	41
2.5.3 Non-linearity in the NBSS in the western Tasman Sea.	45

2.5.4 Concluding remarks	46
Chapter 3 : Spatial and temporal patterns of springtime zooplankton biomass and size in the Tasman Sea	47
3.1 Abstract.....	47
3.2 Introduction	48
3.3 Methods.....	51
3.3.1 Study region	51
3.3.2 Data collection and model development.....	51
3.3.3 Data analysis	52
3.3.4 Model assessment	54
3.4 Results.....	55
3.4.1 Temporal and spatial variability in zooplankton distribution	55
3.4.2 Using linear models to map zooplankton distribution over large scales.....	65
3.4.3 Model assessment	65
3.5 Discussion.....	67
3.5.1 Spatial patterns of zooplankton in the Tasman Sea	67
3.5.2 Temporal decline in zooplankton biomass	69
3.5.3 Implications of the zooplankton size spectrum on trophic efficiency	71
3.5.4 Model assessment	71
3.5.5 Dynamic Ocean Management.....	72
3.5.6 Concluding remarks	73
Chapter 4 General discussion	74
4.1 Zooplankton size distribution in the western Tasman Sea.....	75
4.2 Incorporation of zooplankton into fisheries management.....	77
References	80
Appendix A.....	91
Appendix B	100

List of Acronyms

OPC	Optical Plankton Counter
LOPC	Laser Optical Plankton Counter
LED	Light Emitting Diode
CPR	Continuous Plankton Recorder
SST_{sat}	Satellite Sea Surface Temperature
SLA_{sat}	Satellite Sea Surface Anomaly
Chl_{sat}	Satellite Chlorophyll- α
NBSS	Normalised Biomass Size Spectrum
GMS	Geometric Mean Size
EAC	East Australian Current
NBSS_{slope}	Normalised Biomass Size Spectrum Slope
NBSS_{intercept}	Normalised Biomass Size Spectrum Intercept
ESD	Equivalent Spherical Diameter
MEP	Multiple Element Particle
SEP	Single Element Particle
AI	Attenuance Index
IMOS	Integrated Marine Observation System
MODIS	Moderate Resolution Imaging Spectroradiometer
ENSO	El Niño Southern Oscillation
NSW	New South Wales
CCE	Cold Core Eddy
WCE	Warm Core Eddy
PPMR	Predator Prey Mass Ratio
DCM	Deep Chlorophyll Maximum
DVM	Diel Vertical Migration
DOM	Dynamic Ocean Management

Table of Figures

Figure 1.1 Summary of the possible dynamics of the normalised biomass size spectrum of zooplankton (redrawn from Moore & Suthers 2006). a) shows the steepening of the slope (and increased intercept) due to nutrient enrichment, b) flattening of the slope (and sustained intercept) with continued primary production or c) a steepening of the slope due to predation.	8
Figure 1.2 Figure reproduced from Krupica et al. (2012) summarising the main metrics used to compare zooplankton size spectra; a) the pareto distribution with a fitted least squares line showing simple size based metrics, and b) an NBSS spectrum with the more complex size based metrics. The horizontal lines from upper to lower, show the size ranges of four typical copepods from the east coast of Canada <i>Pseudocalanus</i> spp. (-3.08 mg to -1.97 mg), <i>Temora longicornis</i> (-2.82 mg to -1.01 mg), <i>Calanus finmarchicus</i> (-2.31 mg to -0.47 mg), and <i>Calanus hyperboreus</i> (-1.69 mg to 0.68mg).	10
Figure 1.3 a) Zooplankton particles in water flow through a beam of six light emitting diodes (LEDs) on one side of the sampling tunnel, which is received on the opposite side of the tunnel. The size of the particle is calculated from the detected change in light intensity (Herman 1992). b) the underwater version of the Optical Plankton Counter (OPC) (GoMA 2018a) and c) the Laser-Optical Plankton Counter (LOPC) (GoMA 2018b).	13
Figure 1.4 Triaxus (left) and Sea Soar (right). The Laser-OPC is a sampling instrument which is mounted on a towed body (circled on Triaxus); the LED-OPC on the Sea Soar is arrowed.	15
Figure 1.5 The study area (bordered by the black box) is located on the south-eastern Australian coastline (inset map). The colour shows the north to south gradient in sea surface temperature as measured by satellite. The arrows indicate the direction and strength of currents and the presence of cyclonic (upwelling) and anticyclonic (downwelling) eddies.	16
Figure 1.6 This conceptual diagram shows the flow of analysis through my thesis to achieve the stated aims. The maps in chapter 2 (top row) show the four environmental variables (Satellite temperature, chlorophyll- <i>a</i> , sea level anomaly and bathymetry) that were linearly modelled against <i>in situ</i> ship acquired measurements of size spectra metrics. In chapter 3 (Bottom row), these relationships were applied to archived satellite data of the same	

environmental variables to create maps of zooplankton size distributions (left). The hindcast abundance was compared for the same date and location with corresponding <i>in situ</i> CPR abundance measurements (right)	21
Figure 2.1 Each transect from the study are shown on the map of eastern Australia. The colours represent the voyage year. The inset shows a map of Australia with boundaries of the larger site map marked by a dashed line.....	28
Figure 2.2 Plot of the data points as assigned to watermasses based on bathymetry, location and satellite temperature properties. Bathymetry is plotted on a \log_{10} scale. Shelf North, Shelf South, EAC (East Australian Current), Tasman and Mixed.	32
Figure 2.3 Bar plots comparing a) mean \log_{10} abundance b) \log_{10} biomass, c) geometric mean size (GMS) d) NBSS slope, e) NBSS intercept f) NBSS slope Linearity between watermasses. Error bars represent Standard Error. Matching letters on the bars represent no significant difference between corresponding water masses.	35
Figure 2.4 Normalised Biomass Size Spectra of the A) EAC, B) Tasman, C) Mixed, D) Shelf North, E) Shelf South. The black circles represent the normalised biomass in each size class. The grey line is the linear regression through the points, calculated using the average of biomass in each size class bin. The solid black line represents a fixed slope of -1 for comparison.	36
Figure 3.1 Mean A) sea surface temperature ($^{\circ}\text{C}$), B) Chlorophyll- a (mg m^{-3}), C) sea level anomaly (m), D) bathymetry (m) of the study area. Data averaged from springtime averages from 2003 - 2016	56
Figure 3.2 Springtime continental shelf (<200 m, blue) and offshelf (>1000 m depth, red) mean zooplankton a) Abundance (ind-m^{-3}), b) Biomass ($\log_{10}(\text{mg m}^{-3})$), c) GMS (μm) and d) NBSS _{slope} , from 2003 to 2016, with standard error bars.....	57
Figure 3.3 Coefficient of variation of a) Abundance, b) Biomass c) GMS and d) NBSS _{slope} on <200 m, blue) and off the shelf (>1000 m depth, red), from -28 $^{\circ}\text{S}$ to -36 $^{\circ}\text{S}$	57
Figure 3.4 Linear regressions of mean a) Abundance (ind-m^{-3}), b) Biomass ($\log_{10}(\text{mg m}^{-3})$), c) Geometric Mean Size (GMS) (μm), d) NBSS _{slope} , from 2003 to 2016.....	58
Figure 3.5 AOV Barplots of a) Abundance (ind-m^{-3}), b) Biomass ($\log_{10}(\text{mg m}^{-3})$), c) GMS (μm), d) NBSS _{slope} of the Years 2003 to 2016, labelled with Tukey significant difference test. Years with matching labels show no significant difference between each other.....	59

Figure 3.6 Annual springtime zooplankton Abundance (ind-m ⁻³), from 2003 to 2016.....	61
Figure 3.7 Springtime zooplankton Biomass ($\log_{10}(\text{mg m}^{-3})$) over the study area, from 2003 to 2016	62
Figure 3.8 Springtime mean Geometric Mean Size (GMS) ($\mu\text{m ESD}$) of zooplankton from 2003 to 2016.....	63
Figure 3.9 Springtime zooplankton NBSS _{slope} from 2003-2016.....	64
Figure 3.10 Scatterplot of CPR vs modelled abundance (ind-m ⁻³). Log ₁₀ Model Abundance = 3.455 + 0.09395(log ₁₀ CPR Abundance)	66

List of Tables

Table 1.1 Summary of the major improvements instrument resolution between the LED-OPC and L-OPC.....	11
Table 2.1 OPC deployment and voyage details	29
Table 2.2 Criteria used to define water masses.....	32
Table 2.3 Coefficient values of the linear models. Significant coefficients are marked with asterisks ($P < 0.05$). Coefficients marked with a dot (.) were not included in the final model. See Appendix A Table 8 - 12 for full model results.....	38
Table 3.1 Linear Model coefficient values. Significant coefficients are marked with asterisks ($P < 0.05$). Coefficients marked with a dot (.) were not included in the final model.....	52
Table 3.2 Coefficient values for linear models of zooplankton abundance, biomass, GMS and NBSS _{slope} of the study period over the years 2003-2016. Significant coefficients are marked with asterisks ($P < 0.05$) (*).	58
Table 3.3: Linear Model of log ₁₀ Abundance measured by the Continuous Plankton Recorder (CPR) compared to log ₁₀ Abundance as predicted by the model using the date and coordinates of satellite temperature, chlorophyll- <i>a</i> , sea level anomaly and bathymetry.....	65

Chapter 1 General Introduction

Zooplankton are the missing link between phytoplankton and fisheries harvests (Everett et al. 2017). To fill this knowledge gap I have analysed historical data from optical plankton counters in relation to environmental data of the western Tasman Sea – to convert a satellite view of the ocean into a zooplankton ecosystem. This chapter introduces some aspects of the diversity and ecology of zooplankton, and the size-structure of zooplankton. I describe the optical plankton counter and the various statistics that summarise the size distribution, and introduce the western Tasman Sea.

1.1 Zooplankton diversity and ecology

Plankton are defined as marine organisms that drift with the ocean currents (Everett et al. 2017), including the single celled primary producers (phytoplankton) and bacteria; and the consumers. Zooplankton range from single celled protozoa (ciliates) to jellyfish 2 m diameter, and to siphonophores over 30 m long. The biomass of zooplankton is dominated by small crustaceans such as copepods (over 10,000 species) and krill (80 species) (Slotwinski et al. 2014). In fact all marine phyla are found in the zooplankton either as larval stages (meroplankton) such as most cnidarian jellyfish, molluscs, annelid worms, echinoderms and fish, or as holoplankton, such as copepods, chaetognaths and salps, which spend their entire life as zooplankton.

Phytoplankton bloom during spring as sunlight hours increase and mixed surface layers shallow, retaining cells in the surface layer photic zone. Zooplankton may exploit this phytoplankton rich photic zone during the night, where they are protected from predation by the darkness, and migrate to deeper, darker depths during the day. Diel vertical migration (DVM) is a strategy undertaken by the zooplankton to avoid the photic zone during the day, where they could be eaten by predators (Ritz et al. 2003). Larger zooplankton such as krill with some swimming

ability (i.e. nekton) may undertake large daily vertical migrations up to 500 m depth, whereas copepods and other small zooplankton undertake smaller vertical migrations.

The small sizes of zooplankton allow fast rates of production and population turnover, which is advantageous to quickly grow and multiply while the phytoplankton resource is available. Zooplankton are the trophic link from primary production to fish, fuelling the higher trophic levels, as they are consumed by carnivorous zooplankton, larval fish, and forage fish which are themselves consumed by top predators such as tuna, shark and dolphins.

Zooplankton reproduction cycles are linked to the timing of the phytoplankton bloom so that they can exploit the period of high phytoplankton resources. Copepods hatch from their eggs as larvae (the nauplius stage) and through moulting have 6 naupliar stages, followed by 5 copepodid stages (Johnson and Allen 2005). Life cycles of zooplankton vary along latitudinal gradients. The higher latitudes are affected by pronounced spring blooms, as well as cold, dark winters which suppress phytoplankton growth. Zooplankton such as copepods diapause as food resources, light levels and temperatures become low. During this time, the copepods either release eggs which overwinter until spring, or females overwinter in a quiescent state until the warming temperatures stimulate reproduction. Some copepods will overwinter in the copepodid stage, with the final mature stage occurring during the following spring when food resources increase (Johnson and Allen 2005). During this time individuals survive off their rich reserves of oil droplets, which they accumulated during the previous phytoplankton production period.

In warmer low latitude regions where sunlight hours are less variable, stratification is stronger and mixed layers are deeper, leading to lower nutrient levels in the photic zone (Baird et al. 2008). These areas experience a milder seasonality cycle, and a less pronounced springtime phytoplankton bloom. There, the spring zooplankton bloom is also less pronounced, leading to a low biomass in spring compared with higher latitude regions, and more stable production and biomass over the year. As such, the copepods do not build up such rich lipid reserves or cease reproduction to the extent

of polar/temperate copepods. This also leads to a lower abundance of herbivorous zooplankton than the higher latitude regions, resulting in dominance of omnivorous/carnivorous zooplankton (Henschke et al. 2015).

The community makeup of zooplankton assemblages are associated with different water mass properties (Baird et al. 2011) and oceanographic processes such as upwelling or slope water intrusions (Henschke et al. 2011). Seasonal changes in zooplankton assemblages are also apparent; it is common for salps to bloom in the spring/summer months (Baird et al. 2011) after the phytoplankton spring bloom (Henschke et al. 2011).

Tropical, temperate and cold water zooplankton have been noted for their presence in the south eastern Tasman Sea including copepods, euphausiids, hyperiid amphipods, pteropods, chaetognaths, salps (*Thalia democratica*) and larvaceans (Henschke et al. 2015). The dispersion of zooplankton and other marine organisms at the larval stages can influence range shifts of species with climate change. The strengthening East Australian Current (EAC) has resulted in shifts in Tasmanian zooplankton communities, from cold species relative dominance in the 1970's to warm species relative dominance in most years of 2000-2009 (Johnson et al. 2011).

1.2. Zooplankton size-structure

The father of ecology Charles Elton suggested an inverse relationship between body size and abundance in 1927 (after Sprules and Barth (2016)). Greater population growth rates at the base of the food chain create ecosystems containing high abundances of small organisms, and increasingly scarce abundances as organism size increases. His theories were based on observation, as at the time there was no realistic means to count all the organisms in a community. Electronic methods in the 1960's and 1970's made quantification of body size possible, such as the Coulter Counter (Sheldon et al. 1972), for plankton particles sized 1-100 µm in the ocean. The development of the biomass size spectrum using this technology revealed that

particles occur in roughly equal amounts in logarithmically equal size class bins (Sheldon et al. 1972).

Size is important in biology. Biological functions such as resting metabolism scale with body size to the power law function ($M^{0.75}$) (Andersen et al. 2016). Therefore mortality, prey consumption, development time, production rates, population growth rates and swimming speed are all examples of organism functions that express relationships with size. Metabolic rate is also a function of temperature, so temperature was included into size based/allometric equations to form the metabolic theory of ecology equations (Brown et al. 2004). Because of temperature's influence on chemical reactions, rates such as ontogenetic development of eggs will decrease with decreasing temperature, therefore size relationships may be temperature corrected. Temperature has an exponential effect on metabolic rate, and body size and temperature are taken to be the two most important variables affecting metabolic rate of an individual.

The biomass size frequency distribution (i.e. "size-spectrum") is a useful way of studying biomass and energy flow in ecosystems from the lowest trophic levels to the highest trophic levels. As metabolic rate and biological rates are a function of size, sized based ecosystems are a simplified way of calculating the energy dynamics of an ecosystem. The environment may also modify the size spectrum. Reduced predation pressures on the lower trophic levels may amplify the steepening of the size spectrum, as the small size classes may become more abundant in the spectrum (Sprules and Barth 2016). A steepening in the slope of the normalised biomass spectrum has also been observed when temperature of an ecosystem increases (Sprules and Barth 2016). Not all studies show changes in zooplankton biomass spectra, with a multitude of invasions and major fish species changes having no apparent effect on biomass size spectra over an 8 year study of Lakes Erie and Ontario (Sprules and Barth 2016).

The size spectrum is a balance between gains in energy through growth and losses of energy though respiration and predation/mortality in a size based community (Blanchard et al. 2017). Therefore changes in slope between times or environments

can be used to assess the energy transfer efficiency among environments (Zhou 2006). Slope, biomass and intercept of a spectrum are therefore affected by production and predation in an environment, and growth and respiration rates, trophic dynamics and energy transfer efficiency of the zooplankton in a community (Fig. 1.1).

Environments like fjords and estuaries can often experience large changes in physical properties over short spatial scales, such as salinity, temperature, turbidity and nutrient concentration, hosting different populations and size structures (Checkley et al. 2008; Basedow et al. 2010; Vandromme et al. 2014). For example flatter slopes and higher chlorophyll- α levels occur at the saline end of a fjord, while steeper slopes and lower chlorophyll- α occur at the glacial cold freshwater end (Trudnowska et al. 2014). Estuaries typically have steeper Normalised Biomass Size Spectrum (NBSS) slopes. Slopes of -3 have been found in estuaries (Moore and Suthers 2006) and highest biomass and the steepest slopes were seen near the estuary regions when conducting transects from coastal to offshore areas (Vandromme et al. 2014). Slopes of -1 with very little scatter around the line were observed in the oligotrophic south Coral Sea, with significantly steeper slopes in an island wake, compared to the adjacent, undisturbed ocean (Suthers et al. 2006).

Coastal to offshore gradients often exhibit higher productivity and zooplankton biomass near the coast (Vandromme et al. 2014) and low biomass and lower slopes in open ocean conditions (Marcolin et al. 2015). Coastal to offshore transects in the Bay of Biscay showed patterns of steep slope, high intercept and high zooplankton biomass nearest the coast, where productivity is fuelled by nutrient rich runoff from the land as well as mixing due to the shallower water depths. Coastal regions exhibit high seasonal and annual variability (Vandromme et al. 2014). Wind and rainfall conditions often lead to variations in primary productivity along the coast, with their influence on coastal rainfall runoff (Skarðhamar et al. 2007; Vandromme et al. 2014) and wind driven upwelling processes (Everett et al. 2014) influencing the vertical stratification of the surface layer and introducing nutrients to the photic zone (Skarðhamar et al. 2007; Everett et al. 2014).

Flatter slopes occur over the continental shelf (Vandromme et al. 2014) where waters are more stratified and have less nutrient enrichment, therefore less productivity and an older zooplankton community that have grown to a larger mean body size. NBSS slope can steepen near the shelf break where sporadic mixing of nutrient rich deeper waters into the surface increases the productivity, increasing small herbivorous zooplankton which steepens the NBSS slope (Fig. 1.1). The open ocean regions experience lower variability, due to stratification or lack of terrestrial runoff creating nutrient limited surface waters. The lack of nutrients reduces the primary production, and small herbivorous zooplankton at the base of the food web (Vandromme et al. 2014), contributing to the low biomass and shallower slopes seen in the open ocean.

Patterns in the size spectrum can represent characteristics of an ecosystem. For example, non-linearity of the NBSS slope or domes may be observed as a secondary structure in a size spectrum (Sprules and Barth 2016). Domes appear when a particular size class is present in high abundance or biomass relative to other size classes in the spectrum, which can sometimes relate to a trophic group (Schwinghamer 1981; Mullaney and Suthers 2013; Blanchard et al. 2014; Guiet et al. 2016) or an abundant population of a particular species (Boudreau and Dickie 1992) in that size range. Instability in an ecosystem, due to fluctuations in primary production such as phytoplankton blooms, can create a non- linear size spectrum slope. Initially an increase in primary productivity creates a dome of increased biomass in the size class relating to phytoplankton. Through predation of the phytoplankton by higher trophic levels, this dome appears as a travelling wave, through the smaller to larger size classes over time (Boudreau and Dickie 1992; Heneghan et al. 2016). Travelling waves in the size spectrum may also be due to upsets in the size balance caused by predator effects (Guiet et al. 2016; Sprules and Barth 2016).

1.3. Metrics of the size spectrum

A biomass size frequency distribution is usually converted to a **NBSS**, by dividing the biomass of each size category by the width or range of each size category with units

of m^{-3} (i.e. $\text{mg} \cdot \text{m}^{-3}/\Delta \text{mg}$, (Krupica et al. 2012)). This enables inter-comparison of studies which may use different size categories (linear, or \log_2). A log-log plot of normalised biomass on size creates a negative relationship, as biomass in the natural world is approximately distributed logarithmically. The NBSS has various statistics to convey the zooplankton biomass and productivity. The NBSS slope ($\text{NBSS}_{\text{slope}}$) essentially indicates the biomass ratio of larger sized organisms to smaller sized organisms, indicating a community's growth, respiration, mortality and trophic dynamics (Zhou 2006). Energy preserved as body mass results in higher efficiency of energy/biomass transfer through the food chain resulting in a less negative $\text{NBSS}_{\text{slope}}$, whereas high loss of energy from primary to secondary producers results in steeper NBSS slopes (Trudnowska et al. 2014). Environments with higher temperatures and therefore higher metabolic demands result in increased energy loss and steeper NBSS slopes. Therefore factors that are thought to increase the zooplankton $\text{NBSS}_{\text{slope}}$, can include increases in primary production driving an increase in the abundance of small zooplankton and removal of the larger size classes for example from increased predation by fish (Fig. 1.1) (Zhou 2006). However, sustained primary production can result in a zooplankton community with less negative slopes, due to the abundant energy supply to support zooplankton growth into larger size classes, with the sustained energy supply required to support the higher abundance of larger size classes (Fig. 1.1).

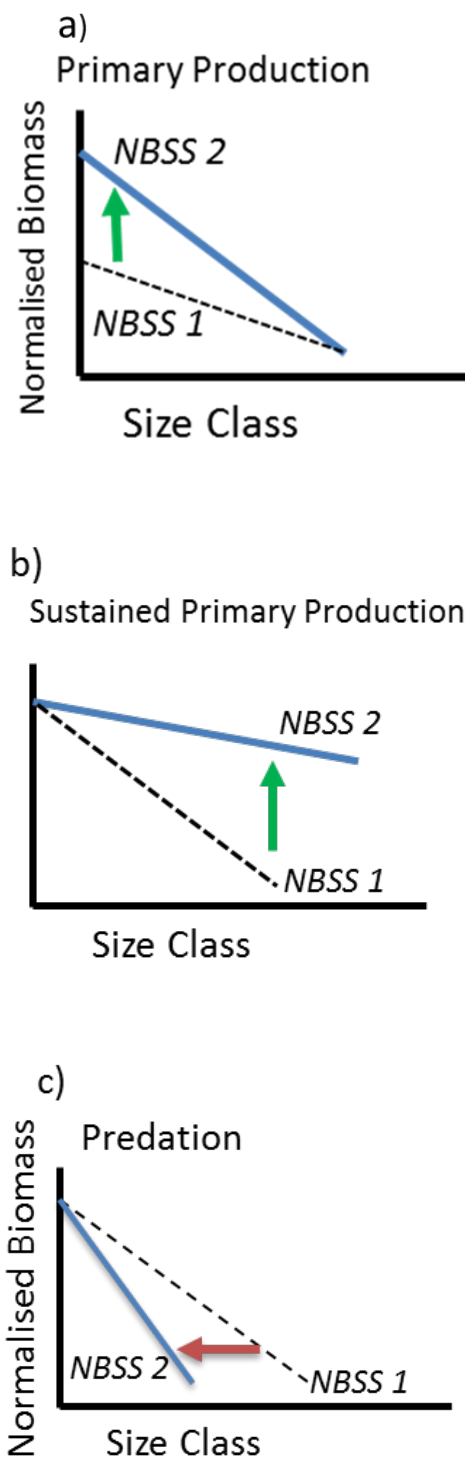


Figure 1.1 Summary of the possible dynamics of the normalised biomass size spectrum of zooplankton (redrawn from Moore & Suthers 2006). a) shows the steepening of the slope (and increased intercept) due to nutrient enrichment, b) flattening of the slope (and sustained intercept) with continued primary production or c) a steepening of the slope due to predation.

The size based parameters of the NBSS were evaluated by Krupica et al. (2012), using broadscale data from the east coast of Canada (Fig. 1.2). They found that simple size-based indices were good indicators of temporal and spatial variations in size structure, such as the geometric mean and arithmetic mean of body size, and coefficient of variation which can tell how much variation lies around the mean size (Krupica et al. 2012). Other indices derived from the NBSS, such as the x and y vertex of a non-linear NBSS, as well as the curvature of the non-linear line, were not as effective at explaining spatio-temporal trends as the size-based indices (Fig. 1.2). These NBSS derived indices only explained secondary patterns in spatial and temporal variations in zooplankton community size structure (Krupica et al. 2012). It is pointed out that the NBSS is fitted to data, so the accuracy of the NBSS derived indices are only as good as the fit of the modelled line to the data (Krupica et al. 2012).

1.4 Measuring particle size with an optical plankton counter (OPC)

The OPC consists of a sampling tunnel through which water and particles flow (Fig. 1.3b) and an LED or a laser beam which is directed across the sampling tunnel (Fig. 1.3c). As a particle flows across the light beam, the detector records a change in light (attenuance) in millivolts, which is calibrated for a range of particle sizes as equivalent spherical diameter (ESD) (Fig. 1.3a). The OPC assumes each fluctuation in light is one particle and therefore multiple particles travelling through the OPC at the same time will be measured and counted as a single particle (termed “coincidence”) (Herman 1992). As zooplankters are not distinguished from other particles by the detector, the OPC is alternatively called the Optical Particle Counter by some authors (Marcolin et al. 2013). The LED-OPC (OPC) has only 6 LEDs and can resolve particles 0.25 to 20 mm ESD whereas the Laser-OPC (LOPC) has a row of 70 1 x 1 mm detectors and can resolve particles 0.1 to 35 mm, at a 1000 fold greater concentration (Herman et al. 2004). The multiple detectors give greater count accuracy (densities of 10^6 m^{-3} (Herman et al. 2004)) and size accuracy. The LOPC has a particle concentration capacity of an estimated 10^6 m^{-3} , with the OPC having a coincidence limit of 10,000 particles. m^{-3} (Herman et al. 2004). The LOPC measures particles of 100-1500 μm as Single Element Particles (SEPS's) and 1500 μm -35000 μm as Multiple Element

Particles (MEP's) which can convey some understanding of shape or even translucence profiles.

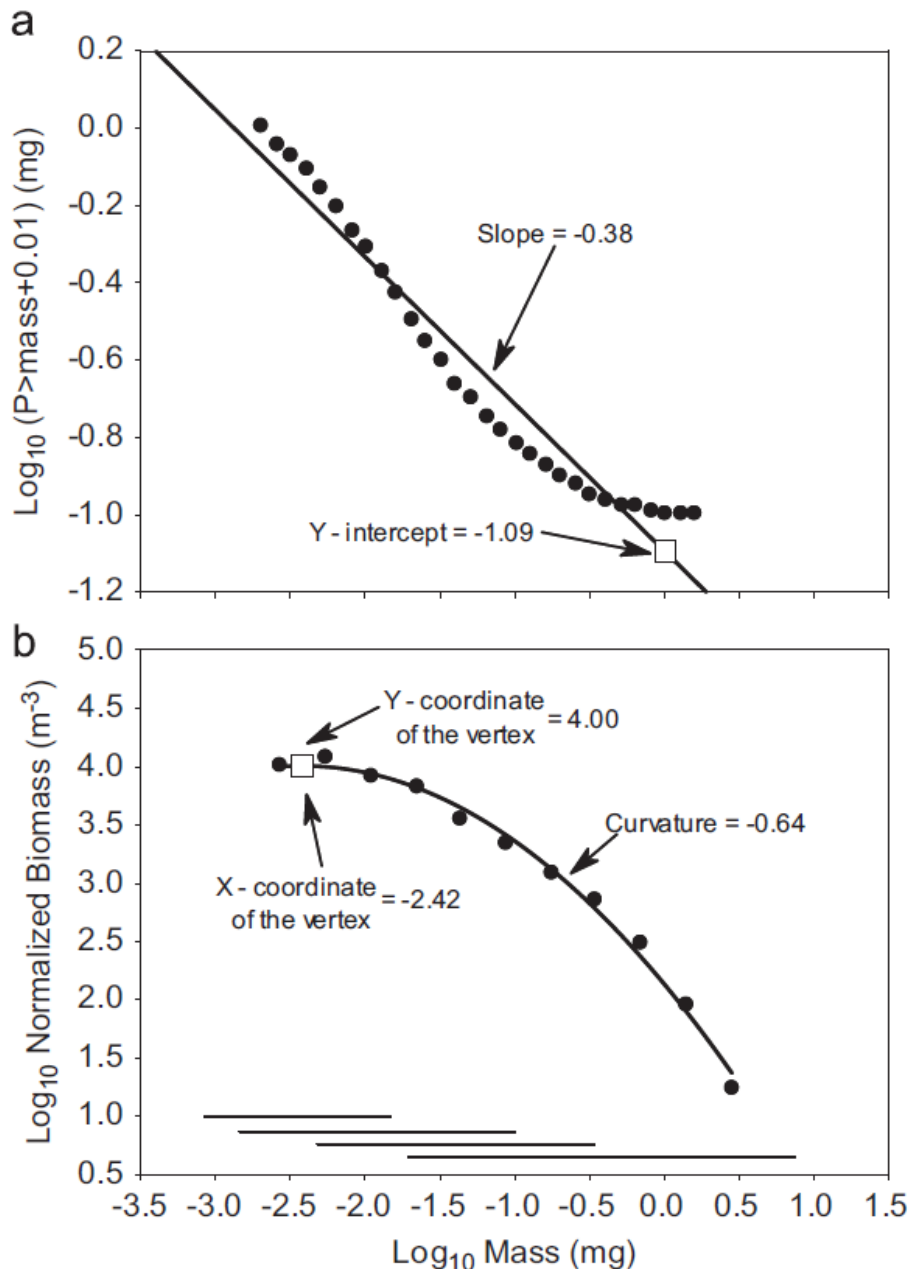


Figure 1.2 Figure reproduced from Krupica et al. (2012) summarising the main metrics used to compare zooplankton size spectra; a) the pareto distribution with a fitted least squares line showing simple size based metrics, and b) an NBSS spectrum with the more complex size based metrics. The horizontal lines from upper to lower, show the size ranges of four typical copepods from the east coast of Canada *Pseudocalanus* spp. (-3.08 mg to -1.97 mg), *Temora longicornis* (-2.82 mg to -1.01 mg), *Calanus finmarchicus* (-2.31 mg to -0.47 mg), and *Calanus hyperboreus* (-1.69 mg to 0.68mg).

Table 1.1 Summary of the major improvements instrument resolution between the LED-OPC and L-OPC.

	LED-OPC	Laser-OPC
Light-beam	Light Emitting Diode	Laser
Sampling interval	4 mS	0.55 µS
Size range	0.25 mm-20 mm	0.1- 35 mm
Max concentration	25,000 m ⁻³	1 x 10 ⁶ m ⁻³
Particle detection	Single element particle	Single (100-1500 µm) and multiple element (1500-35000 µm) particle,

The background light attenuation is continuously monitored and adjusted to provide a constant light intensity across the tunnel (to account for sediment or chlorophyll), such that any sudden fluctuation is interpreted as a particle. The OPC counts any particle greater than the minimum size with an optical refractance – living zooplankton, or non-living matter of the same size range (Herman et al. 2004; Trudnowska et al. 2014) such as detritus, empty larvacean houses and pteropod webs (Checkley et al. 2008). Sheldon et al. (1972) observed that the majority of the larger suspended ocean particles in the zooplankton size range were in fact zooplankters, and phytoplankton sized particles collected in the open ocean were organic and plankton or planktonic detritus, with living phytoplankton cells making up about half of this. Elliot & Tang (2011) found up to 30% of copepod nauplii were dead, but these larval stages are smaller than the 300 µm lower limit of this study. Although the particles passing through the OPC that fall within the zooplankton size range are assumed to be living zooplankters, this is likely inaccurate due to contamination by some non-living and detrital particles. Most detrital particles fall below the 300 µm size limit used in this study. Dead zooplankton is still useful carbon that enters the scavenging food web and passes productively up the size-based food chain.

Evaluation of LOPC data with net samples and Zooscan analysis can be used to distinguish the living and detrital proportions of particles measured by the OPC. However, it is important to note that all sampling gear has limitations of net avoidance, net extrusion, or damage and particle creation. Nets can have sampling errors, due to net avoidance by larger copepods/organisms, and damage and loss of more fragile taxa such as tunicates and gelatinous zooplankton and detritus. This is a reality of all plankton studies. In regard to my use of the LOPC however:

- 1) Elliott and Tang (2011) found up to 30% of copepod nauplii were dead – but these larval stages are smaller than the 300 µm lower limit of my study.
- 2) Dead zooplankton is still useful carbon that enters the scavenging food web, and passes productively up the size-based food chain.

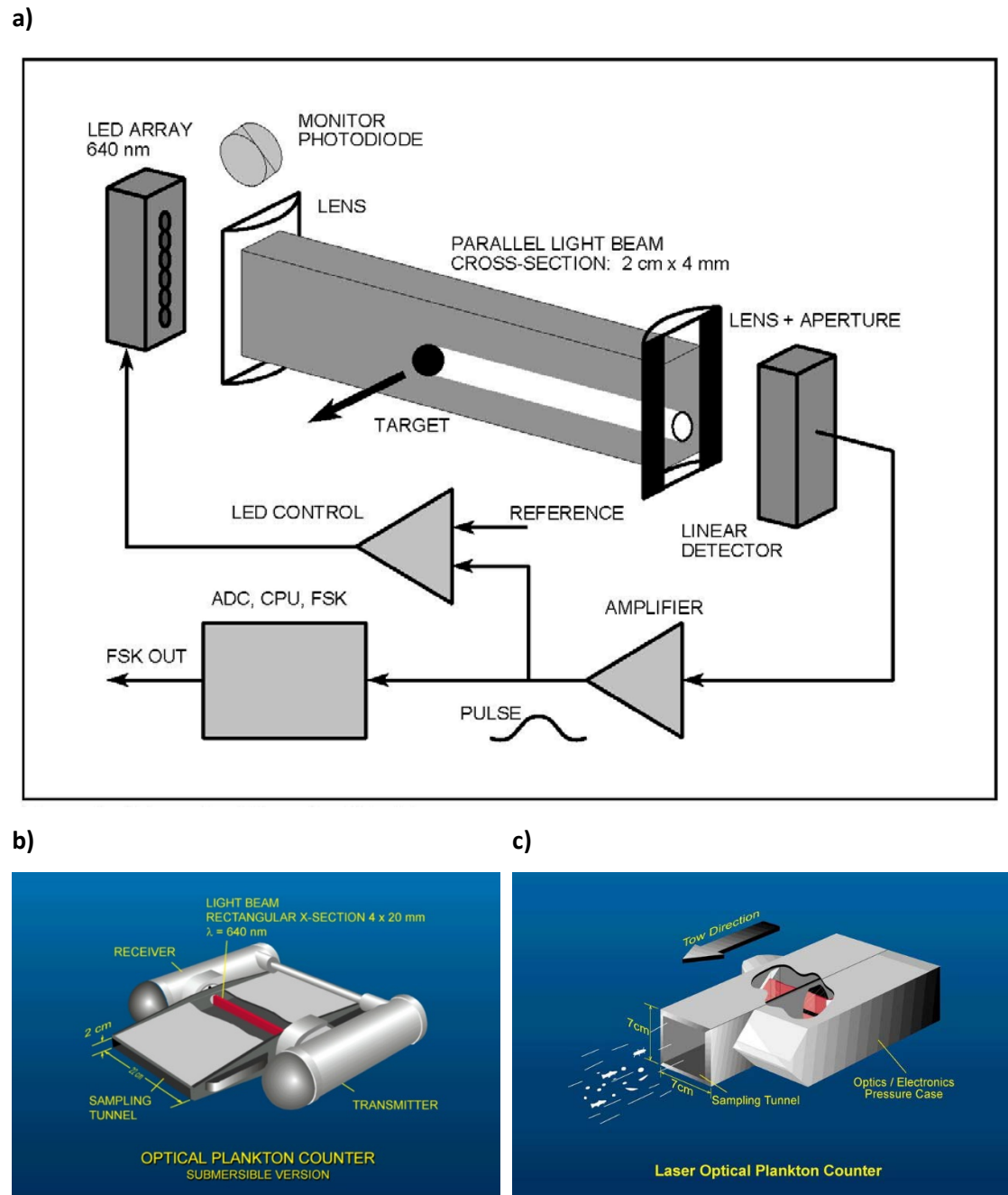


Figure 1.3 a) Zooplankton particles in water flow through a beam of six light emitting diodes (LEDs) on one side of the sampling tunnel, which is received on the opposite side of the tunnel. The size of the particle is calculated from the detected change in light intensity (Herman 1992). **b)** the underwater version of the Optical Plankton Counter (OPC) (GoMA 2018a) and **c)** the Laser-Optical Plankton Counter (LOPC) (GoMA 2018b).

As a light intensity is measured (and not a “shadow”), the OPC is not sensitive to the angle at which a zooplankton is orientated as it passes through the light beam. For example, a long narrow zooplankton could pass through the tunnel head or tail first and the shadow cast consist of its entire length by height profile, or longitudinal plane. Conversely, it may pass through the tunnel side on, casting a shadow equivalent to its transverse plane, or height by width. The change in light intensity of the two situations would yield a much lower value and ESD for the latter situation, despite being the same individual (Herman 1992).

There may be sampling inefficiencies at either end of the sampling size limits of the OPC and LOPC instruments. The OPC is designed to measure particles of size 250 µm to 2 cm ESD (Herman 1992) and the LOPC has a greater sample size range of particle sizes (100 µm to 35 cm). It is possible that sampling inefficiencies at the extreme ends of the spectrum occur due to low natural density of larger particles or sample gear inefficiencies at the extreme ends of their size measuring capabilities, resulting in a tailing off of counts at the larger and smaller particle sizes. Data points of size bins can be removed from the spectrum if the counts are too low, or the coefficient of variation of the size bin is too high (Sprules and Barth 2016).

The OPC and newer LOPC have similar operational practices and principles, however there have been no studies that compare the sampling differences between the two. In this study, the LOPC data was analysed more coarsely than the LOPC’s sampling capabilities. To make the data collected by the two instruments consistent the LOPC data was reduced to match the size range and resolution limits of the OPC and the size range of 0.3 to 12 mm ESD was used for analyses.

Measurements of NBSS_{slope} constructed using size data collected by net and size data collected by OPC are significantly correlated (Vandromme et al. 2014), particularly at high abundances (Checkley et al. 2008), but with variability in the relationship reducing at low abundances (Checkley et al. 2008). Intercept may be higher when measured using the OPC size data (Vandromme et al. 2014) but greater accuracy can be achieved using methods to correct for the aggregates collected by the OPC (Petrik et al. 2013). Difficulty can arise when comparing LOPC with net measurements due to

the fragility of organisms resulting in under sampling of fragile taxa such as tunicates and coelenterates and aggregates in the net samples (Checkley et al. 2008). Also a nets filtering efficiency needs to be considered, with Checkley et al. (2008) using a filtering efficiency of 0.75 to allow consistent comparison of net abundance estimates of large copepods with LOPC abundance measurements.



Figure 1.4 Triaxus (left) and Sea Soar (right). The Laser-OPC is a sampling instrument which is mounted on a towed body (circled on Triaxus); the LED-OPC on the Sea Soar is arrowed.

1.5 Study Area and the western Tasman Sea

The study area is in the western Tasman Sea off the south eastern Australian coast from 28°S to 37°S and eastward to the Lord Howe Seamount chain. The narrow continental shelf, bounded by the 200 m isobath, fluctuates between 15 and 50 km width. This region is characterised by three main water types; shelf water, the warm oligotrophic East Australian Current (EAC) and the cooler Tasman Sea (Suthers et al. 2011). The EAC is a warm western boundary current, flowing poleward at an average speed of 1 ms^{-1} (Baird et al. 2008). At approximately latitude 32°S, the EAC separates from the coast and either turns eastward to form the Tasman Front, or continues south forming the EAC extension (Everett et al. 2014). The separation latitude and quantity of EAC water that enters the southern region is affected by EAC flow, which fluctuates with changes in El Nino Southern Oscillation (ENSO) (Baird et al. 2011). The EAC extension off Tasmania varies in strength approximately every 10-15 years (Hill et al. 2008).

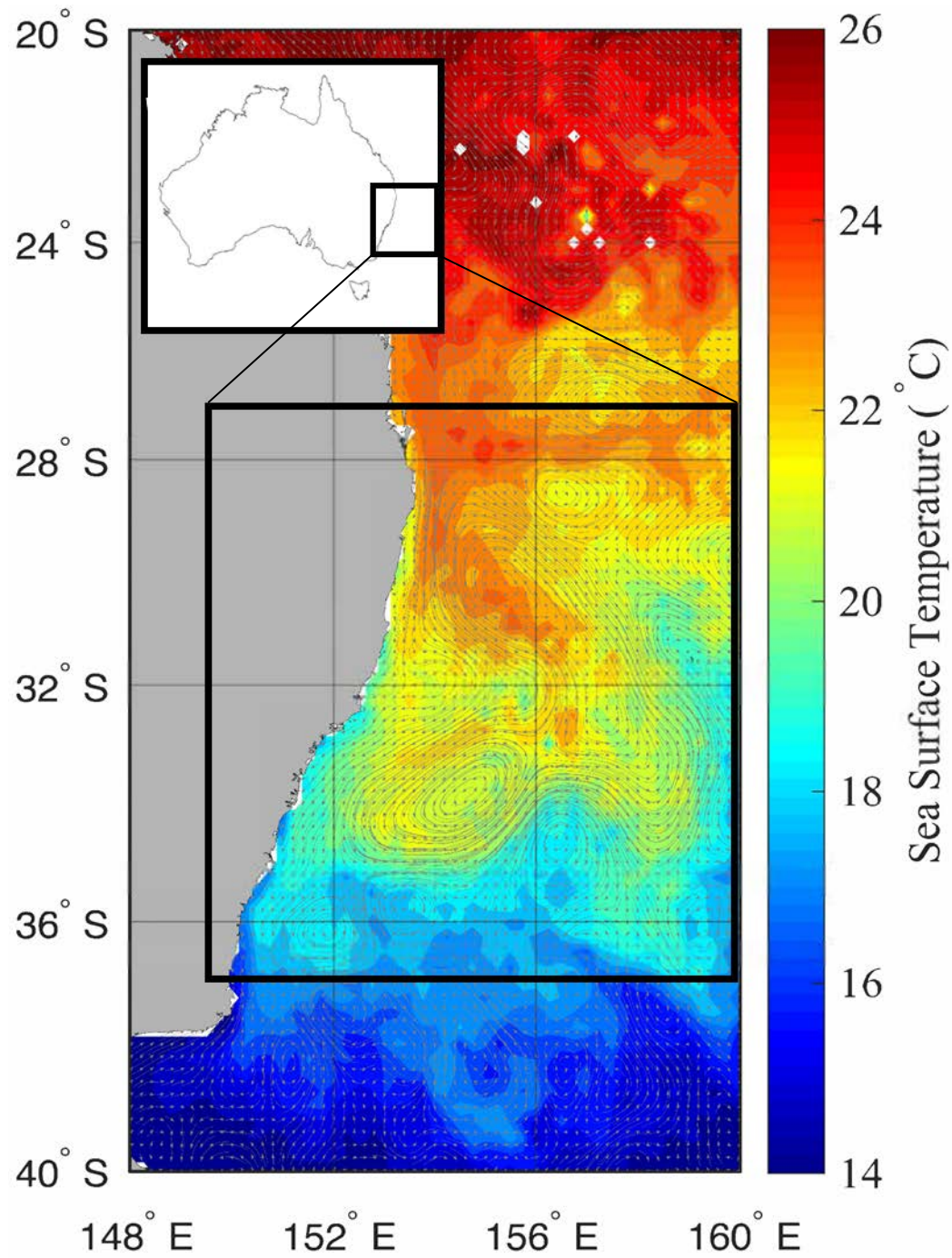


Figure 1.5 The study area (bordered by the black box) is located on the south-eastern Australian coastline (inset map). The colour shows the north to south gradient in sea surface temperature as measured by satellite. The arrows indicate the direction and strength of currents and the presence of cyclonic (upwelling) and anticyclonic (downwelling) eddies.

The EAC may be described in four stages – from its formation in the south Coral Sea (15-24°S); to the intensification off SE Queensland and northern NSW (22-31°S); the separation off the coast and formation of a large “retroflection” eddy and Tasman Front (31-34°S); and the southward moving eddy field into the waters of eastern Tasmania (Ridgway and Dunn 2003). Eddies form along the length of the EAC, bringing spatial diversity to the water-types and plankton, and are particularly abundant in a region described as “Eddy Avenue” off the Sydney-Newcastle coast (31-34°S, (Everett et al. 2012)). Eddy avenue contains a higher frequency of eddies than the rest of the study area and the eddies formed here display greater rotational speeds than elsewhere in the Tasman Sea (Everett et al. 2012). Cold core eddies (CCE's) have an average of 16 % more chlorophyll-*a* than the surrounding Tasman Sea waters (Everett et al. 2012). The coastal CCE's often form from productive shelf waters and as the isotherms shallow the upwelled nutrient rich waters within the eddy centre continue to fuel production (Mullaney and Suthers 2013). Warm core eddies (WCE's) are often formed from the oligotrophic Coral Sea waters and have on average of 28% less chlorophyll-*a* than their surrounds (Everett et al. 2012) due to the deepened and stratified surface layer inhibiting mixing of the deeper nutrient rich waters.

The EAC has a less pronounced seasonal phytoplankton production cycle because it is a stable, low nutrient, stratified water mass with a mixed layer depth of 25-50 m (Baird et al. 2008; Suthers et al. 2011). The Tasman Sea has a mixed layer depth of between 80-120 m (Baird et al. 2008) and is prone to mixing with deeper layers, exposing nutrients to the euphotic zone. This region experiences a seasonal springtime phytoplankton bloom when sea surface temperature increases, dissolved nitrates and silicates increase and the mixed layer becomes shallower (Everett et al. 2014).

These two water types are characterised by different zooplankton and fish communities due to their different environmental properties. The EAC harbours tropical zooplankton assemblages and there is an increase in the size spectrum slope of 30% between the Coral Sea (approx. -1) (-0.95 to -1.3) (Suthers et al. 2006)) and

Tasman Sea (-0.59 to -0.8) (Baird et al. 2008). The cooler Tasman Sea supports a higher biomass of phytoplankton, with larger phytoplankton cells (Baird et al. 2008) and a higher biomass and proportion of larger size classes of zooplankton than the EAC (Baird et al. 2008).

Upwelling occurs along the continental shelf as a result of current and wind driven upwelling. Upwelling favourable bottom stress and wind stress can increase chlorophyll-*a* levels along the shelf. At 29 and 32°S wind stress has a particularly strong influence on surface chlorophyll-*a* levels (Everett et al. 2014). Cape Byron (28.5°S) and Smokey Cape (31°S), are areas of consistent upwelling. However, productivity is particularly low at these locations because the upwelling waters reach the surface downstream at 29-29.5°S and 32°S, respectively, due to the strong southward flow of the EAC. Here Chlorophyll-*a* productivity is high, creating favourable conditions for zooplankton and larval fish development. Physical processes, such as separation of the EAC from the coast at the separation zone, cause uplift of slope waters onto the shelf (Everett et al. 2012). These processes set up consistent patterns of productivity along the shelf. Overall, south of the separation zone chlorophyll-*a* levels are driven more by seasonal changes and north of the separation zone chlorophyll-*a* has less of a seasonal signature and is more influenced by upwelling processes (Everett et al. 2014).

1.6 Aims of this research.

In summary, zooplankton are a food resource to fish, and biomass and NBSS intercept of the zooplankton size spectrum are ultimately an indicator of the availability of zooplankton to support the biomass of fish. Zooplankton biomass is determined by the richness of the supply of phytoplankton or lower trophic resources as a food resource to support zooplankton. A greater biomass of phytoplankton results in a greater biomass of zooplankton, seen as a higher intercept in the NBSS. The mediating factors that determine the proportion of primary production that translates into zooplankton biomass, are related to temperature, and the properties of the zooplankton size structure.

My overall goal was to integrate the zooplankton size-structure and oceanographic data from several voyages in the western Tasman Sea, and develop a statistical model for the region which could be used for dynamic ocean management of fisheries (e.g. Hobday et al. 2011). These voyages were conducted on Australia's Marine National Facility – RV Southern Surveyor (2004-2010) and RV Investigator (2014-2015). This was done using *in situ* data collected using the OPC/LOPC on a towed platform (a SeaSoar or Triaxus, Fig. 1.3) to measure zooplankton sized particles and assess the particle size structure (size range 300-12000 µm ESD), along with concurrent *in situ* measurements of environmental variables (temperature, chlorophyll-a, bathymetry and sea level anomaly). The environmental variables were chosen as they are available over large areas through satellite data. Chlorophyll-a concentration affects the growth rate and body size of zooplankton. Zooplankton size is also controlled by temperature, with larger individuals observed in colder environments. Sea level anomaly is used to identify cold and warm core eddies, which can entrain zooplankton populations and often harbour different physical and biological properties to the surrounding environment. Bathymetry may affect zooplankton communities, through upwelling and sea floor mixing processes adding nutrients to the water column and enriching primary production at the shelf break and on the shelf. All the voyages were conducted during the austral spring because of specific objectives related to fisheries and oceanography. My specific research aims were to:

- 1) Determine relationships of zooplankton community size structure with environmental variables in the western Tasman Sea; and
- 2) Apply the relationships to spatial satellite data of the study region, using springtime (Sept-Oct-Nov) averages of the physical oceanography for 2003 to 2016, to map zooplankton community size structure in the western Tasman Sea.

This was achieved in two steps. Simple linear models were used to model zooplankton size structure parameters as they related to the ocean environmental conditions they were under at the time. Backstep regressions were used to determine

which environmental conditions were important and retained in the model. The relationships determined in this first step were then used to hindcast the zooplankton community size structures over the study area in the spring seasons from 2003 to 2016. This was done by applying the modelled relationships to archived satellite data of the study area, averaged over the spring months, and using the results to create hindcast maps of zooplankton community size structure over the study area. Finally, a comparison between the hindcast modelled abundance values and archived *in situ* abundance data collected by Continuous Plankton Recorder was made, to assess whether the two methods show a similar pattern of zooplankton abundance over the study area.

I concluded my thesis by considering the potential of these findings for seascape ecology of the western Tasman Sea, which underpins the modern methods of dynamic ocean management (Hobday and Hartmann 2006). Note that the two data chapters (Chapter 2 and Chapter 3) were written in the form of journal articles, therefore there are some duplications (i.e. in methods) between the two.

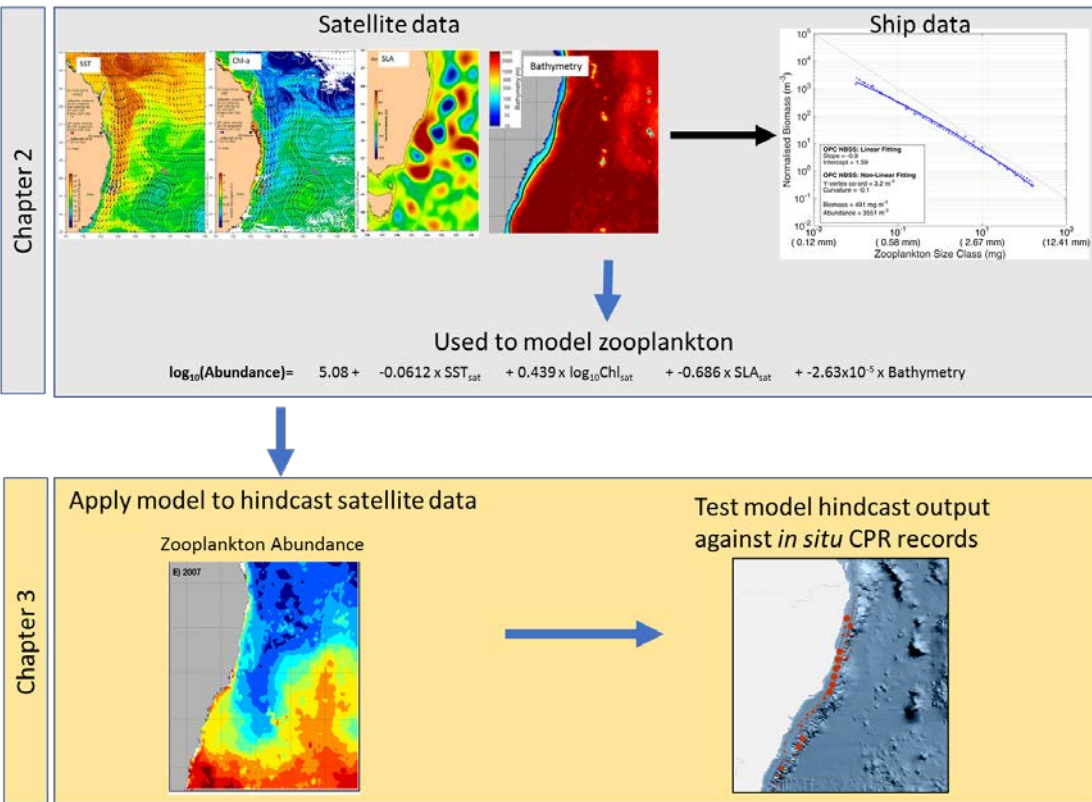


Figure 1.6 This conceptual diagram shows the flow of analysis through my thesis to achieve the stated aims. The maps in chapter 2 (top row) show the four environmental variables (Satellite temperature, chlorophyll- α , sea level anomaly and bathymetry) that were linearly modelled against *in situ* ship acquired measurements of size spectra metrics. In chapter 3 (Bottom row), these relationships were applied to archived satellite data of the same environmental variables to create maps of zooplankton size distributions (left). The hindcast abundance was compared for the same date and location with corresponding *in situ* CPR abundance measurements (right).

Chapter 2 : Quantifying the link between the size-distribution of zooplankton and satellite-derived oceanographic variables

2.1 Abstract

The size-structure of the zooplankton community in the western Tasman Sea was investigated to further our understanding of how oceanographic processes drive changes in the zooplankton size structure. I assembled five size-based indices in the upper mixed layer (<30 m from the surface) from 39 deployments of an Optical Plankton Counter towed for a total of 3,661 km, during the austral winter and spring in 2004, 2006, 2008, 2015 and 2016. I compared the zooplankton abundance, biomass, geometric mean size (GMS), and the slope and intercept from the normalised biomass size spectrum (NBSS) among 5 characteristic habitats, and then examined these indices on a continuum with satellite Sea Surface Temperature (SST_{sat}), satellite Sea Level Anomaly (SLA_{sat}), satellite Chlorophyll- α (Chl_{sat}) and bathymetry using linear models. Overall the cooler Tasman Sea waters had greater abundance, biomass, GMS, and NBSS-intercept ($NBSS_{intercept}$) than waters derived from the warmer East Australian Current, which had a steeper NBSS-slope ($NBSS_{slope}$). There was no difference between the continental shelf and the adjacent ocean. The linear models explained between 18% ($NBSS_{slope}$) and 46% (GMS) of the variability. The relationships of the zooplankton size-based ecosystem with remotely sensed environmental variables reveal the potential to generate estimates of zooplankton biomass and production over broad temporal and spatial scales.

2.2 Introduction

Zooplankton are a key trophic link between phytoplankton and fish communities in the deep ocean (Kiyashko et al. 2014), on continental shelves (Young et al. 1996), on coral reefs (Hamner et al. 1988) and temperate reefs (Champion et al. 2015). Yet little is known about how zooplankton biomass and production varies at the temporal and spatial scales of dynamic oceanographic features, such as eddies and ocean currents (Piontkovski et al. 1995). Biogeochemical parameters, such as sea-surface temperature, nitrate and chlorophyll- α underpin dynamic ocean management (Hobday and Hartmann 2006; Maxwell et al. 2015; Dunn et al. 2016), yet a stronger focus on understanding the processes of the lower trophic levels, such as zooplankton, is needed to reconcile the divergent fisheries biomass estimates (Jennings and Collingridge 2015). Compared to biogeochemical parameters, zooplankton estimates offer a deeper mechanistic understanding of fishery production processes (Friedland et al. 2012) and when coupled with satellite observations of the oceanographic conditions, is the first step towards better understanding prey-fields for fish communities.

Similar to phytoplankton (Barnes et al. 2011) and fish (Jennings and Mackinson 2003), zooplankton communities are strongly size-structured (Baird et al. 2008; Barton et al. 2013). Analysing the size structure is a pragmatic approach to address the complexity of the pelagic ecosystem. These size distributions are commonly referred to as size-spectra (Stephens et al. 1967). At a basic level, the size spectrum reveals how abundance (or biomass) of a community varies with body size (Edwards et al. 2017). The size spectrum also provides an estimate of energy transfer through the food-web (Dickie et al. 1987; Jennings et al. 2008), as size determines a zooplankter's predator-prey relationships, along with many vital rates such as growth, fecundity, and metabolism (Zhou 2006; Kiørboe and Hirst 2008).

Size spectra are generally described by the relationship between the logarithm of total body mass (or abundance) binned to body mass classes, irrespective of species identity. Typically, a size-spectrum is linear on logarithmic axes and is quantified by the slope and y-intercept (Edwards et al. 2017) where the slope is approximately -1,

as first proposed by Sheldon et al. (1972) to hold from bacteria to whales. There is of course much variability around this -1 approximation (e.g. Baird et al. 2008; Basedow et al. 2010; Krupica et al. 2012; Zhou et al. 2010; Suthers et al. 2006). Non-linear patterns are also seen within the size-spectra and generally result from either short-term perturbations of the community from nutrient inputs (Moore and Suthers 2006), or the bloom of a single-species (Mullaney and Suthers 2013) or from longer-term patterns such as seasonality (Jennings 2005), limits of sampling gear (Krupica et al. 2012) or inefficiencies in the predator-prey relationship in the size-ranges related to a switch in taxa (i.e. phytoplankton-zooplankton or zooplankton-fish; (Kerr and Dickie 2001; Blanchard et al. 2017)). Nonetheless, the linear size-spectrum is a powerful tool for understanding predator-prey relationships and energy transfer within the food-web.

As biomass in a food web moves from lower trophic levels through to higher trophic levels energy is lost. As such, a higher biomass at smaller size classes is required to support the biomass of larger sizes classes, resulting in a negative size spectrum slope. The rate of energy loss is affected by environmental conditions such as temperature, oceanographic processes (eddies, upwelling) and food availability. The size-spectrum of the zooplankton community is known to vary between locations (Baird et al. 2008), times (Basedow et al. 2010) and environmental conditions (Krupica 2006), but no studies have developed continuous linear relationships between the zooplankton size-spectra and environmental conditions, as has occurred for phytoplankton (Barnes et al. 2011). This is a significant knowledge gap.

Mean phytoplankton biomass and cell size increases with decreasing temperature and increasing chlorophyll-*a* (Barnes et al. 2011), and an increase in the mean cell-size of the phytoplankton community can result in a greater abundance of large-sized fish (Woodworth-Jefcoats et al. 2013). We know from zooplankton-resolved size-spectrum models, that changes in the size-spectra and feeding characteristics of the zooplankton community can significantly alter the productivity and biomass of the fish community (Heneghan et al. 2016). Without understanding how the zooplankton size-spectrum mediates the food-web, we are neglecting a significant factor in how

energy is transferred from phytoplankton to fish. Understanding how the size-spectra of zooplankton change with environmental conditions is the first step in this process, and will help to bridge the gap between the phytoplankton and fish community size structure.

The marine region off eastern Australia is characterized by a range of watermasses (Henschke et al. 2011), including the warm, oligotrophic East Australian Current (EAC) which flows down from the Coral Sea and typically has a mixed layer depth of 25 - 50 m (Baird et al. 2008; Suthers et al. 2011), and the temperate, relatively eutrophic Tasman Sea (Baird et al. 2008; Suthers et al. 2011) which typically has a mixed layer depth of between 80 – 120 m (Baird et al. 2008). The continental shelf (<200 m) is strongly influenced by over-washing from the EAC in the north and the Tasman Sea in the south, and is also susceptible to eddy intrusions (Young et al. 2001), intermittent upwelling (Roughan and Middleton 2002) and phytoplankton blooms (Everett et al. 2014). The zooplankton size-spectra of the oligotrophic Coral Sea and EAC waters are generally very linear and vary between -0.87 and -1.14 (Rissik et al. 1997; Suthers et al. 2006; Baird et al. 2008). Conversely, the Tasman Sea generally displays a flatter slope of between -0.59 and -0.78 (Baird et al. 2008).

The size-spectra of particles in the zooplankton size range are rapidly obtained from particle size data as measured by instruments such as an optical plankton counter (OPC) (Herman 1992; Herman et al. 2004). Despite the OPC's inability to distinguish detritus and non-living particles from living zooplankters, the OPC is frequently used to convey empirical estimates of zooplankton biomass and abundance, and has previously been used to model a variety of size-dependent rates such as growth, mortality and production (Zhou 2006; Zhou et al. 2009; Basedow et al. 2010). The goal of this chapter is to use multiple deployments of an OPC to determine the abundance, biomass and size-distribution of zooplankton communities within the western Tasman Sea in relation to remotely sensed environmental variables (SST_{sat} , Chl_{sat} and SLA_{sat}) and bathymetry. Specifically, I aim to determine:

1. How zooplankton size-spectra differ among characteristic water-masses off eastern Australia; and

2. What environmental variables drive these differences in zooplankton size-communities.

Satellite data are used for this analysis as they have high spatial and temporal coverage so can be applied or compared between many global regions. Satellite data collect chlorophyll-*a* of the first optical layer which can vary depending on water clarity or turbidity and captures an overall value for the water column. As such, small scale features, or more complex vertical properties of the water column can be overlooked (Durham and Stocker 2012). The satellite physical variables have been chosen to broadly represent the physical oceanographic conditions. OPC data was collected from the upper 30 m of water (the upper mixed layer) and satellites also observe the upper mixed layer - either the ocean skin (Sea Surface Temperature) or upper few metres. Neither method includes the Deep Chlorophyll Maximum (DCM) which is why we chose the upper 30 m of OPC data.

2.3 Methods

2.3.1 Study Region

The study region (Fig. 2.1) lies in the western Tasman Sea, bordered by eastern Australia's coastline and between 28 °S and 37 °S and east to the Lord Howe Seamount Chain (159.40 °E). In this region the continental shelf fluctuates in width from 15 - 50 km (Suthers et al. 2011). The East Australian Current, a western boundary current originating in the Coral Sea, is one of the two dominant watermasses of the western Tasman Sea area, flowing at up to 2 m s⁻¹ (Suthers et al. 2011) through the Tasman Sea watermass (the other dominant watermass). The region is also characterised by southward moving eddies (Everett et al. 2012), intermittent upwelling (Roughan and Middleton 2004; Everett et al. 2014), and the Tasman Front (Baird et al. 2008).

2.3.2 In-situ Data Collection

Data was collected using an OPC mounted on a modified SeaSoar (2004, 2006, 2008) and a Laser OPC (LOPC) mounted on the Triaxus (2015, 2016). The OPC (Herman 1992) and LOPC (Herman et al. 2004) count and estimate the size of particles as they pass through the sampling tunnel and interrupt a light emitting diode or laser array (respectively). The shadow cast by the particles passing through the array are converted into a corresponding Equivalent Spherical Diameter (ESD). Coincident measurements of salinity, temperature, depth, flow, longitude and latitude were recorded using a Seabird CTD mounted on the SeaSoar (SBE3 and SBE4) and Triaxus (SBE9+).

A total of 39 deployments were made on voyages between 2004 and 2016 measuring 3661 km and sampling 1731 m³ of water (Table 2.1). Each deployment (Fig. 2.1) consisted of a number of undulations between the surface and 120 m (SeaSoar) or 200 m (Triaxus). Each pair of up/down casts were separately analysed as an independent sample. In this analysis, only the 5 - 30 m is included. This is to ensure

the data analysed is within the surface mixed layer (Baird et al. 2008, 2011) and corresponds with remotely sensed observations (below).

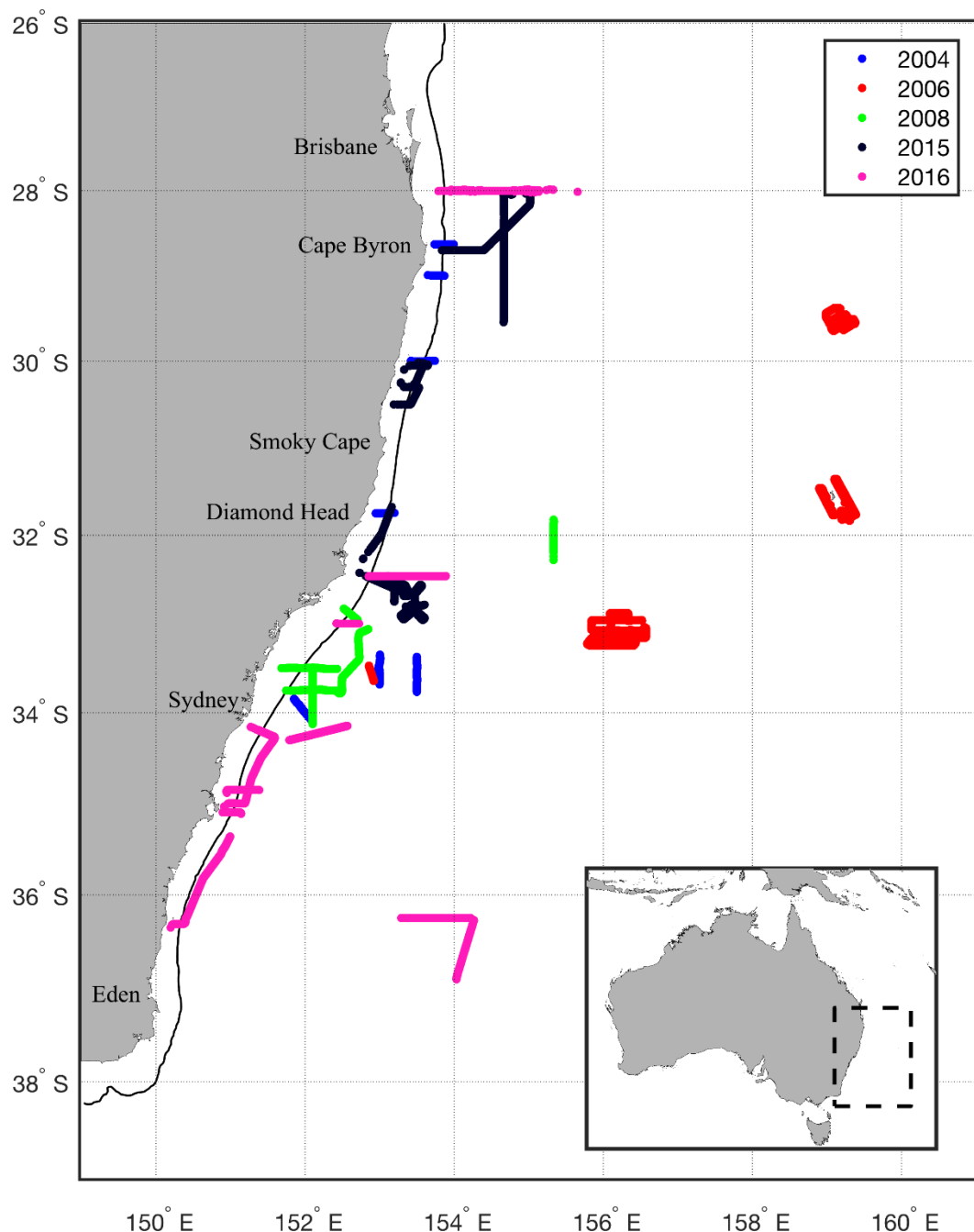


Figure 2.1 Each transect from the study are shown on the map of eastern Australia. The colours represent the voyage year. The inset shows a map of Australia with boundaries of the larger site map marked by a dashed line.

Table 2.1 OPC deployment and voyage details

Date Range	Vessel	Platform	Deployments	Distance (km)	Volume (m ³)	Particles Counted
2 September - 13 September 2004	RV Southern Surveyor	SeaSoar	8	255	93.51	772,685
27 September – 11 October, 2006	RV Southern Surveyor	SeaSoar	9	1120	561.16	3,012,667
10 October – 20 October, 2008	RV Southern Surveyor	SeaSoar	5	383	166.55	820,573
2 –June – 18 June, 2015	RV Investigator	Triaxus	8	1033	551.46	1,774,319
30 August – 23 September 2016	RV Investigator	Triaxus	9	868	358.43	2,306,398
		TOTAL	39	3660	1731.11	8,686,642

2.3.3 Remotely Sensed Observations

Satellite data for the linear models were derived from a number of products. MODIS Level 3 sea surface temperature (SST_{sat}), and ocean-colour data (chlorophyll- a) (Chl_{sat}) were obtained from the Integrated Marine Observing System (IMOS) Data Portal (<http://imos.aodn.org.au/imos/>) at 1 km resolution. Chlorophyll- a was derived using the OC3 algorithm. MODIS data was retrieved for 5x5 pixels ($\sim 25 \text{ km}^2$) surrounding the centre of each sample, on the day of sampling. The chlorophyll- a concentration is measured by a daily satellite pass of the area and all data points are assigned the closest daily Chlorophyll- a value, to show an overall pattern of primary productivity in the area. Chlorophyll- a fluctuates through the day and night, but these small, short term fluctuations are negligible when compared to the longer timescale of zooplankton production. Satellite altimeter data, for sea-surface height anomaly (SLA_{sat}) were obtained from NASA/CNES (Jason-1 and 2) and ESA (ENVISAT) and mapped in near-real time for the Australian region. Bathymetry data was sourced from GEBCO (GEBCO 2018).

2.3.4 Zooplankton Size Spectra

For each sample, the zooplankton community were quantified from OPC particle size data using five metrics: Zooplankton Biomass (mg m^{-3}), Zooplankton Abundance (ind. m^{-3}), GMS (ESD; μm), and the $\text{NBSS}_{\text{slope}}$ and $\text{NBSS}_{\text{intercept}}$ of the NBSS. Biomass was calculated using the volume equation of a prolate spheroid (size ratio of 3:1) and a specific gravity of 1 (Moore and Suthers 2006). The summed biomass for each net tow was standardised by the processed volume.

In order to calculate the $\text{NBSS}_{\text{slope}}$, the particle-biomass data (between the sizes of 300 to 12000 μm ESD) from each deployment was binned into a series of logarithmically equal size intervals of 0.2 mg. This resulted in a total of 32 bins. This biomass size spectrum was then normalised by dividing the biomass of each bin by the width of the bin ($\text{mg m}^{-3}/\Delta \text{mg}$). The NBSS is independent of any specified body size interval allowing for comparison across different studies and systems (Sprules and Munawar 1986). The $\text{NBSS}_{\text{slope}}$ was derived by fitting a least-squares polynomial

regression to the NBSS (Krupica et al. 2012). The r^2 of the linear fit of NBSS_{slope} was used to define the linearity of the NBSS_{slope}, which is referred to as NBSS linearity. NBSS_{intercept} is the y-intercept of the NBSS_{slope}.

It is important to note that the data collected by the OPC does not distinguish between living zooplankton and debris, aggregates or zooplankton carcasses. Most detrital particles are smaller than the 300 µm lower size limit that is used in this study. Up to 30% of copepod nauplii may consist of carcasses (Elliott and Tang 2011) but these stages are also smaller than this studies lower size limit. However, the NBSS constructed from this data may still include some larger detrital or moribund zooplankton artefacts.

2.3.5 Determining watermasses

The study area was divided into watermasses defined by the satellite sea surface temperature, bathymetry and location (Fig. 2.2, Table 2.2) of the data points, following previous Tasman Sea work (Henschke et al. 2011; Mullaney and Suthers 2013). Shelf depth was defined to be less than 200 m, as this is the depth where the continental shelf transitions to the shelf break. Deeper than 200 m, the shelf drops steeply to 2000 m after which the deep ocean and shallow seafloor gradients limit mixing due to seafloor interactions and characterise the oceanic properties (seen) eastward of the 200 m isobath. The latitude north and south of 33°S was chosen to represent the Shelf-north and Shelf-south areas, as this is where separation of the EAC from the shelf occurs (Cetina-Heredia et al. 2014). Depths less than 200 m and located offshore ($>155^{\circ}$ E), such as offshore islands and seamounts, were grouped by their temperatures and classified as EAC, Mixed or Tasman, as continental inputs are assumed to be negligible.

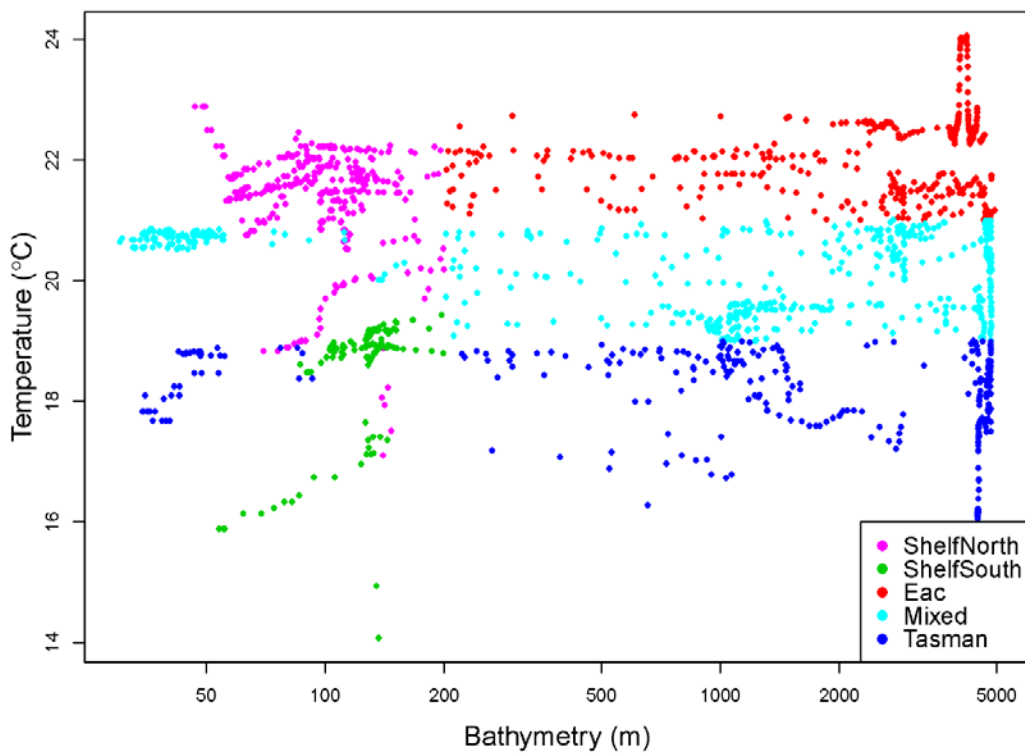


Figure 2.2 Plot of the data points as assigned to watermasses based on bathymetry, location and satellite temperature properties. Bathymetry is plotted on a \log_{10} scale. Shelf North, Shelf South, EAC (East Australian Current), Tasman and Mixed.

Table 2.2 Criteria used to define water masses

Watermass	Temperature (°C)	Water Depth (m)	Latitude	Longitude
Tasman	< 19	≥ 200	-	
		<200		>155°E
EAC	>21	≥ 200	-	
		<200		>155°E
Mixture	19 – 21	≥ 200	-	
		<200		>155°E
Shelf North	-	< 200	> -33°S	
Shelf South		< 200	$\leq -33^{\circ}\text{S}$	

2.3.6 Statistical Analysis

Analysis of Variance (ANOVA's) were performed to indicate significant differences between watermasses, of $\log_{10}(\text{biomass})$, abundance, GMS, NBSS_{slope}, and NBSS_{intercept}. Tukey post hoc testing was then performed to determine the level of significance in differences between each watermass.

I used linear models in R (R Core Team 2017) to assess the relationships between zooplankton size structure metrics ($\log_{10}\text{biomass}$, $\log_{10}\text{abundance}$, GMS, NBSS_{slope} and NBSS_{intercept}) and environmental variables. The explanatory environmental variables included in the original models were SST_{sat}, SLA_{sat}, water depth and Chl_{sat}. Chl_{sat} was right skewed, so it was \log_{10} transformed. Environmental variables were checked for co-linearity using pairplots. No variables were co-linear. Backward elimination stepwise regressions were performed and variables were retained in the models if they reduced the model AIC. Non-significant variables ($p>0.05$) were removed if doing so also further reduced the AIC of the models. The final linear models were checked for normality and homogeneity of variance using normal quantile plots and residual plots. Model coefficients were standardised using Package lm.beta (Behrendt 2014) and effects plots of model terms were produced using Package effects (Fox 2003) in R (R Core Team 2017).

2.4 Results

This study presents zooplankton data for 39 deployments of an OPC on a towed undulating vehicle in the western Tasman Sea. The OPC recorded the individual size of 8.7 million zooplankton sized particles along transects totalling 3661 km (Table 2.1). For all samples, the GMS ranged from 388 µm to 717 µm ESD and biomass ranged from 5.7 to 38 g m⁻³. The NBSS_{slope} ranged from -1.59 to -0.365. During sampling, the mean in-situ temperature (0 - 30 m) ranged from 15.3°C to 24.0°C and the salinity ranged from 35.40 to 35.78. Table 2.1 data includes both day and night tows and as such it incorporates the variability in zooplankton counts through the 24 hour period.

2.4.1 Water-mass specific differences

Each OPC profile was assigned to one of the 5 watermasses (EAC, Tasman Sea, Mixed and Continental Shelf North and South), using Temperature and Depth (Table 2.2). Significant differences were observed, using ANOVA, between watermasses (Fig. 2.3) for zooplankton abundance ($F_{4,1795} = 76.69$, $p < 0.001$), biomass ($F_{4,1795} = 124.6$, $p < 0.001$), GMS ($F_{4,1795} = 217.5$, $p < 0.001$), NBSS_{slope} ($F_{4,1795} = 101.4$, $p < 0.001$), NBSS_{intercept} ($F_{4,1795} = 140.8$, $p < 0.001$), and NBSS linearity ($F_{4,1795} = 44.91$, $p < 0.001$).

Compared to the EAC, the Tasman Sea had significantly higher mean zooplankton abundance (2884 ind. m⁻³, 6166 ind. m⁻³ respectively), higher mean biomass (244 mg m⁻³, 1318 mg m⁻³ respectively), larger mean GMS (441 µm, 525 µm respectively), shallower mean NBSS_{slope} (-0.985, -0.774 respectively) and higher mean NBSS_{intercept} (1.3, 2.00 respectively) (Fig. 2.3, Appendix A Table 1-5). In addition, the southern shelf had significantly higher zooplankton abundance, biomass, and GMS compared to the northern shelf, as well as a shallower NBSS_{slope} and higher NBSS_{intercept} (Fig. 2.3).

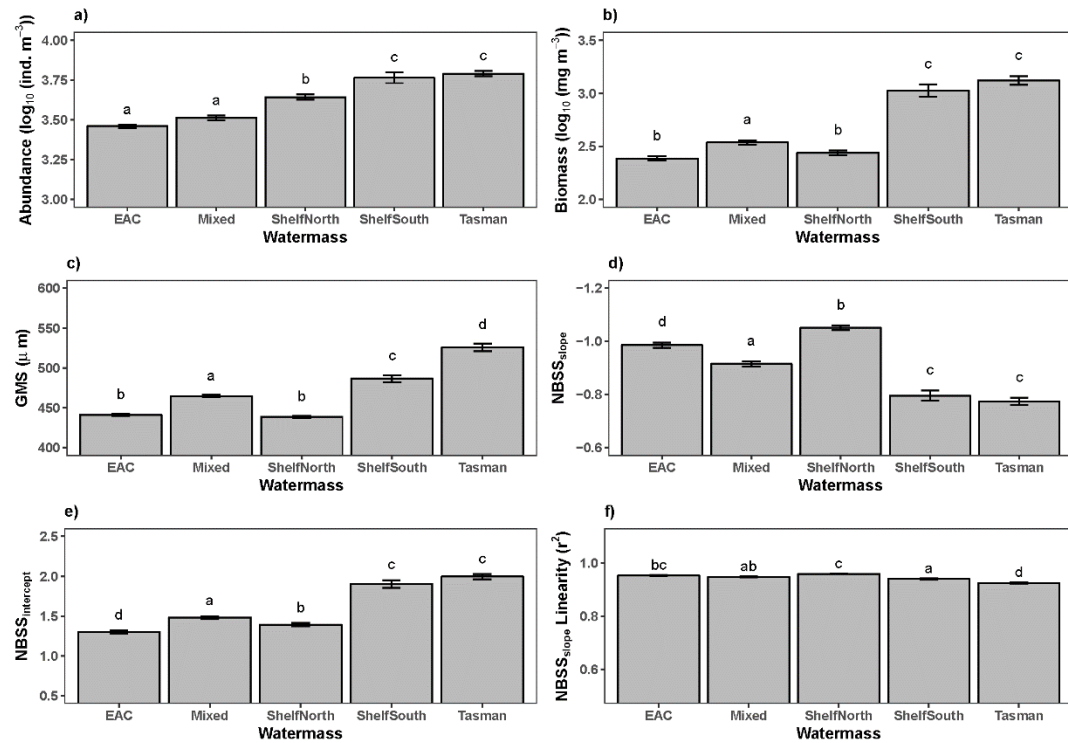


Figure 2.3 Bar plots comparing a) mean \log_{10} abundance b) \log_{10} biomass, c) geometric mean size (GMS) d) NBSS slope, e) NBSS intercept f) NBSS slope Linearity between watermasses. Error bars represent Standard Error. Matching letters on the bars represent no significant difference between corresponding water masses.

The NBSS slopes of the EAC and northern shelf are more linear, ($r^2 = 1.00$ and 0.99 respectively (Fig. 2.4)) and steeper (mean NBSS_{slope} = -0.985 and -1.05, respectively (Fig. 2.3)) than the NBSS_{slope} of the Tasman Sea ($r^2 = 0.96$ (Fig. 2.4), mean NBSS_{slope} = -0.774 (Fig. 2.3)) and southern shelf ($r^2 = 0.98$ (Fig. 2.4), mean NBSS_{slope} = -0.800; (Fig. 2.4)). The EAC and northern shelf NBSS_{slope} linearities are significantly different to the southern shelf and Tasman sea watermasses (Fig. 2.3 f). The southern watermasses (Tasman Sea and Shelf-South) show distinct doming (non-linearities) between 1 and 10 mg m^{-3} . (Fig. 2.4 B, E).

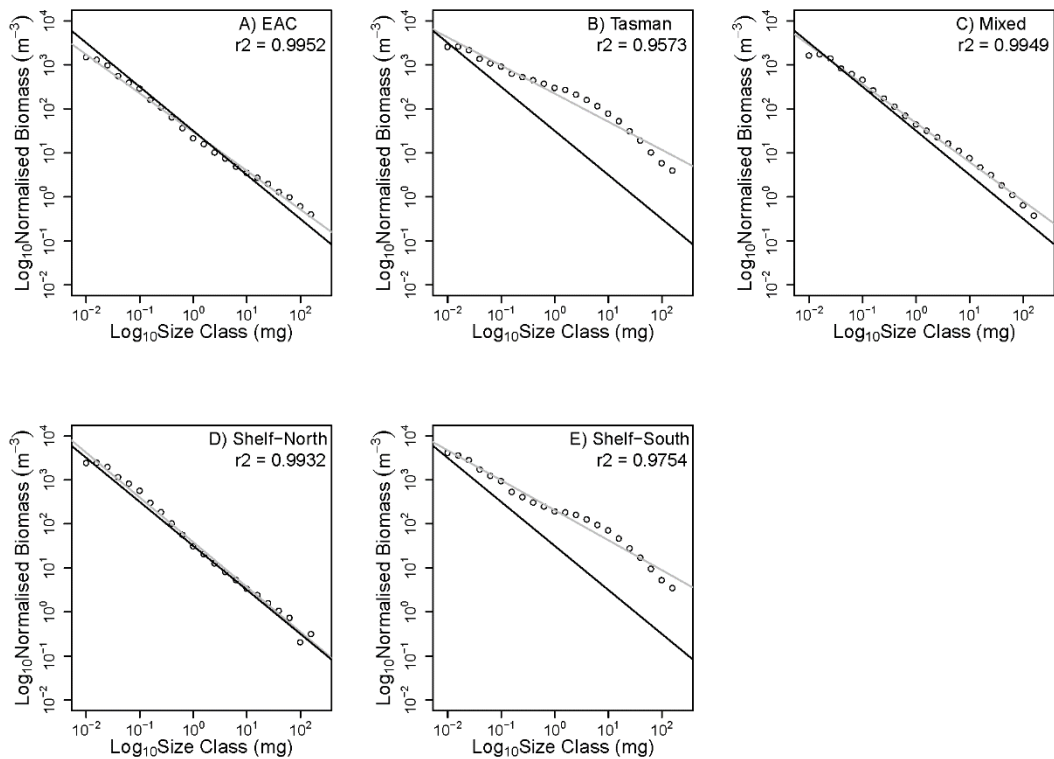


Figure 2.4 Normalised Biomass Size Spectra of the A) EAC, B) Tasman, C) Mixed, D) Shelf North, E) Shelf South. The black circles represent the normalised biomass in each size class. The grey line is the linear regression through the points, calculated using the average of biomass in each size class bin. The solid black line represents a fixed slope of -1 for comparison.

2.4.2 Environmental drivers of zooplankton size spectra

Given temperature's role in shaping Tasman Sea watermasses (Fig. 2.2) and the significant differences in response variables between watermasses, linear models were initially used to assess the response of each variable against SST_{sat}. Increasing temperature resulted in decreasing zooplankton abundance ($r^2 = 0.10$, $p < 0.001$), biomass ($r^2 = 0.21$, $p < 0.001$), GMS ($r^2 = 0.35$, $p < 0.001$) and NBSS_{intercept} ($r^2 = 0.24$, $p < 0.001$). NBSS_{slope} also became more negative as water temperature increases ($r^2 = 0.17$, $p < 0.001$; Appendix A Fig. 1).

Linear models containing additional satellite-derived covariates – SST_{sat} , Chl_{sat} , SLA_{sat} , with bathymetry – were subsequently developed. All the included covariates were significant and the final models explained between 18 and 46% of the variability (Table 2.3). SST_{sat} , Chl_{sat} and SLA_{sat} were significant in all models, while water-depth was significant in the models for abundance, GMS and $NBSS_{intercept}$. Chl_{sat} showed a positive relationship with all response variables (Table 2.3), indicating higher chlorophyll- a biomass drove increased abundance, biomass, GMS and a flatter (less negative) $NBSS_{slope}$. SST_{sat} and SLA_{sat} displayed a negative relationship with all response variables. Water-depth had a negative relationship with abundance and $NBSS_{intercept}$, but a positive relationship with GMS.

SST_{sat} has the greatest standardised coefficient value (-0.308 to -0.575) (negative relationships) for all models (Appendix A Table 8 - 12) except for abundance, in which SLA_{sat} has the greatest standardised coefficient value (-0.336), with SLA_{sat} and Chl_{sat} contributing in almost equal parts (standard coefficients of -0.336 and 0.330 respectively). Water Depth has the lowest standardised coefficient value for all models in which it was retained (-0.085 to 0.15). The relationships in this study are also driven by Chl_{sat} (standardised coefficient values of 0.075 to 0.330) (positive relationships), and SLA_{sat} (standardised coefficients of -0.106 to -0.336) (negative relationships), having the second highest standardised coefficient values for abundance, and biomass, GMS, $NBSS_{slope}$, and $NBSS_{intercept}$, respectively. See Appendix A, Fig. 3 - 7 and Table 8 - 12 for full model details.

Table 2.3 Coefficient values of the linear models. Significant coefficients are marked with asterisks ($P < 0.05$). Coefficients marked with a dot (.) were not included in the final model. See Appendix A Table 8 - 12 for full model results.

	Intercept	SST _{sat}	log ₁₀ Chl _{sat}	SLA _{sat}	WaterDepth	r ²
log₁₀(Biomass)	6.301*	-0.166*	0.685*	-0.866*	.	0.34
log₁₀(Abundance)	5.08*	-0.0612*	0.439*	-0.686*	-2.63x10 ⁻⁵ *	0.29
GMS	870.397*	-19.117*	49.486*	-50.477*	0.004	0.46
NBSS_{slope}	0.280*	-0.058*	0.070*	-0.151*	.	0.18
NBSS_{intercept}	5.043*	-0.158*	0.539*	-1.000*	-2.481x10 ⁻⁵ *	0.38

2.5 Discussion:

This study has revealed how the size-distribution of the zooplankton community changes between distinctive water-masses off eastern Australia and, for the first time, along a continuum of oceanographic variables. Water-masses are evident in the climatology of the western Tasman Sea, with seasonal northern and southern regimes either side of the Tasman Front driven by temperature, salinity, mixed-layer depth and nutrients (Baird et al. 2008; Everett et al. 2014). Analysing the Tasman Sea zooplankton communities, defined by the temperature and bathymetry characteristic of these water-masses, also revealed two significantly different size-based planktonic ecosystems. The warmer water-mass had less zooplankton biomass, steeper slopes and smaller GMS associated with the East Australian Current and Coral Sea (higher SST_{sat}). The colder water-mass had greater biomass, shallower slopes and larger GMS associated with the Tasman Sea (lower SST_{sat}). A third water mass is usually evident in the region – shelf water (Cresswell 1994; Henschke et al. 2011) – but in this study, differences in the zooplankton size spectra were not evident in the northern or southern shelf waters, most likely due to the influence of the surrounding offshore watermasses.

2.5.1 Zooplankton Biomass and Abundance in the western Tasman Sea

Zooplankton showed a 5-fold increase in biomass between the EAC (244 mg m^{-3}) and the more eutrophic Tasman Sea waters (1318 mg m^{-3} ; Figure 2.3b), and a doubling in abundance (3136 ind. m^{-3} to 7457 ind. m^{-3}). These results suggest a greater standing-stock of prey to support communities of planktivores such as forage fish in the cooler Tasman Sea, compared to the EAC waters. The greater nutrient concentrations and phytoplankton biomass in the Tasman Sea (Everett et al. 2014) support a higher biomass of zooplankton, as well as larger mean zooplankton size. Conversely, the warmer EAC and Coral Sea waters, which have lower nutrient concentrations and phytoplankton biomass have significantly lower zooplankton biomass and a smaller mean size of zooplankton. Similarly to the results presented here, in the subtropical North Pacific, the highest zooplankton biovolume and abundance ($126.1 \pm 70.1 \text{ mm}^3$

m^{-3} and $379.9 \pm 34.7 \text{ ind.m}^{-3}$ respectively) were linked to regions of high primary productivity and upwelling (Dai et al. 2016). The lowest biovolume and abundance ($12.0 \pm 4.6 \text{ mm}^3 \text{ m}^{-3}$ and $58.7 \pm 20.4 \text{ ind. m}^{-3}$ respectively) of zooplankton were observed in the regions with lowest primary production and chlorophyll-*a*, as is consistent with the positive relationships between zooplankton size metrics and Chl_{sat} in this study.

The abundance of particles in the ocean declines exponentially with size, and therefore particle abundance has to be made in the context of a size range. Our results lie within the abundances seen in other studies when the particle size ranges are considered. LOPC abundances in differing habitats and in the size range of 350 – 2000 μm are between 453 particles. m^{-3} to 44544 particles. m^{-3} (Espinasse et al. 2018), and in another study the OPC recorded abundances of 16.8 to 1076 ind. m^{-3} for 500–5000 μm , (Sato et al. 2015).

It was expected that the Tasman Sea and EAC watermasses would host different communities of zooplankton due to the differences in physio-chemical properties (Suthers et al. 2011; Everett et al. 2014). Surprisingly however, there was no significant difference in zooplankton biomass between the northern shelf and the EAC, nor the southern shelf and Tasman Sea. It was expected that the upwelling of nutrient-rich water and higher chlorophyll-*a* biomass on the shelf relative to offshore (Young et al. 1996; Everett et al. 2014; Vandromme et al. 2014), would have resulted in a higher biomass of zooplankton. It is likely however, that the degree of mixing between the shelf and offshore due to wind, currents and eddies (Everett et al. 2012; Schaeffer et al. 2013; Wood 2014), occurs at a timescale which is shorter than the response (generation) time of zooplankton.

For my analysis, there are no concurrent net samples to be able to analyse for agreement between net and LOPC samples or classify the environment (ie high density of primary producers or gelatinous zooplankton). Zooscan is not a perfect method either – net samples suffer extrusion or avoidance and will not sample the aggregates noted above.

Perhaps an assessment of the *in situ* Chlorophyll-*a* levels and analysis of Attenuance Index and %Multiple Element Particles's (Schultes and Lopes 2009; Espinasse et al. 2018) from the LOPC data could help suggest where data samples may not be accurate due to contamination of the LOPC data with high concentrations of detritus. My analysis however is more concerned with assessing zooplankton biomass and NBSS between different regions/ecosystems. Due to the limits in comparing the data obtained by two different sampling methods it is recommended for consistency that interregional comparisons be made using data sourced by one method only (Schultes and Lopes 2009).

2.5.2 Zooplankton size-spectra and its implications for trophic ecology

Zooplankton communities are strongly size-structured (Barton et al. 2013). Size determines the predator – prey dynamics of zooplankton, and many vital rates such as growth, fecundity, and metabolism (Kiørboe and Hirst 2008). The GMS of the zooplankton community increased by ~20% between the EAC (~445 µm) and the Tasman Sea (~525 µm; Figure 3d) and the NBSS_{slope} was significantly steeper in the EAC (~-1.0) compared to the Tasman Sea (~-0.8). Globally, these results agree with previous studies which have shown that the average zooplankton body size decrease and slopes steepen in the oligotrophic gyres and convergence zones, relative to the higher latitudes (San Martin et al. 2006). Steeper slopes may occur initially in environments with intermittent bursts of productivity such as estuaries (Moore and Suthers 2006) or upwelling zones (Piontkovski et al. 1995) as small herbivorous zooplankton proliferate, but the slope generally flattens as the energy is transferred to larger size classes and productivity of the lower trophic levels returns to the baseline.

The NBSS_{slope} can be used to determine the energy transfer efficiency through the size spectrum. Steeper slopes, such as we observed in the EAC, indicate a higher loss of energy and the inability for the energy to transfer to larger size classes (Blanchard et

al. 2009). This is due to the insufficient availability of food to both replace metabolic expenses and support the growth rates required to replace losses due to mortality (Blanchard et al. 2009), with the increased temperature increasing the energy required to maintain the metabolic costs. Alternatively, a shallower slope is indicative of a more efficient flow of energy to higher size classes (Trudnowska et al. 2014; Vandromme et al. 2014).

Zooplankton can have multiple feeding strategies, but when primary production is low, such as in the EAC or other oligotrophic regions, carnivory is usually the dominant strategy (Clark et al. 2001; Henschke et al. 2015). Therefore smaller predator prey mass ratios (PPMR) and longer food chains with more trophic levels are characteristic (Jennings and Warr 2003). The addition of thermodynamic losses associated with feeding and digesting food at each of the trophic steps in these longer food chains results in an overall greater energy loss (Atkinson and Sibly 1997). In contrast, more productive regions such as the Tasman Sea, are characterised by flatter slopes, larger PPMR and shorter food chains. The reduction in trophic steps may reduce the combined energy losses that result at each step (Barnes et al. 2010; Heneghan et al. 2016), therefore increasing energy transfer efficiency in the form of a higher proportion of energy and biomass available to support the larger zooplankton size classes.

Recent studies have shown the importance of defining zooplankton when modelling energy flow through food chains. Increased herbivorous feeding strategies result in flatter zooplankton slopes and unstable ecosystems, with the shorter, more efficient food chains resulting in greater fish community abundance, productivity and resilience (Heneghan et al. 2016). The flatter slopes of the Tasman Sea are likely a result of adequate food resource availability, allowing metabolic replacement, plus growth into larger size classes (Guillet et al. 2016). We can speculate that the Tasman Sea, with increased productivity and flatter slopes, is less stable but more resilient with a greater PPMR. Conversely, smaller PPMR and longer food chain length of generalist carnivorous strategies sets up a stable system, but have a low energy transfer rate, as is reflected in the warm, oligotrophic, stable EAC environment.

The zooplankton biomass, abundance and size spectra in this study exhibited strong links with environmental variables (Table 2.3; Fig. 2 A 5-9). The negative relationships of temperature with zooplankton biomass, abundance, GMS and size spectra found in this study is in accordance with other studies finding temperature to be consistently important in the prediction of zooplankton biomass (Woodd-Walker et al. 2001) and having a negative relationship (Pretorius et al. 2016). Steeper NBSS_{slope} (Baird et al. 2008) and lower zooplankton biomass associated with low chlorophyll-*a* (Woodd-Walker et al. 2001) are a result of a positive relationship of chlorophyll-*a* with zooplankton biomass (Pretorius et al. 2016). This is consistent to the findings of a positive relationship of Chl_{sat} with all zooplankton size metrics in the Tasman Sea. Enrichment of zooplankton biomass at cyclonic eddy centres, as is evident in this study by the negative relationship between SLA_{sat} and Tasman Sea zooplankton size metrics, has been shown in other studies, but the relationship is more variable as high biomasses can also be associated with anticyclonic eddies (Labat et al. 2009). Size structure has previously been observed to change on a coastal to offshore gradient, from steep slopes in the coastal zone, to flatter slopes on the continental shelf and higher abundances on the shelf break (Vandromme et al. 2014; Albaina & Irigoien 2004), but here bathymetry was only significant in some models and showed a relatively poor fit (Appendix A Fig. 8-12). However, shelf and offshore zooplankton size structure may fluctuate seasonally with seasonal changes in the presence of upwelling cells and watermass locations (Pretorius et al. 2016), therefore marring clear trends.

The models explained 18 to 46 % of the variability, showing some models have promising results but there remains considerable uncertainty. A linear trend is adopted for this study so that the relationship can be applied to variable oceanic environments.

Zooplankton are subject to environmental variables beyond the variables included in the linear model analyses. The satellite variables used in this study are easy to obtain for widespread areas and so the relationships are able to be applied to, or compared

with, other areas and time periods. Other variables that are not readily or accurately available through remote sensing methods, such as salinity (Karlsson 2018, Uriarte 2006), recruitment of individuals into an area rich in productivity (Basedow 2014) can affect the community size structure. The incorporation of chlorophyll-*a* as the food source is simplistic, as zooplankton can acquire their energy requirements from other pathways such as from the detrital foodweb. Additionally, incorporating a time series of the persistence period of chlorophyll-*a* prior to the model date could provide additional information on the level of growth that has previously occurred in the zooplankton community. Growth rates of zooplankton are species specific as food source varies with species, affecting assimilation efficiency. This level of detail is dismissed in a size based model which simplifies growth rate to being a function of size. Predation and fishing in the area are unaccounted for in the model. Fishing has a top down effect, removing large individuals with flow on effects through the food web.

These variables have all been shown to influence zooplankton community size characteristics, yet are unaccounted for in the models. *In situ* temperature/salinity profiles, CTD casts and analysis of net samples and further subsetting of oceanic environments or regions into different models could provide additional variables to improve model prediction.

The model outputs point to temperature's importance in driving zooplankton size metrics, however the other environmental variables make notable contributions to the models. This shows the increased potential of using linear models with multiple environmental variables over temperature alone in the prediction of zooplankton community size structure. The zooplankton size spectra presented here varied in similar ways to phytoplankton size spectra along an environmental continuum (Barnes et al. 2011). Interestingly however, the magnitude of the response was larger for zooplankton. The change in slope of the size spectra in response to temperature was much greater for zooplankton (steepened by 0.6 between 16 and 24 °C), compared to phytoplankton (steepened by 0.2 between 16 and 24 °C; Figure 3a in Barnes et al. 2011). Understanding how the phytoplankton and zooplankton size-

spectra vary, both independently with environmental variables (as in this study and Barnes et al. 2011) is important, but so is quantifying how they co-vary at the same location. Due to the technical considerations of the range of instruments required, phytoplankton and zooplankton size-spectra are rarely measured simultaneously, with some exceptions (e.g. García-Muñoz et al. 2014). Understanding how the size-spectra of zooplankton changes with environmental conditions, including how it covaries with the phytoplankton size-spectra, will help to bridge the gap to understanding the global fish biomass and size structure. Fish community size spectra are less sensitive to environment predictors (Guillet et al. 2016), and given it is strongly mediated by the size-distribution of plankton (Heneghan et al. 2016), we expect that increasing our understanding of how the zooplankton size-spectra varies across time and space will greatly improve estimates of global fisheries biomass.

2.5.3 Non-linearity in the NBSS in the western Tasman Sea.

Linearity, or the coefficient of determination (r^2), of the $\text{NBSS}_{\text{slope}}$ is an indicator of the stability and productivity of an ecosystem (Suthers et al. 2006). In stable watermasses, such as pelagic or offshore environments, linear slopes fitted to the NBSS have greater r^2 values indicating less variation around the linear fit of the $\text{NBSS}_{\text{slope}}$. Less stable environments such as inland lakes have greater secondary structuring around the linear $\text{NBSS}_{\text{slope}}$, therefore lowering the r^2 value of the linear fit (Sprules and Barth 2016). Fluxes of energy through the spectrum are mediated by the growth and respiration rates (Boudreau and Dickie 1992) of individuals in the spectrum, which in turn shape the biomass spectrum slope (Basedow et al. 2010). Pulses of primary production result in peaks, or domes, being present along the size continuum, representing the wave of the energy from primary production blooms, passing successively as biomass through the size classes (Silvert and Platt 1978). These dome features are characteristic of productive ecosystems with greater influence of oceanographic variability (García-Muñoz et al. 2014).

In stable, oligotrophic water masses the $\text{NBSS}_{\text{slope}}$ has a positive relationship with NBSS linearity (García-Comas et al. 2014; García-Muñoz et al. 2014), as a result of

steady nutrient concentrations over time, and spreading of biomass evenly through the size bins at close to steady state (García-Muñoz et al. 2014). The EAC and the adjacent shelf have the highest linearity (EAC: $r^2=1.00$, SE=0.08; Shelf-North: $r^2=0.99$, SE=0.11) (Fig. 2.3) and are not significantly different (Fig. 2.4) which reflects the stable, oligotrophic conditions of the water mass and the limited seasonality in tropical phytoplankton dynamics off Australia (Everett et al. 2015). By contrast, the southern shelf ($r^2 = 0.98$, SE = 0.1403) and Tasman Sea ($r^2 = 0.96$, SE=0.175) demonstrate increased non-linearity and are not significantly different (Fig. 2.4). However, the EAC and Tasman sea exhibit a significant difference in NBSS_{slope} linearity (Fig. 2.4). This indicates the difference between the two water masses, with the southern shelf and Tasman sea being dynamic water masses, the shelf experiencing frequent upwelling of nutrient rich waters and the Tasman sea being subject to a shallower mixed layer depth and an eddy field propagating southward of the separation zone.

2.5.4 Concluding remarks

This study has given us insights into the utility of using remotely sensed variables to predict the size structure of zooplankton communities at a high resolution. Previous work has highlighted the benefit of using environmental variables to predict phytoplankton community size structures (Barnes et al. 2011) and manage different ocean habitats dynamically over large spatial and temporal scales (Hobday et al. 2011). As the size structure of the zooplankton community will mediate the energy transfer to higher trophic levels, applying the relationships developed here over large spatial scales will inform prey fields and likely distributions of fish communities.

Chapter 3 : Spatial and temporal patterns of springtime zooplankton biomass and size in the Tasman Sea

3.1 Abstract

Zooplankton provides the trophic link between phytoplankton and fisheries. The spatial and temporal distribution of zooplankton in the ocean will therefore control the distributions of prey fish and fisheries. Using linear models derived from relationships of satellite observations and bathymetry with zooplankton size-structure data collected by an Optical Plankton Counter (OPC), various metrics of the size spectrum were modelled using bathymetry and the 2003 - 2016 springtime averages of satellite observations of sea surface temperature (SST_{sat}), chlorophyll- α (Chl_{sat}) and sea level anomaly (SLA_{sat}), in the western Tasman Sea. Springtime zooplankton abundance, biomass and Geometric Mean Size (GMS) increased in a poleward direction, both on and off the shelf. The open ocean exhibited greater variability than the shelf. Springtime zooplankton size parameters and distribution varied spatially and annually, significantly altering the total productivity within the study area for most spring seasons. Model output was then compared to in-situ observations from the Continuous Plankton Recorder (CPR), collected independently during the periods which zooplankton were modelled. Model output abundance was significantly correlated with CPR abundance (Pearson's correlation coefficient $r = 0.34$). Overall the findings show that zooplankton size parameters can be modelled using satellite variables, as a guide to real-time zooplankton distribution, however more extensive model assessment is required to determine their accuracy. These results are of significance to dynamic ocean management and the modelling of inter-annual potential fish productivity of the western Tasman Sea.

3.2 Introduction

The Tasman Sea is a global hotspot of climate change due to a strengthening of the East Australian Current (EAC), and increased EAC transport to more southerly locations (Wu et al. 2012). In addition, the point of separation of the EAC from the coast is moving further south (Cetina-Heredia et al. 2014). The consequences of this are warmer sea surface temperatures, altered nutrient regimes, different assemblages of phytoplankton and reduced primary production during spring in southerly areas previously occupied by the Tasman Sea (Thompson et al. 2008). Climate shifts are causing southward extension and overwintering of warm water marine species (Johnson et al. 2011), but little is known about changes in zooplankton.

The monitoring of inter-annual fluctuations of zooplankton as the trophic link between phytoplankton and fish allows a mechanistic means of estimating the fish productivity and distribution in the oceans. We need to be able to map *in situ* zooplankton biomass in real-time, to monitor distribution changes in zooplankton communities over the past and as they are currently occurring. Knowledge of the spatial and temporal distribution of zooplankton in the Tasman Sea is important because the patterns can indicate potential fish abundance of an area, changes in distribution and productivity patterns over time with physical phenomenon such as climate change, and be used for management purposes such as setting fishery quotas (Hobday and Hartog 2014).

The distribution of zooplankton production can indicate where certain species of interest, for protection or targeted fishing purposes, may congregate to exploit zooplankton production hotspots. In turn, the seascape provides real time guidance for managing resources such as southern bluefin tuna and yellowfin tuna which migrate, or are attracted to these locations, to feed on planktivores (Young et al. 1996, 2001). This approach, known as Dynamic Ocean Management (DOM), moves away from the traditional fixed representations of marine habitats (Payet 2006; Blanchard et al. 2012), to better represent the dynamic marine environment, which experiences annual and seasonal variations as well as shifting locations of watermasses with climate change. In the Tasman Sea, analyses have defined the distribution of eddies (Everett et al. 2012), the fluctuations of the East Australian Current (Cetina-Heredia et al. 2014), phytoplankton patterns (Everett et al. 2014) and seasonal fish distribution, which are relevant to the fisheries industry (Hobday and Hartmann 2006). However, there has been much less effort given to determining the distribution of zooplankton (Everett et al. 2017). This is surprising as zooplankton are the trophic link between phytoplankton and fisheries (Stock et al. 2017). Furthermore, many models that attempt to map fish abundance and distribution use phytoplankton (or a proxy - chlorophyll-a) (Blanchard et al. 2017; Everett et al. 2017) and generally have a positive relationship with fisheries (Friedland et al. 2012). Phytoplankton are a trophic level away from fish, and are therefore a less reliable indicator of fish production (Heath 2012) as it discounts the variations in energy transfer through the zooplankton trophic link, which is modified by different zooplankton food web structures and energy transfer efficiencies (Stock et al. 2017). These variations are modified by environmental process (García-Muñoz et al. 2014; Guiet et al. 2016). Zooplankton community size structure is a useful proxy for energy transfer (Sprules and Barth 2016) yet has never been modelled and mapped spatially using satellite environmental data to explore this link.

In this chapter I map zooplankton community size structure by using statistical models constructed from satellite data, with zooplankton community size structure estimated using Optical Plankton Counter (OPC) data in the zooplankton size range, to assess whether annual changes in zooplankton temporal and spatial distribution have occurred during the period of satellite data availability (2003 to 2016). We then test the model outputs using *in situ* CPR data that are available over the same time frame, from 2009 to 2016, to assess the *in situ* viability of the measurements.

Specifically, the aims of this study are to:

- 1) Quantify the spatial and temporal patterns of zooplankton biomass and size in the Tasman Sea; and
- 2) Assess the spatial and temporal model outputs of zooplankton abundance using the continuous plankton recorder (CPR) data sets.

The OPC data used in the study was collected from the upper 30 m of water (the upper mixed layer) and satellites also observe the upper mixed layer - either the ocean skin (SST) or upper few metres. The Tasman typically has a mixed layer depth of 80 – 120 m and the EAC of 25 – 50 m (Baird et al. 2008; Suthers et al. 2011).

Therefore only the upper 30 m of OPC data were used so as to avoid the Deep Chlorophyll Maxima (DCM) zooplankton communities, as these layers are not captured by satellite ocean colour observations (Blondeau-patissier et al. 2014).

The sampling method of the CPR differs to the LOPC and each method results in its own unique bias of the data. A direct comparison is likely to yield quite different abundance measurements between the two. Therefore the assessment is to compare the patterns of relative abundance over different areas and seasons as individually measured by each method.

The results indicate that spatial models of zooplankton distribution, have the potential to become powerful tools in the assessment of real-time zooplankton (and fisheries) production in the Tasman Sea.

3.3 Methods

3.3.1 Study region

The study area spanned from 27.75 – 36.25° S, and 149 – 159 °E in the western Tasman Sea off eastern Australia (Fig. 2.1). The major water masses included the Tasman Sea water mass in the southern and offshore study site areas; the East Australian Current (EAC) in the north, flowing southward along the continental shelf; and the EAC separation zone occurring at approximately 31°S (Cetina-Heredia et al. 2014). The warm oligotrophic EAC water mass originates in the Coral Sea and supports a zooplankton community that is distinct from the zooplankton community in the cooler, eutrophic Tasman Sea (Baird et al. 2008).

3.3.2 Data collection and model development

The data collection and linear model development (Chapter 2) is outlined briefly below. Particle size data in the zooplankton size range (300 to 12000 µm) was collected using an Optical Plankton Counter (OPC) mounted on a modified SeaSoar (2004, 2006, 2008) and a Laser Optical Plankton Counter (LOPC) mounted on a Triaxus (2015, 2016). Coincident measurements of salinity, temperature, depth, flow, longitude and latitude were recorded using a Seabird CTD mounted on the SeaSoar and Triaxus. A total of 39 deployments were made on voyages between 2004 and 2016, measuring a total of 3661 km and sampling 1731 m³ of water (Table 3.1). Each deployment (Fig. 3.1) consisted of a number of undulations between the surface and 120 m (SeaSoar) or 200 m (Triaxus).

Satellite data for the linear models were derived from a number of products. MODIS Level 3 sea surface temperature (SST_{sat}), and ocean-colour data (chlorophyll-*a*, Chl_{sat}) was obtained from the Moderate Resolution Imaging Spectroradiometer Aqua Satellite (MODIS-Aqua; V2016.4.3; OC3 4 km L3) at 4 km resolution. Chl_{sat} was derived using the OC3 algorithm. MODIS data was retrieved for 5x5 pixels (~25 km²) surrounding the centre of each sample, on the day of sampling. Satellite altimeter data for sea-surface height anomaly (SLA_{sat}) were obtained from the IMOS Data Portal

for the same spatial area as the SST_{sat} and Chl_{sat} data. Bathymetry data was sourced from GEBCO (GEBCO 2018).

Size spectra metrics of zooplankton abundance, biomass, GMS, normalised biomass size spectrum (NBSS) slope ($NBSS_{slope}$) and NBSS intercept ($NBSS_{intercept}$) were calculated from the OPC/LOPC data (Section 2.2). Backward stepwise regression was performed to identify which of the explanatory variables, from SST_{sat} , Chl_{sat} , SLA_{sat} and bathymetry (Section 2.2), were significant for each size metric (Table 3.1). The linear models were derived from the size and abundance of zooplankton sized particles at 5 - 30m depths in the years 2004, 2006, 2008, 2015 and 2016, during springtime in the western Tasman Sea (Section 2.2). Biomass was used and $NBSS_{intercept}$ was excluded for analyses here, as the $NBSS_{intercept}$ metric is highly correlated with biomass density (Boudreau and Dickie 1992).

Table 3.1 Linear Model coefficient values. Significant coefficients are marked with asterisks ($P < 0.05$). Coefficients marked with a dot (.) were not included in the final model.

	Intercept	SST_{sat}	$\log_{10}Chl_{sat}$	SLA_{sat}	WaterDepth	r^2
$\log_{10}(Biomass)$	6.30*	-0.166*	0.685*	-0.866*	.	0.34
$\log_{10}(Abundance)$	5.08*	-0.0612*	0.439*	-0.686*	$-2.63 \times 10^{-5}*.$	0.29
GMS	870*	-19.1*	49.5*	-50.5*	0.004	0.46
$NBSS_{slope}$	0.280*	-0.058*	0.070*	-0.151*	.	0.18

3.3.3 Data analysis

The satellite SST_{sat} , SLA_{sat} and Chl_{sat} data averages from September/October/November of 2003-2016 were used to generate climatology figures for the study area (Fig. 3.1). The linear model relationships were applied to monthly composite data from Sept/Oct/Nov, of the satellite variables of SST_{sat} , Chl_{sat} and SLA_{sat} , with the inclusion of bathymetry for abundance and GMS. The zooplankton abundance, biomass, GMS and $NBSS_{slope}$, estimated using the (L)OPC

particle size and abundance data, were mapped for spring (Sept - Nov) using satellite variables data from 2003 to 2016 and bathymetry. Mapped yearly anomalies were also generated for the same variables from 2003 to 2016 (Appendix B Fig. 1-4).

In order to assess the difference in the zooplankton community between the shelf and offshore regions, the study area was stratified into two regions, 0-200 m depth and 1000-4000 m respectively (ignoring the slope 200-1000 m). The shelf and offshelf areas were latitudinally divided into bands of 0.5°, with the displayed latitude being central in the band (i.e. 31°S calculated from 30.75-31.25 °S). The means and standard errors of abundance, biomass, GMS, and NBSS_{slope} were determined by averaging the pixels within each latitudinal band for each annual springtime model output.

To assess the coefficient of variation, a north to south section of the offshore region was subset in order to represent the range of offshore zooplankton environments but with a similar number of data points to the shelf region.

The significance of differences in the yearly means of abundance, biomass, GMS and NBSS_{slope} were tested with a one-way Analysis of Variance (ANOVA), with post-hoc Tukey tests, performed in R version 3.4.0 (R Core Team 2017) (Fig. 3.3, Table 3.3). The abundance, biomass, GMS and NBSS_{slope} in the Tasman Sea and Coral Sea regions (determined from the maritime boundaries (Marineregions.org 2016)) were calculated by averaging the pixels within each sea boundary for the spring season of each year from 2003 to 2016.

Net collections were not available for evaluation of the living and dead particles as counted by the OPC. CPR abundance data was available for the region and has been used as the next best assessment of the OPC derived model output. However due to sampling errors encountered to different degrees in all sampling gear, it is difficult to compare data sets collected by OPC and other collection methods such as nets, Zooscan and CPR due to net extrusion, gear avoidance and damage to fragile particles and taxa. It is recommended for consistency that only one type of sampling device be used when making interregional comparisons (Schultes and Lopes 2009).

3.3.4 Model assessment

The modelled zooplankton distribution was compared to in-situ observations of zooplankton abundance. Archived Continuous Plankton Recorder (CPR) data was retrieved from the Australian Ocean Data Network (Australian Ocean Data Network 2016). The CPR is towed behind commercial ships of opportunity at 7 m depth and the frequency of sampling is dependent on shipping schedules. The CPR channels water samples through a square 1.25 cm entrance and onto a filtering 200 µm silk mesh, which is wound across the sampling tunnel (Warner and Hays 1994). A second silk is rolled onto the filtering mesh to cover and hold the captured plankton in place, and the combined mesh are wound onto a storage drum. This is later removed for lab processing of the samples for abundance and taxonomic information. CPR zooplankton abundance data, for the months September – November, were available in the study area in the years of 2009, 2010, 2012, 2014, 2015 and 2016.

To assess the correspondence between CPR abundance measurements and the model abundance outputs as input with the satellite and bathymetry data for the corresponding date and co-ordinates, linear regression was performed in R version 3.4.0 (R Core Team 2017). Pearson's correlation coefficient was also used to compare the CPR abundance (ind. m⁻³) with the modelled abundance, by aligning model results with co-ordinates and dates of CPR data points, calculated using the satellite data corresponding with the same location and date (Fig. 3.8).

3.4 Results

3.4.1 Temporal and spatial variability in zooplankton distribution

The mean climatology (Fig. 3.1) shows warmer sea surface temperatures in the north of the study area, with the highest temperatures located along the northern section of coastline and stretching southward along the coastline (Fig. 3.1A). Chl_{sat} is highest in the south of the region, grading to lower levels with northward progression (Fig. 3.1B). Sea level anomaly (SLA_{sat}) generally shows a pattern of heightened SLA_{sat} near to the coastline as well as in the southern region of the study area (Fig. 3.1C). The centre of the study area shows a negative SLA_{sat}. Interannual differences in springtime SST_{sat}, Chl_{sat} and SLA_{sat} distribution are apparent but SST_{sat} and Chl_{sat} follow the same north to south trend (Appendix B Fig.'s 5 – 7). The bathymetry is shallow nearest to the coast with depths less than 200m, then steeply drops off along the continental shelf break to an area of depths of 1000 - 5000 m with offshore islands and seamounts (Fig. 3.1D).

There is trend of a latitudinal increase in mean abundance, mean biomass, mean GMS, and mean NBSS slope (NBSS_{slope}), both in the shelf and offshelf areas (Fig. 3.2). The offshelf area has a higher coefficient of variation (CoV) than the shelf area (Fig. 3.3), for mean abundance, biomass, GMS and NBSS_{slope}.

Mean abundance significantly decreased over the study period from 2003 to 2016 ($r^2 = 0.46$, $p < 0.005$) (Table 3.2, Fig. 3.4a). Mean biomass significantly decreased over the study period ($r^2 = 0.38$, $p < 0.005$) (Table 3.2, Fig. 3.4b), as well as GMS ($r^2 = 0.36$, $p < 0.05$) (Table 3.2, Fig. 3.4c). NBSS_{slope} became steeper (more negative) over the study period ($r^2 = 0.34$, $p < 0.017$) (Table 3.2, Fig. 3.4d).

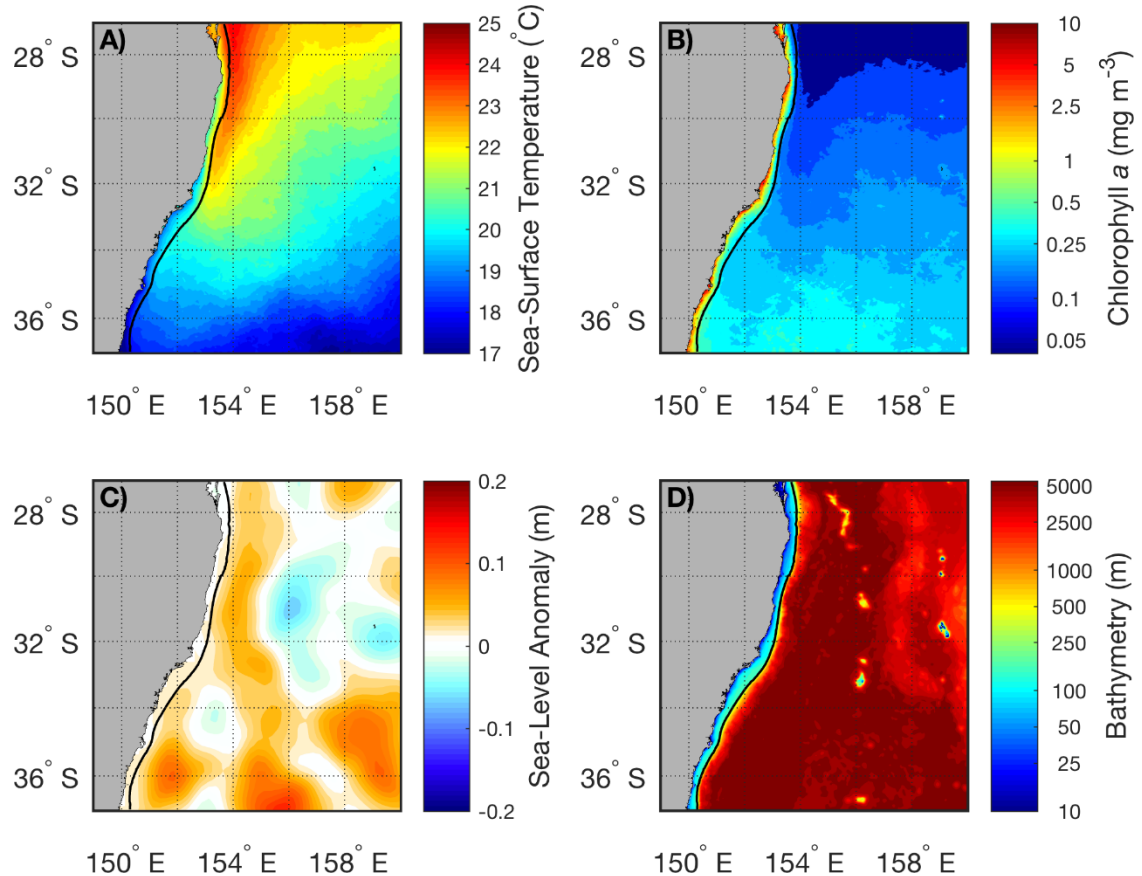


Figure 3.1 Mean A) sea surface temperature (°C), B) Chlorophyll- α (mg m^{-3}), C) sea level anomaly (m), D) bathymetry (m) of the study area. Data averaged from springtime averages from 2003 - 2016

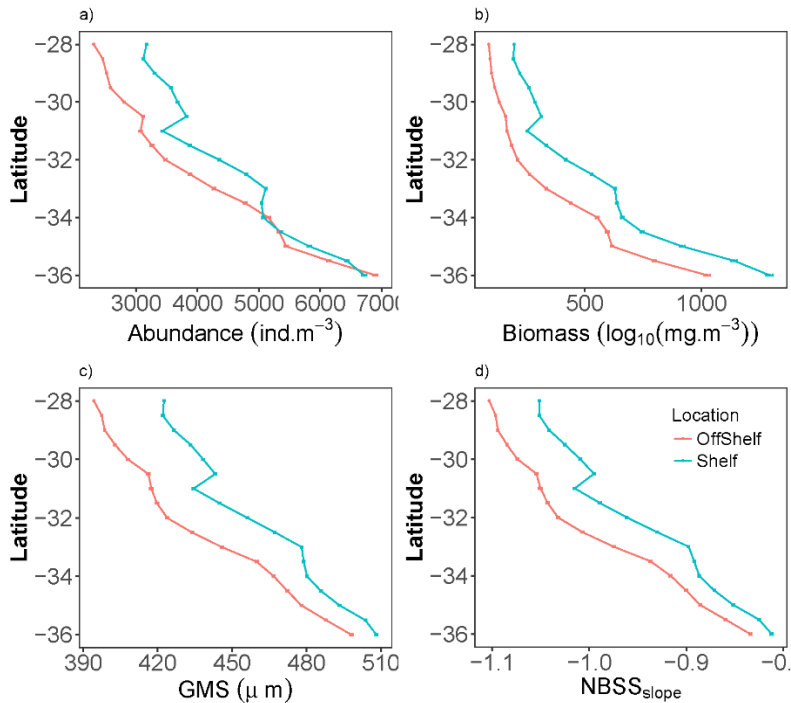


Figure 3.2 Springtime continental shelf (<200 m, blue) and offshelf (>1000 m depth, red) mean zooplankton a) Abundance (ind.m^{-3}), b) Biomass ($\log_{10}(\text{mg.m}^{-3})$), c) GMS (μm) and d) NBSS_{slope}, from 2003 to 2016, with standard error bars.

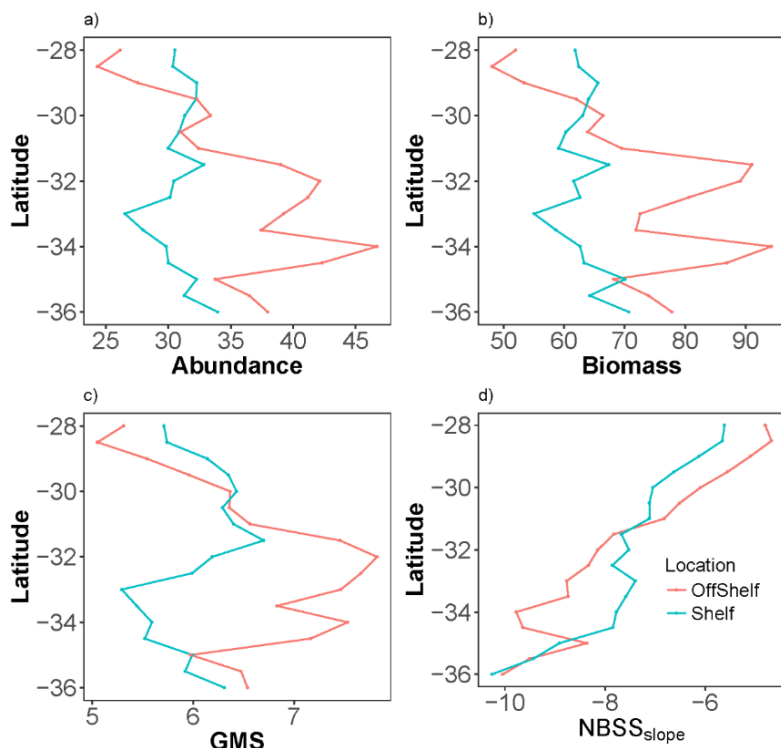


Figure 3.3 Coefficient of variation of a) Abundance, b) Biomass c) GMS and d) NBSS_{slope} on <200 m, blue) and off the shelf (>1000 m depth, red), from -28 °S to -36 °S.

Table 3.2 Coefficient values for linear models of zooplankton abundance, biomass, GMS and NBSS_{slope} of the study period over the years 2003-2016. Significant coefficients are marked with asterisks ($P < 0.05$) (*).

	Intercept	Year	r^2
Mean log₁₀(Abundance)	19.16*	-0.00772*	0.456
Mean log₁₀(Biomass)	29.22*	-0.0133*	0.379
GMS	0.0031*	-1.304*10 ⁻⁶ *	0.358
NBSS_{slope}	5.75*	-0.0033*	0.337

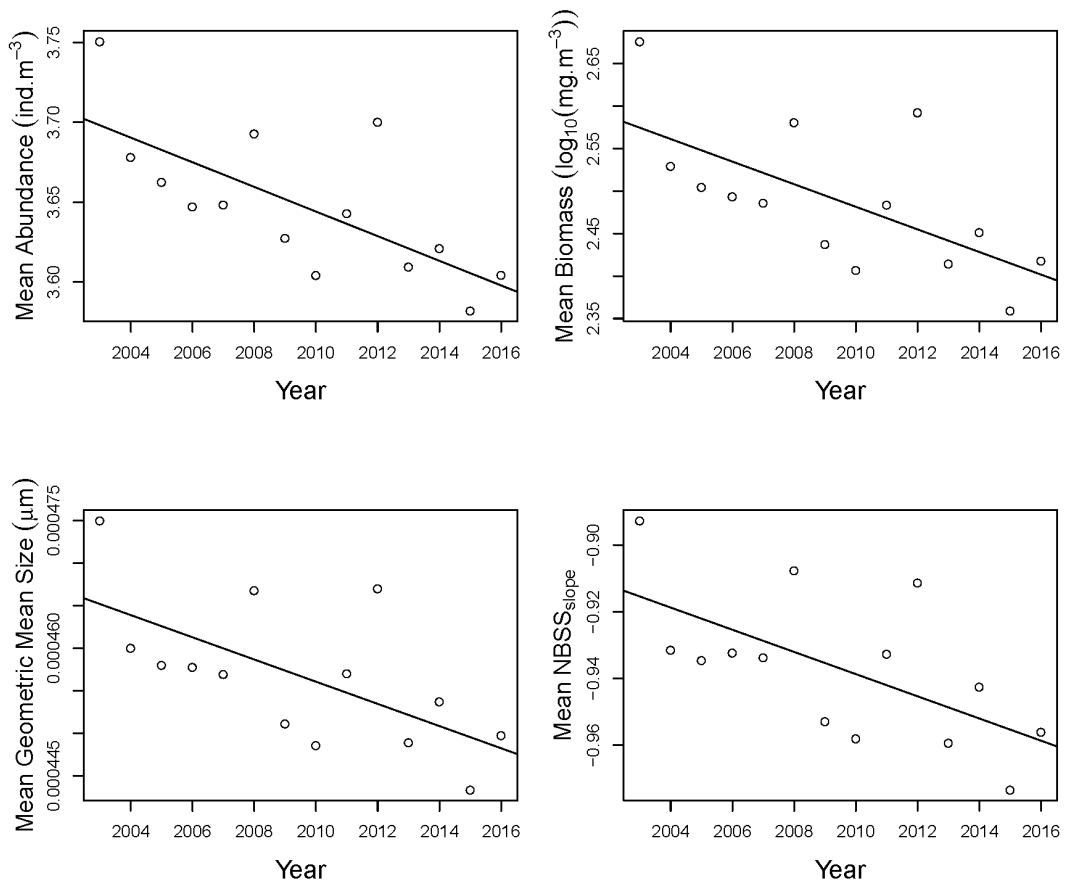


Figure 3.4 Linear regressions of mean a) Abundance (ind. $\cdot m^{-3}$), b) Biomass ($\log_{10}(mg \cdot m^{-3})$), c) Geometric Mean Size (GMS) (μm), d) NBSS_{slope}, from 2003 to 2016.

Analyses of variance (Appendix B Table 1) showed significant differences between years for abundance ($F_{13,620626} = 2908, p < 0.001$), biomass ($F_{13,627712} = 2574, p < 0.001$), GMS ($F_{13,627712} = 2439, p < 0.001$) and NBSS_{slope} ($F_{13,627712} = 2420, p < 0.001$). Tukey test results revealed significant differences between the abundance of all years except for 2006 and 2007 (Fig. 3.5a). Biomass of the study area was significantly different for most years. 2003, 2008 and 2012 had significantly high biomass, with 2015 having significantly low biomass (Fig. 3.5b). GMS showed significant differences and was significantly greater in 2003, 2008 and 2012 and significantly lower in 2015 (Fig. 3.5c). NBSS_{slope} is significantly greater in the years 2003, 2008, 2012 and significantly lower in 2015 (Fig. 3.5d).

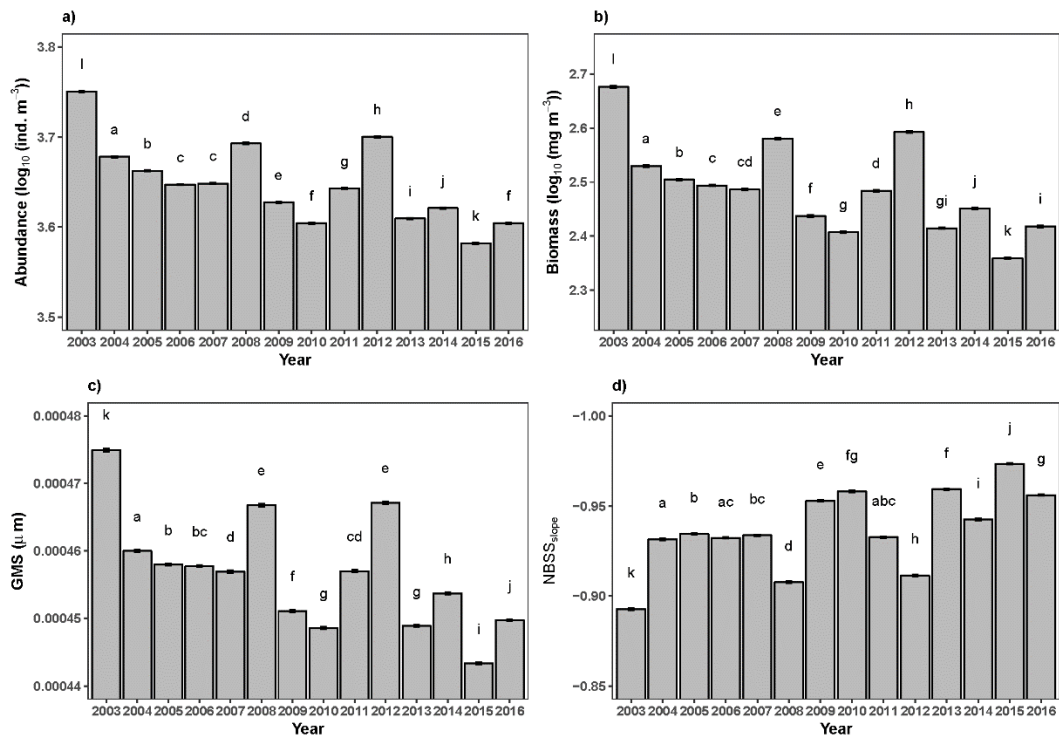


Figure 3.5 AOV Barplots of a) Abundance (ind-m^{-3}), b) Biomass ($\log_{10}(\text{mg m}^{-3})$), c) GMS (μm), d) NBSS_{slope} of the Years 2003 to 2016, labelled with Tukey significant difference test. Years with matching labels show no significant difference between each other.

The distribution and extent of zooplankton mean abundance varies from year to year (Fig. 3.6). The Tasman Sea always has higher abundance than the Coral Sea area (Appendix B Fig. 5). Some years such as 2003 show strong blooms / positive zooplankton abundance anomalies in the south of the study region (Appendix B Fig 1), driving increases in the Tasman Sea study area abundance (Appendix B. Fig. 5). Other years such as 2015 show poorer abundance and lower abundance anomalies in both the southern and northern regions (Appendix B Fig. 1 and 5). This affects the overall abundance of the entire study area (Appendix B Fig. 9).

Zooplankton mean biomass is high in 2003 with strong positive biomass anomalies (Appendix B Fig. 2) and lower in 2013 with neutral to negative biomass anomalies (Fig. 3.7, Appendix B Fig. 10). The Tasman Sea area always has higher biomass than the Coral Sea area (Appendix B Fig. 6).

Mean zooplankton size (GMS) is low in years such as 2015 (Appendix B Fig. 11), when mean GMS in both the Tasman Sea and Coral Sea areas were the lowest, (Appendix B Fig. 7) and GMS anomaly was generally negative over the study area (Appendix B Fig. 3). Mean GMS is high in 2003 in the Tasman Sea area (Fig. 3.8), and high in the Coral Sea area in 2006, when GMS anomalies were more positive in these areas (Fig. 3.8, Appendix B Fig. 3). For the overall study area, the highest GMS was in 2003 and lowest in 2015 (Appendix B Fig. 11). The GMS is always higher in the Tasman Sea than the Coral Sea areas (Appendix B Fig. 7).

NBSS_{slope} is least negative in 2003 and most negative in 2015 for the entire study area (Fig. 3.9, Appendix B Fig. 12), with predominantly negative NBSS_{slope} anomalies in 2015 (Appendix B Fig. 4). The Coral Sea and Tasman Sea areas both have their most negative NBSS_{slope} values in 2015, with the Tasman Sea having the least negative slope in 2003 (Appendix B Fig. 8) along with strong positive NBSS_{slope} anomalies (Appendix B Fig. 4).

Chapter 3

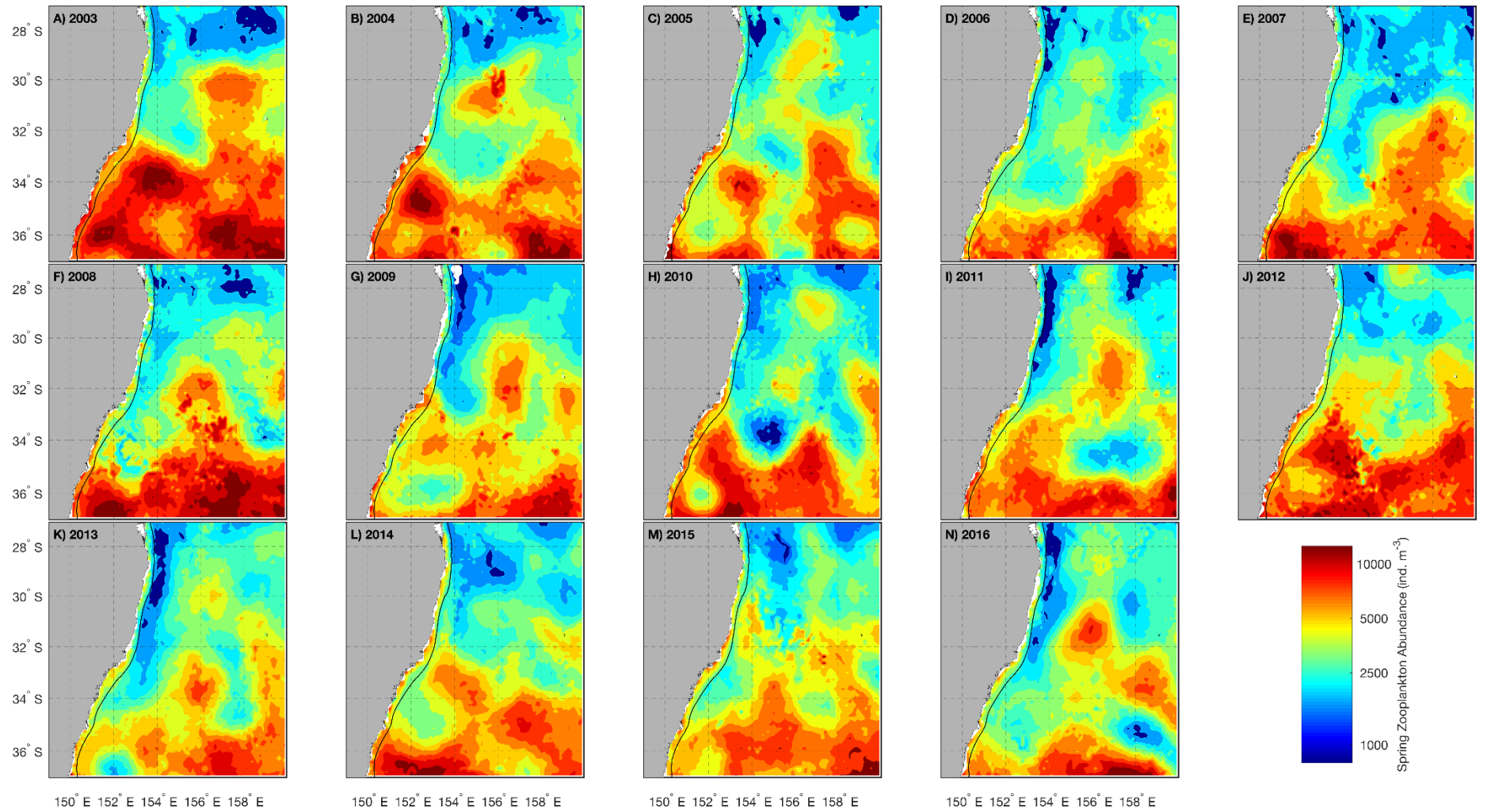


Figure 3.6 Annual springtime zooplankton Abundance (ind·m⁻³), from 2003 to 2016

Chapter 3

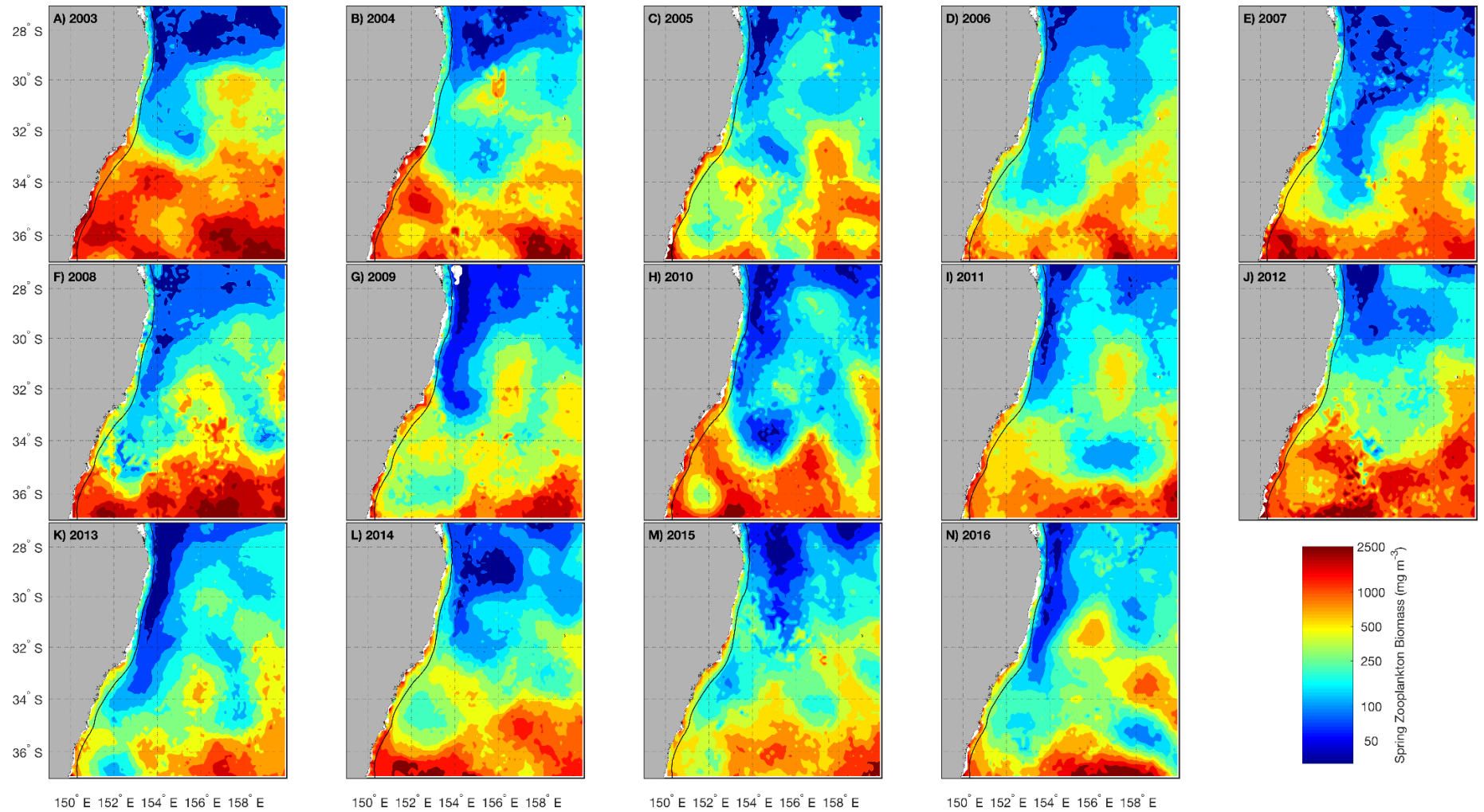


Figure 3.7 Springtime zooplankton Biomass ($\log_{10}(\text{mg m}^{-3})$) over the study area, from 2003 to 2016.

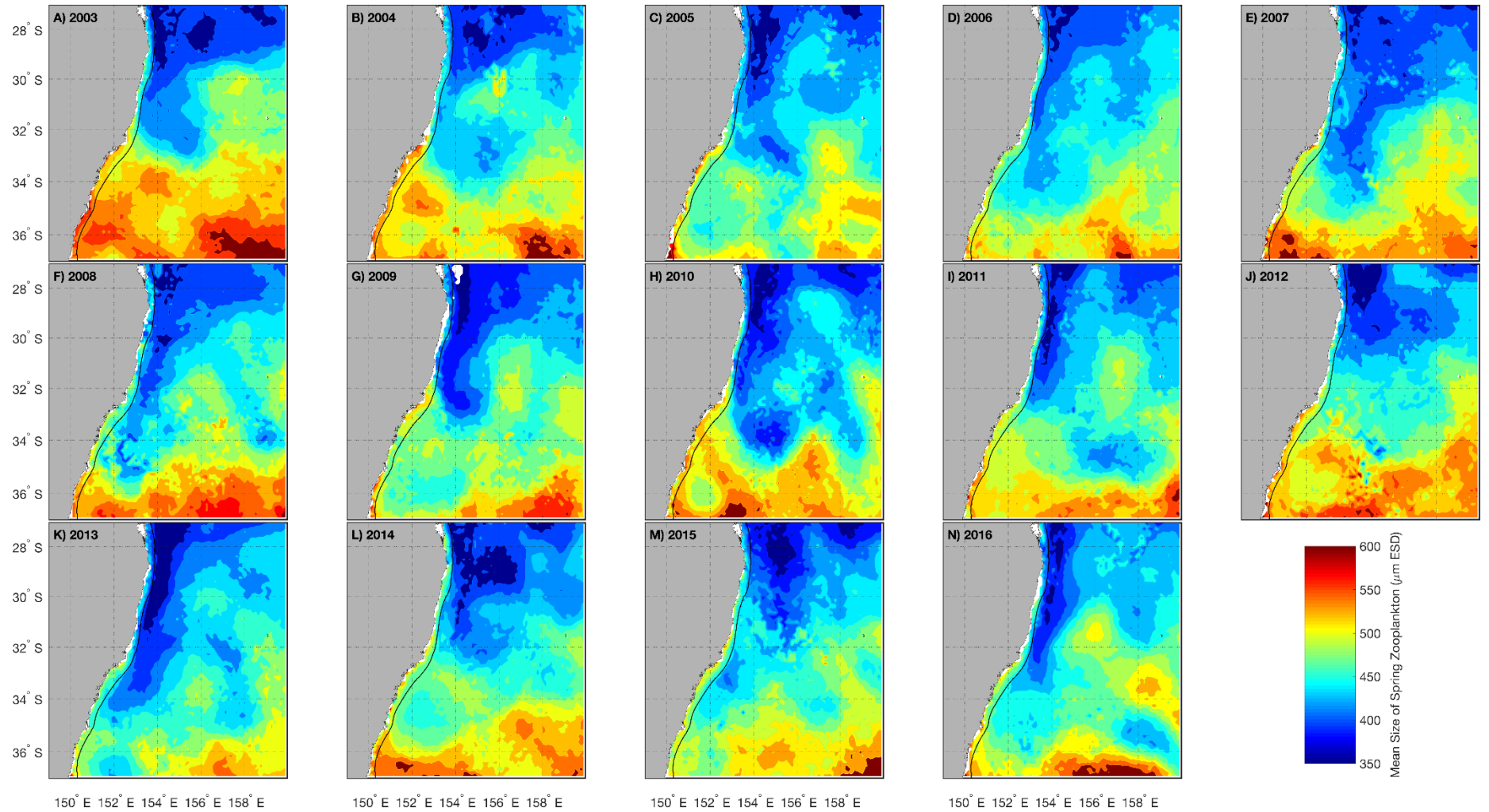


Figure 3.8 Springtime mean Geometric Mean Size (GMS) (μm ESD) of zooplankton from 2003 to 2016.

Chapter 3

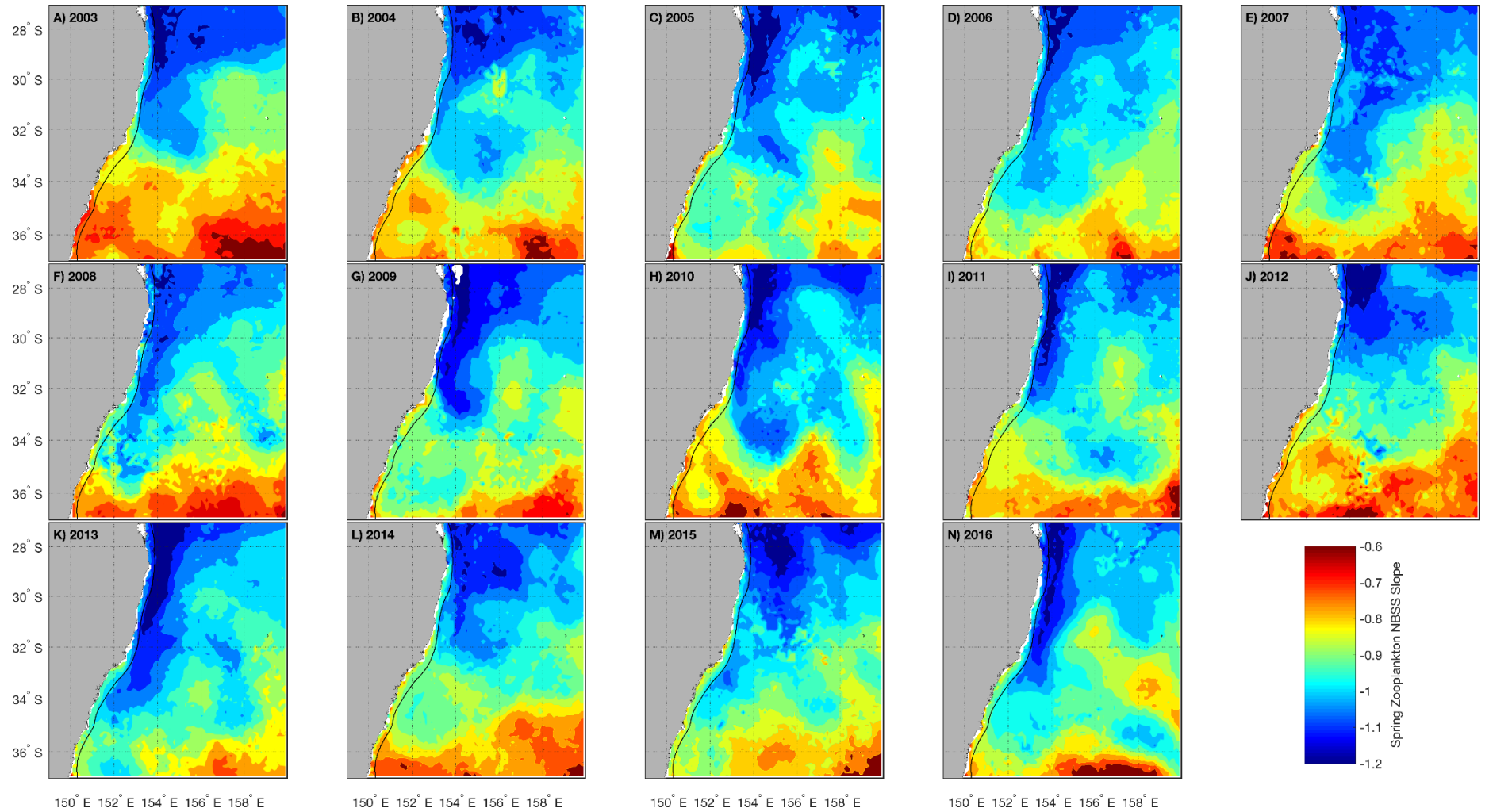


Figure 3.9 Springtime zooplankton NBSS_{slope} from 2003-2016

3.4.2 Using linear models to map zooplankton distribution over large scales

The spatial application of the linear models (Fig. 3.6-3.9) show annual variation in the distribution of springtime zooplankton biomass, abundance, GMS and NBSS_{slope}. High springtime biomass, abundance, GMS and NBSS_{slope} are consistently seen in the south of the study area and mean biomass, abundance, GMS and NBSS_{slope} are consistently higher in the Tasman Sea relative to the Coral Sea watermasses (Appendix B Fig. 5-8). The boundary between productive southern and less productive northern regions fluctuates each springtime, driving the mean productivity of the overall study area (Fig. 3.6-3.9). Annual abundance, biomass, GMS and NBSS_{slope} anomalies (Appendix B Fig. 1-4) do not show any clear spatial pattern of annual fluctuations. However, the extreme positive and negative anomalies of the southern region are in accordance with the years of highest and lowest, respectively, biomass, abundance, GMS and NBSS_{slope} of the study area.

3.4.3 Model assessment

A linear regression comparing the abundance model output values to corresponding date and coordinate values of abundance as recorded by CPR showed a significant positive correlation ($r^2 = 0.11$, $p < 0.001$) (Table 3.3, Fig. 3.10) with a Pearson's correlation coefficient of 0.34. CPR abundance data was recorded in the years 2009, 2010, 2012, 2014, 2015 and 2016.

Table 3.3: Linear Model of \log_{10} Abundance measured by the Continuous Plankton Recorder (CPR) compared to \log_{10} Abundance as predicted by the model using the date and coordinates of satellite temperature, chlorophyll- α , sea level anomaly and bathymetry.

	Estimate	St. Error	t-value	p-value	r2
MdlAbund ~Log₁₀CPRAbundance					
(Intercept)	3.455	0.0470	73.49	<0.001	0.11
Log₁₀CPRAbund	-0.09395	0.0259	3.633	<0.001	

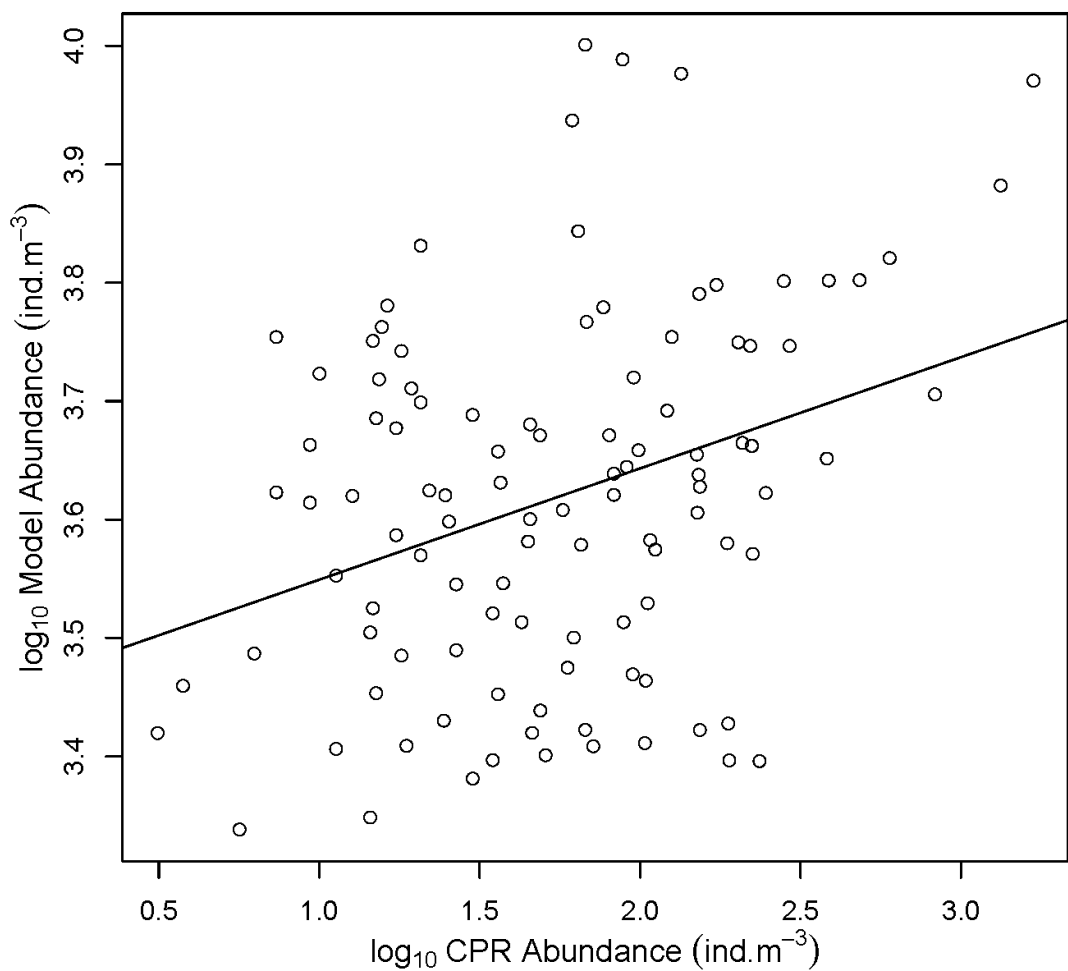


Figure 3.10 Scatterplot of CPR vs modelled abundance (ind. m^{-3}). $\text{Log}_{10}\text{Model Abundance} = 3.455 + 0.09395(\log_{10}\text{CPR Abundance})$

3.5 Discussion

Zooplankton size structure varied temporally and spatially, with a north to south gradient of increasing zooplankton abundance, biomass, GMS and NBSS_{slope}. A latitudinal increase in phytoplankton and fish productivity is typical of the study region, but geographical patterns of zooplankton size structure vary temporally. Mapping of the annual springtime size structure using satellite oceanographic variables revealed spatio-temporal patterns which can be incorporated into ecosystem models as a potentially important correlate for management of fisheries. Interestingly, a decrease in zooplankton community size structure metrics was found for the study area over the study period, highlighting the urgent need for more studies into the implications of declining zooplankton resources for fisheries productivity in the Tasman Sea.

3.5.1 Spatial patterns of zooplankton in the Tasman Sea

The distribution of zooplankton community size spectrum broadly maps to the Tasman and Coral Sea watermasses. As expected, the zooplankton size spectrum displays more negative zooplankton NBSS slopes, lower biomass, lower GMS and lower abundances in the northern Coral Sea waters, when compared to the southern, and cooler, Tasman Sea (Fig. 3.6-3.9). The higher abundances of the Tasman Sea likely relate to increased nutrient availability which drives production of the lower trophic levels (Everett et al. 2014).

The Coral Sea zooplankton community is subject to warm, oligotrophic and stratified waters, limiting the production of the lower trophic levels and giving rise to lower zooplankton abundance and biomass. With increasing temperature and lower primary production levels, body-size declines (Vidal 1980), and therefore the zooplankton size-spectrum in the warmer Coral Sea waters has a smaller GMS and steeper NBSS_{slope}. The mapping of zooplankton size spectra shows that zooplankton communities characteristic of warmer Coral Sea water are also distributed along the coast and shelf break into more southerly reaches of the western Tasman Sea. These

intrusions are likely the result of inter-annual variability in the EAC strength and the movement of the EAC separation zone southward (Cetina-Heredia et al. 2014).

At the smaller scale, eddies were apparent in the mapped zooplankton data (Fig. 3.6-3.9). Eddies are common in the region (Everett et al. 2012), transporting watermasses (Baird and Ridgway 2012), entrained zooplankton (Everett et al. 2011, 2015) and larval fish (Mullaney and Suthers 2013). Many of these eddies are generated around the EAC separation zone, where the EAC is diverted eastward and is commonly retroflected into anticyclonic eddies, and can persist up to a year (Rykova and Oke 2015). These eddies can stay in the vicinity for long periods of time (Everett et al. 2015), but will eventually travel south around Tasmania and westwards toward the Great Australian Bite (Pilo et al. 2015). These eddies, such as the anticyclonic eddies in 2009 and 2010 (Fig. 3.6-3.9), clearly show that the zooplankton size structure differs from the surrounding watermass. These large anti-cyclonic eddies are known to be important to the south eastern Australian southern bluefin tuna and yellowfin tuna fisheries (Young et al. 2001). Smaller cyclonic ‘frontal’ eddies (Everett et al. 2015) are known to alter the zooplankton size spectrum through increased production (Labat et al. 2009; Mullaney and Suthers 2013), but are too short lived to be visible in this seasonal analysis. Understanding the impact of these eddies will be important to quantifying the temporal and spatial variability of zooplankton size-structure within the study region.

Variability of the zooplankton size-spectrum was expected to be higher on the continental shelf, compared to the offshore region, due to processes such as sporadic upwelling which intermittently bring cooler nutrient rich waters to the surface (Roughan & Middleton 2002) increasing the production of the lower trophic levels (Everett et al. 2014). Interestingly, the shelf region showed a lower coefficient of variation (CoV) across all zooplankton size spectrum parameters when compared to the offshore region (Fig. 3.3). It was expected that variability would be higher along

the shelf due to sporadic upwelling, however the mixing of waters and enhanced zooplankton productivity along the shelf could reduce the variability in the zooplankton size spectrum along the shelf. In contrast, off the shelf there are the very low productivity waters of the Coral Sea in the north and higher productivity Tasman Sea waters in the south, and transient eddies moving through the area. Combined, these different environments off the shelf result in high variability of zooplankton.

3.5.2 Temporal decline in zooplankton biomass

This study showed a negative trend in zooplankton abundance, biomass, GMS and NBSS_{slope} of the study area through time. This is in agreement with other global and regional studies which have also shown a decline in phytoplankton, zooplankton and fish over recent decades (Roemmich and McGowan 1995; Beaugrand and Reid 2003; Turner et al. 2011; Capuzzo et al. 2018).

Reduction in primary production in the North Sea and the associated declines in small copepods and fish stock recruitment between 1988 and 2013 have been attributed to sea surface warming (Capuzzo et al. 2018). Likewise, a reduction in zooplankton volume by 80% has been recorded with warming sea surface temperatures in the California Current between 1951 to 1993 (Roemmich and McGowan 1995). Total zooplankton abundance has declined over 1998 to 2008 in Massachusetts Bay, correlated not with temperature but with declines in Chlorophyll-*a* (Turner et al. 2011).

Shifts of zooplankton community assemblages to higher latitudes are also associated with climate change. Warm water copepod species extended northward by 10° latitude in the North Atlantic Sea, reducing the abundances of the previously cold water zooplankton assemblages from 1982 to the study date (Beaugrand and Reid 2003). Valdes et al. (2007) observed trends of increased seasonal persistence of subtropical zooplankton species in the Bay of Biscay, where warm water zooplankton species persisted from 2 months of the year in the early 1990's to 5 months of the

year in the late 1990's. Moreover, previous to 1978 one of these warm water species, *Temora stylifera*, had never before been observed in the area. In many areas increased stratification and reduced upwelling intensity are attributed to climate change, reducing nutrients in the photic layer and leading to reduced phytoplankton biomass and reduced zooplankton biomass (Roemmich and McGowan 1995; Valdes et al. 2007). However increased stratification is not apparent off the South-eastern Australian coast (Thompson et al. 2009). The consequences of ocean warming on fish biomass of the Tasman Sea remains unknown, but changes in fish biomass have been shown to be related to changes in zooplankton biomass in other warming regions of the global ocean (Sherman et al. 2011).

As the EAC strengthens (Wu et al. 2012) and the EAC separation zone moves south (Cetina-Heredia et al. 2014), there is a decline in phytoplankton biomass (Johnson et al. 2011). Phytoplankton species such as the dinoflagellate *Noctiluca scintillans* (McLeod et al. 2012) and zooplankton species such as the sea urchin *Centrostephanus rodgersii* (Johnson et al. 2011) are transported further south. It is not surprising that with the intrusion of warmer Coral Sea waters into the Tasman Sea, there is a decline in zooplankton abundance, biomass and GMS, and therefore a steepening of the NBSS_{slope}. The lower silicate concentrations introduced by EAC water may be a cause of the shift from diatoms to dinoflagellates in the region. Dinoflagellates have lower nutritional value to the higher trophic levels than diatoms (Thompson et al. 2009). This is likely to affect zooplankton productivity in the region. The concern for regional fisheries managers, is that the decline in zooplankton availability will have flow on effects into the resources available to sustain fisheries of the region. There is speculation that as the EAC intensifies, more frequent / stronger upwelling events may occur along the continental shelf, thereby enhancing primary production and increasing overall productivity of the area (Everett et al. 2014). Unfortunately, the temporal resolution of this study is too broad to resolve finer scale details such as localised upwelling. Whether more frequent upwelling events will occur, or occur at a scale that outweighs the influence of the southward penetration of the lower productivity Coral Sea waters, is as yet unknown.

3.5.3 Implications of the zooplankton size spectrum on trophic efficiency

In this study the Tasman Sea area has a higher abundance, biomass, GMS and flatter NBSS_{slope} than the Coral Sea area. Increases in Chlorophyll- α have been associated with greater mean size of phytoplankton cells and flatter phytoplankton size spectrum slopes (Barnes et al. 2011). In this study (and Chapter 2) I show that increases in Chlorophyll- α also increases the mean size of zooplankton and results in flatter NBSS_{slope}. A flatter NBSS_{slope} indicates a shorter food chain length from prey to predator, increased energy transfer efficiency (Jennings and Collingridge 2015; Heneghan et al. 2016; Stock et al. 2017) and more herbivorous feeding strategies (Stock et al. 2017). Omnivorous zooplankton in the Tasman Sea can change their feeding strategy to become more carnivorous when chlorophyll- α in an environment is low (Henschke et al. 2015). This implies that the zooplankton communities in the Coral Sea waters may have a more carnivorous feeding strategy than the Tasman Sea. This agrees with my observations of a smaller mean size and steeper NBSS_{slope}, which indicates an increasing number of trophic steps and greater energy losses (Jennings and Warr 2003).

3.5.4 Model assessment

An assessment of the linear model against in-situ Continuous Plankton Recorder data (CPR) showed a positive trend, indicating general agreement between the model and observed data. The weak correlation ($r=0.34$) may be attributed to a number of sampling differences between instruments. In particular, the CPR is known to under sample zooplankton abundance, particularly at the larger sizes, sizes smaller than 270 μm (the CPR mesh size (Batten et al. 2003)) and of delicate zooplankton (Owens et al. 2013). The small opening aperture of the CPR reduces catchability of zooplankton as they avoid the CPR (Batten et al. 2003). In comparison, the (L)OPC has sampling limitations in having no way to classify whether a counted particle is in fact a zooplankton or a particle of detritus, yet each particle within this study's size range is included to make up the zooplankton abundance. In addition, my study uses (L)OPC data obtained throughout the top 30m of the sea surface, whereas the CPR is towed at a constant 7 m depth. However, the CPR does capture seasonal, long-term and spatial zooplankton trends. The comparison

between the two instruments is used to assess whether patterns of relative abundance over the area as sampled per instrument show similar trends.

In addition, there are temporal discrepancies between the data sources, as the model outputs are based on a seasonal average of the satellite data, whereas the CPR data point is based on the observation of that location at the given date and time. The positive relationship between model and observations is a good outcome and indicates that the broad patterns described here are likely accurate. Further ground truthing could be undertaken to improve the accuracy and calibration of the model outputs, and also used to compare differences between CPR and OPC sampling results.

3.5.5 Dynamic Ocean Management

The use of satellite data to model zooplankton allows real-time assessment of physical and biological ocean properties over large spatial and high temporal scales. This study shows the potential for mapping zooplankton biomass and size structure, which can be used as an indicator of productive fishery grounds that are of commercial and conservational importance (Young et al. 1996, 2001; Hobday and Hartmann 2006). Habitat predictions can be modelled and applied to oceanographic variables in real time (Hahlbeck et al. 2017), and has recently become more viable due to improvements in technology, with real time updates sent by mobile phone apps or email (Dunn et al. 2016).

This real time modelling approach has been used to conserve and protect migratory species, by studying the species habitat use and defining these habitats as they occur over time with satellite data. For example, where loggerhead and leatherback turtles coincide with swordfish fishing grounds in Hawaii, dynamic ocean management (DOM) in the form of daily maps of predicted turtle habitats, using SST and ocean currents, are used by fishermen to avoid these specific areas. (Howell et al. 2015). The introduction of DOM has resulted in reduced closure times, reduced fuel costs associated with fruitless fishing attempts, better management of quotas and increased efficiency of fisheries (Dunn et al. 2016; Hahlbeck et al. 2017).

In the Tasman Sea, near real-time habitat models based on temperature have already been developed to determine Southern Bluefin Tuna (SBT) distribution in the Tasman Sea (Hobday and Hartmann 2006). The use of zooplankton as a co-variate within these models would be useful as it provides a direct biological link between the ocean environment and the prey of many of these fish species. Zooplankton abundance, for example, is closely linked with SBT abundance and distribution as zooplankton attract and support jack mackerel, a major prey source of SBT (Young et al. 1996). For this reason, quantification of zooplankton biomass can be a powerful indicator of fishery location and production.

3.5.6 Concluding remarks

The spatial modelling of zooplankton size spectra parameters will allow the assessment of zooplankton in biogeochemical and ecosystem models. Understanding patterns in size, will allow models to more accurately model energy transfer through the food web and better estimate the productivity of the higher trophic levels. Currently, there is inadequate inclusion of zooplankton size spectrum dynamics into ecosystem models (Blanchard et al. 2017). In many models small zooplankton are included as part of the background phytoplankton spectrum and larger zooplankton are lumped in with small fish and their empirical size based relationships, which has been shown to grossly misrepresent the energy dynamics of the zooplankton component and lead to inaccurate estimates of fish productivity (Heneghan et al. 2016; Blanchard et al. 2017). With zooplankton biomass and size spectrum modelled for the Tasman Sea, fish biomass can now be more realistically modelled over the area and provides a platform for dynamic fisheries management of the Tasman Sea. Application of the zooplankton model output can also be combined with primary production and fisheries catch data over the area, to model the entire biological spectrum, from primary production to fish, as an important insight into energy dynamics and how they are changing in the Tasman Sea with climate change.

Chapter 4 General discussion

The blue ocean is far from a uniform saline environment but rather a slowly swirling mix of distinctive habitats. Within a few metres or minutes, one can move from the oceanographic equivalent of a rainforest to a desert. The ecology of these seascapes is driven by photosynthesis of phytoplankton, and by grazing and predation by zooplankton. Seascapes ecology is the new landscape ecology, which examines the relationships of the environment and ecosystem processes (Hobday and Hartog 2014; Kavanaugh et al. 2016). This thesis attempted to improve our present awareness of our physical seascape by including for the first time the biological seascape relationships of planktonic animals. Compared to landscape ecology, simple patterns in chlorophyll-*a* biomass in the ocean are insufficient to describe the ecosystem processes due to the rapid turnover (production) of phytoplankton and zooplankton. It is at the level of zooplankton that the relatively rapid (daily, weekly) dynamics of phytoplankton are integrated, and where fish production is determined (Hobday and Hartog 2014).

This thesis examined how the ocean environment shapes the energy flow and productivity of zooplankton communities, using the size structure parameters of abundance, biomass, geometric mean size (GMS), normalised biomass size spectrum (NBSS) slope ($\text{NBSS}_{\text{slope}}$) and intercept ($\text{NBSS}_{\text{intercept}}$). Temperature and food concentration drive the metabolic and respiration rate (Brown et al. 2004), trophic dynamics (Brown et al. 2004), growth rate (Hirst & Bunker 2003), mortality and final size (Vidal 1980; Brown et al. 2004) of zooplankton. Different oceanographic environments host zooplankton communities that differ in biomass and size structure to those in their surrounding environments (Baird et al. 2008, 2011; Mullaney and Suthers 2013; Henschke et al. 2015). Zooplankton size structure has been widely sampled and recorded over the oceans (see Table 2.2, Everett et al. (2017)), but zooplankton size structure and its relationship to environmental conditions over broad spatio-temporal scales has not been documented before.

Satellite data of sea surface temperature, chlorophyll-*a*, sea level anomaly and bathymetry were used to build relationships with measurements of *in situ* zooplankton size data. The relationships were then applied to archived satellite data, to create maps that explore how zooplankton size structure in the Tasman Sea has varied since 2003. This is an important step towards improving dynamic ocean management of the Tasman Sea area, as zooplankton are the key trophic group linking phytoplankton with fisheries (Champion et al. 2015; Heneghan et al. 2016; Everett et al. 2017). Sampling errors do exist in the gears used to collect the data, such as unknown contributions of detritus to the (Laser) Optical Plankton Counter ((L)OPC) data and the use of satellite sea surface data to represent the upper 30 m of sampled water column. Furthermore, direct comparison of abundance between the LOPC and the Continuous Plankton Recorder (CPR) is flawed due to the differences in sampling bias. However, as there were no net samples available to compare my data with, CPR abundance was the next best evaluation method available for this study. Future studies could benefit from comparison of (L)OPC data with net samples to correct for the detrital and carcass fractions of the samples. With that in mind the study was designed to acquire a broad understanding of the spatial and temporal patterns that occur in the western Tasman Sea. Using these patterns, a better understanding of energy transfer and community size structure of the zooplankton component can be used to inform size-based ecosystem models, for improved estimations of fish production (Heneghan et al. 2016; Blanchard et al. 2017) and more appropriate management of the Tasman Sea resources (Hobday et al. 2011).

4.1 Zooplankton size distribution in the western Tasman Sea

Size of an organism has long been known to be a result of the environment in which it resides. The size of zooplankton increases with lower temperatures as well as high prey concentrations. Temperature controls metabolic rate, and the effect of increased temperature results in increased losses of energy through higher respiration rates (Kerr and Dickie 2001). This allocation of a higher proportion of energy to respiration results in a loss of energy that would have otherwise been

allocated to growth or reproduction, and therefore temperature affects the flow and retention of energy through zooplankton size spectrum and food web (Brown et al. 2004). A way to measure the flow of energy through the food web is through the distribution of biomass, as can be done through the size spectrum (Platt and Denman 1977; Guiet et al. 2016). The balance of growth, respiration, mortality and trophic dynamics of a community controls the slope of the biomass size spectrum (Zhou 2006). More efficient energy transfer in the size spectrum results in a greater proportion of energy moving up the food chain, and therefore a greater biomass of larger organisms in the environment. This is represented in the NBSS as higher biomass in the larger size classes and a shallower slope (less negative). Zooplankton in the Tasman Sea study area showed such patterns.

The oligotrophic Coral Sea waters are low in nutrients and chlorophyll-*a* (Suthers et al. 2006). This is also reflected in the zooplankton communities which had low abundance, low biomass, low GMS, and steeper, more negative NBSS slopes. Warmer temperatures exacerbate the effect of low food availability in tropical areas (Hirst and Bunker 2003), as the loss of energy through allocation to the increased metabolic demands (Savage et al. 2004) require greater energy inputs to sustain the allocation of energy into growth and reproduction (Kerr and Dickie 2001). This is mirrored in the steeper NBSS slopes seen here, as energy is lost along the spectrum, and less biomass is transferred into the higher size classes. Therefore, productivity of the zooplankton is limited by the low food resource available, and by increased environmental temperatures causing decreased energy/biomass transfer efficiency through the zooplankton size spectrum.

The Tasman Sea showed higher abundances, biomass, GMS, flatter (less negative) NBSS slopes and higher NBSS intercepts. This agrees with previous research, showing the Tasman as highly productive (Baird et al. 2008) and supporting an economically important Australian fishery ground (Young et al. 2001). The cooler waters, with elevated chlorophyll-*a* (Baird et al. 2008) and strong springtime phytoplankton blooms (Everett et al. 2014), support a larger zooplankton community (Baird et al. 2008). The lower temperatures and lower respiration rates increase the proportion of

energy allocated into growth and reproduction, therefore increasing energy transfer efficiency through the zooplankton size spectrum. This has resulted in a zooplankton community with a higher abundance of individuals, higher overall biomass, greater GMS and less steep NBSS slope.

4.2 Incorporation of zooplankton into fisheries management

As zooplankton transfer the energy between phytoplankton and fish, the balance of energy and biomass retention through this trophic group is an important determinant of the energy available to support fish productivity. Modelling the zooplankton spectrum, based on empirical data, with real time spatial environmental conditions allows better data input into ecosystem models (Hobday et al. 2011; Sprules and Barth 2016). This allows incorporation of the dynamic nature of the ocean conditions into models thereby giving a more practical and informative input to modelling ecosystem productivity (Friedland et al. 2012). Higher fisheries yield has been associated with lower temperatures, higher latitudes and higher chlorophyll- a concentrations (Friedland et al. 2012). Higher zooplankton z-ratios (the ratio of mesozooplankton to phytoplankton) have been associated with increased primary production (Friedland et al. 2012). Increased primary production drives larger phytoplankton cell sizes (Barnes et al. 2011), as does colder water temperatures (Friedland et al. 2012). Zooplankton processes the energy provided by phytoplankton, with their biological rates and trophic interactions controlling the rate of energy loss and transfer from phytoplankton through the zooplankton. The end result, is the overall biomass of zooplankton that is available as an energy source to support the next higher trophic level.

The common practice in size-based modelling is to allocate small zooplankton to the background resource of phytoplankton, and to allocate larger zooplankton into the size range of small fish, thereby misrepresenting the energy dynamics of zooplankton. This has been shown to give large inaccuracies in model output predictions of fish productivity and ecosystem stability (Heneghan et al. 2016; Blanchard et al. 2017). Other models use chlorophyll- a concentrations as the primary determinant of fish

production, also ignoring the important energy dynamics that occur through zooplankton (Stock et al. 2017).

This sets up a need to represent zooplankton productivity in a simple but informative way that is compatible for incorporation into ecosystem models, in real time and over large spatial coverage (Hobday et al. 2011). The models developed in this study, using satellite co-variates over large spatial and temporal scales, can be used to inform the real time modelling and dynamic ocean management of fisheries production, supplementing the use of phytoplankton and SST to inform current fishery habitat models (Hobday et al. 2011). The monitoring of zooplankton in this way allows assessment in real time, of productivity changes due to water mass shifts, and how the changes in ocean environment affect zooplankton productivity.

The two dominant water masses in the study area are the Tasman Sea and the Coral Sea. Each has its own zooplankton community characteristics, with differences in species, trophic dynamics, size spectrum and productivity. Climate change is driving a greater mass of Coral Sea water further southward, and this is reflected in our results as a change in springtime zooplankton community size spectra and a decline in zooplankton biomass of the study area during the study period of 2003 to 2016. The decline in zooplankton biomass is likely to be from the water mass shift of oligotrophic, warm Coral Sea water with its associated smaller GMS and less productive zooplankton communities. This drives a decline in productivity levels of the study area, reducing the area of productive Tasman Sea waters, with their zooplankton communities that have traditionally characterised the area as a productive, economically important fishing region. This finding shows the current importance and need for zooplankton monitoring, as the effects of water mass distribution shifts with climate change are likely to have a large impact on fisheries productivity, and therefore the local economies. This study shows the great potential of using zooplankton relationships with satellite derived environmental variables, to convert a satellite's view of our planet, to an ecosystem one. Hobday and Hartog (2014) speculated that if improved dynamics of seascape (satellite derived) variables do not improve dynamic ocean management, then "has the pursuit of environment-

biology relationships reached a prediction barrier?" (Hobday & Hartog (2014), p. 143). This seems premature, when the key rate-determining processes from zooplankton size-structure have not until now been determined.

References

- Albaina A, Irigoien X (2004) Relationships between frontal structures and zooplankton communities along a cross-shelf transect in the Bay of Biscay (1995 to 2003). *Mar Ecol Prog Ser* 284:65–75. doi: 10.3354/meps284065
- Andersen KH, Berge T, Gonçalves RJ, et al (2016) Characteristic sizes of life in the oceans, from bacteria to whales. *Ann Rev Mar Sci* 8:217–241. doi: 10.1146/annurev-marine-122414-034144
- Atkinson D, Sibly RM (1997) Why are organisms usually bigger in colder environments? Making sense of a life history puzzle. *Trends Ecol Evol* 12:235–239. doi: 10.1016/S0169-5347(97)01058-6
- Australian Ocean Data Network (2016) Open Access to Ocean Data. <https://portal.aodn.org.au/search>. Accessed 13 Mar 2018
- Baird ME, Everett JD, Suthers IM (2011) Analysis of southeast Australian zooplankton observations of 1938 – 42 using synoptic oceanographic conditions. *Deep Res Part II* 58:699–711. doi: 10.1016/j.dsr2.2010.06.002
- Baird ME, Ridgway KR (2012) The southward transport of sub-mesoscale lenses of Bass Strait Water in the centre of anti-cyclonic mesoscale eddies. *Geophys Res Lett* 39:1–7. doi: 10.1029/2011GL050643
- Baird ME, Timko PG, Middleton JH, et al (2008) Biological properties across the Tasman Front off southeast Australia. *Deep Res Part I Oceanogr Res Pap* 55:1438–1455. doi: 10.1016/j.dsr.2008.06.011
- Barnes C, Irigoien X, De Oliveira J a a, et al (2011) Predicting marine phytoplankton community size structure from empirical relationships with remotely sensed variables. *J Plankton Res* 33:13–24. doi: 10.1093/plankt/fbq088
- Barnes C, Maxwell D, Reuman D, Jennings S (2010) Global patterns in predator – prey size relationships reveal size dependency of trophic transfer efficiency. *Ecology* 91:222–232. doi: 10.1890/08-2061.1
- Barton AD, Pershing AJ, Litchman E, et al (2013) The biogeography of marine plankton traits. *Ecol. Lett.* 16:522–534
- Basedow SL, Tande KS, Zhou M (2010) Biovolume spectrum theories applied: Spatial patterns of trophic levels within a mesozooplankton community at the polar front. *J Plankton Res* 32:1105–1119. doi: 10.1093/plankt/fbp110
- Batten SD, Clark R, Flinkman J, et al (2003) CPR sampling: the technical background, materials and methods, consistency and comparability. *Prog Oceanogr* 58:193–215. doi: 10.1016/j.pocean.2003.08.004

Beaugrand G, Reid PC (2003) Long-term changes in phytoplankton, zooplankton and salmon related to climate. *Glob Chang Biol* 9:801–817. doi: 10.1046/j.1365-2486.2003.00632.x

Behrendt S (2014) *Im.beta*: Add Standardised Coefficients to *Im*-objects

Blanchard JL, Andersen KH, Scott F, et al (2014) Evaluating targets and trade-offs among fisheries and conservation objectives using a multispecies size spectrum model. *J Appl Ecol* 51:612–622. doi: 10.1111/1365-2664.12238

Blanchard JL, Heneghan RF, Everett JD, et al (2017) From Bacteria to Whales : Using Functional Size Spectra to Model Marine Ecosystems. *Trends Ecol Evol* 32:174–186. doi: 10.1016/j.tree.2016.12.003

Blanchard JL, Jennings S, Holmes R, et al (2012) Potential consequences of climate change for primary production and fish production in large marine ecosystems. *Philos Trans R Soc B Biol Sci* 367:2979–2989. doi: 10.1098/rstb.2012.0231

Blanchard JL, Jennings S, Law R, et al (2009) How does abundance scale with body size in coupled size-structured food webs? *J Anim Ecol* 78:270–280. doi: 10.1111/j.1365-2656.2008.01466.X

Blondeau-patissier D, Gower JFR, Dekker AG, et al (2014) A review of ocean color remote sensing methods and statistical techniques for the detection, mapping and analysis of phytoplankton blooms in coastal and open oceans. *Prog Oceanogr* 123:123–144. doi: 10.1016/j.pocean.2013.12.008

Boudreau PR, Dickie LM (1992) Biomass Spectra of Aquatic Ecosystems in Relation to Fisheries Yield. *Can J Fish Aquat Sci* 49:1528–1538. doi: 10.1139/f92-169

Brown JH, Gillooly JF, Allen AP, et al (2004) Toward a metabolic theory of ecology. *Ecology* 85:1771–1789. doi: 10.1890/03-9000

Capuzzo E, Lynam CP, Barry J, et al (2018) A decline in primary production in the North Sea over 25 years, associated with reductions in zooplankton abundance and fish stock recruitment. *Glob Chang Biol* 24:e352–e364. doi: 10.1111/gcb.13916

Cetina-Heredia P, Roughan M, Van Sebille E, Coleman M a. (2014) Long-term trends in the East Australian Current separation latitude and eddy driven transport. *J Geophys Res Ocean* 119:4351–4366. doi: 10.1002/2014JC010071

Champion C, Suthers IM, Smith JA (2015) Zooplanktivory is a key process for fish production on a coastal artificial reef. *Mar Ecol Prog Ser* 541:1–14. doi: 10.3354/meps11529

- Checkley DM, Davis RE, Herman AW, et al (2008) Assessing plankton and other particles in situ with the SOLOPC. *Limnol Oceanogr* 53:2123–2136. doi: 10.4319/lo.2008.53.5_part_2.2123
- Clark DR, Aazem K V., Hays GC (2001) Zooplankton abundance and community structure over a 4000 km transect in the north-east Atlantic. *J Plankton Res* 23:365–372. doi: 10.1093/plankt/23.4.365
- Cresswell G (1994) Nutrient enrichment of the sydney continental shelf. *Mar Freshw Res* 45:677–691. doi: 10.1071/MF9940677
- Dai L, Li C, Yang G, Sun X (2016) Zooplankton abundance, biovolume and size spectra at western boundary currents in the subtropical North Pacific during winter 2012. *J Mar Syst* 155:73–83. doi: 10.1016/j.jmarsys.2015.11.004
- Dickie LM, Kerr SR, Boudreau PR (1987) Size-Dependent Processes Underlying Regularities in Ecosystem Structure. *Ecol Monogr* 57:233–250. doi: 10.2307/2937082
- Dunn DC, Maxwell SM, Boustany AM, Halpin PN (2016) Dynamic ocean management increases the efficiency and efficacy of fisheries management. *Proc Natl Acad Sci* 113:668–673. doi: 10.1073/pnas.1513626113
- Durham WM, Stocker R (2012) Thin Phytoplankton Layers: Characteristics, Mechanisms, and Consequences. *Ann Rev Mar Sci* 4:177–207. doi: 10.1146/annurev-marine-120710-100957
- Edwards AM, Robinson JPW, Plank MJ, et al (2017) Testing and recommending methods for fitting size spectra to data. *Methods Ecol Evol* 8:57–67. doi: 10.1111/2041-210X.12641
- Elliott DT, Tang KW (2011) Spatial and Temporal Distributions of Live and Dead Copepods in the Lower Chesapeake Bay (Virginia, USA). *Estuaries and Coasts* 34:1039–1048
- Espinasse B, Basedow S, Schultes S, et al (2018) Conditions for assessing zooplankton abundance with LOPC in coastal waters. *Prog Oceanogr* 163:260–270. doi: 10.1016/j.pocean.2017.10.012
- Everett JD, Baird ME, Buchanan P, et al (2017) Modeling What We Sample and Sampling What We Model: Challenges for Zooplankton Model Assessment. *Front Mar Sci* 4:1–19. doi: 10.3389/fmars.2017.00077
- Everett JD, Baird ME, Oke PR, Suthers IM (2012) An avenue of eddies: Quantifying the biophysical properties of mesoscale eddies in the Tasman Sea. *Geophys Res Lett* 39:1–5. doi: 10.1029/2012GL053091

- Everett JD, Baird ME, Roughan M, et al (2014) Relative impact of seasonal and oceanographic drivers on surface chlorophyll a along a Western Boundary Current. *Prog Oceanogr* 120:340–351. doi: 10.1016/j.pocean.2013.10.016
- Everett JD, Baird ME, Suthers IM (2011) Three-dimensional structure of a swarm of the salp *Thalia democratica* within a cold-core eddy off southeast Australia. *J Geophys Res* 116:1–14. doi: 10.1029/2011JC007310
- Everett JD, Macdonald H, Baird ME, et al (2015) Cyclonic entrainment of preconditioned shelf waters into a frontal eddy. *J Geophys Res Ocean* 120:667–691. doi: 10.1002/2014JC010301
- Fox J (2003) Effect displays in {R} for Generalised Linear Models. *J Stat Softw* 8:1–27
- Friedland KD, Stock C, Drinkwater KF, et al (2012) Pathways between primary production and fisheries yields of large marine ecosystems. *PLoS One* 7:e28945. doi: 10.1371/journal.pone.0028945
- García-Comas C, Chang C-Y, Ye L, et al (2014) Mesozooplankton size structure in response to environmental conditions in the East China Sea: How much does size spectra theory fit empirical data of a dynamic coastal area? *Prog Oceanogr* 121:141–157. doi: 10.1016/j.pocean.2013.10.010
- García-Muñoz C, García CM, Lubián LM, et al (2014) Metabolic state along a summer north-south transect near the Antarctic Peninsula: A size spectra approach. *J Plankton Res* 36:1074–1091. doi: 10.1093/plankt/fbu042
- GEBCO (2018) General Bathymetric Chart of the Oceans (GEBCO). <https://www.gebco.net/>. Accessed 17 Mar 2018
- GoMA (2018a) Optical Plankton Counter (OPC) » Gulf of Maine Census. In: Opt. Plankt. Count. <http://www.gulfofmaine-census.org/education/research-technology/optical-instruments/optical-plankton-counter-opc/>. Accessed 23 Mar 2018
- GoMA (2018b) Laser-Optical Plankton Counter (LOPC) » Gulf of Maine Census. In: Laser-Optical Plankt. Count. <http://www.gulfofmaine-census.org/education/research-technology/optical-instruments/laser-optical-plankton-counter-lopc/>. Accessed 23 Mar 2018
- Guillet J, Poggiale J-C, Maury O (2016) Modelling the community size-spectrum: recent developments and new directions. *Ecol. Modell.* 337:4–14
- Hahlbeck N, Scales KL, Dewar H, et al (2017) Oceanographic determinants of ocean sunfish (*Mola mola*) and bluefin tuna (*Thunnus orientalis*) bycatch patterns in the California large mesh drift gillnet fishery. *Fish Res* 191:154–163. doi: 10.1016/j.fishres.2017.03.011

- Hamner WM, Jones MS, Carleton JH, et al (1988) Zooplankton, planktivorous fish, and water currents on a windward reef face: Great Barrier Reef, Australia. *Bull. Mar. Sci.* 42:459–479
- Heath MR (2012) Ecosystem limits to food web fluxes and fisheries yields in the North Sea simulated with an end-to-end food web model. *Prog Oceanogr* 102:42–66. doi: 10.1016/j.pocean.2012.03.004
- Heneghan RF, Everett JD, Blanchard JL, Richardson AJ (2016) Zooplankton Are Not Fish: Improving Zooplankton Realism in Size-Spectrum Models Mediates Energy Transfer in Food Webs. *Front Mar Sci* 3:1–15. doi: 10.3389/fmars.2016.00201
- Henschke N, Everett JD, Baird ME, et al (2011) Distribution of life-history stages of the salp *Thalia democratica* in shelf waters during a spring bloom. *Mar Ecol Prog Ser* 430:49–62. doi: 10.3354/meps09090
- Henschke N, Everett JD, Suthers IM, et al (2015) Zooplankton trophic niches respond to different water types of the western Tasman Sea: A stable isotope analysis. *Deep Res Part I* 104:1–8. doi: 10.1016/j.dsr.2015.06.010
- Herman AW (1992) Design and calibration of a new optical plankton counter capable of sizing small zooplankton. *Deep Sea Res Part A Oceanogr Res Pap* 39:395–415. doi: 10.1016/0198-0149(92)90080-D
- Herman AW, Beanlands B, Phillips EF (2004) The next generation of Optical Plankton Counter: The Laser-OPC. *J Plankton Res* 26:1135–1145. doi: 10.1093/plankt/fbh095
- Hill KL, Rintoul SR, Coleman R, Ridgway KR (2008) Wind forced low frequency variability of the East Australia Current. *Geophys Res Lett* 35:1–5. doi: 10.1029/2007GL032912
- Hirst AG, Bunker AJ (2003) Growth of marine planktonic copepods: global rates and patterns in relation to chlorophyll a, temperature, and body weight. *Limnology Oceanogr* 48:1988–2010. doi: 10.4319/lo.2003.48.5.1988
- Hobday AJ, Hartmann K (2006) Near real-time spatial management based on habitat predictions for a longline bycatch species. *Fish Manag Ecol* 13:365–380. doi: 10.1111/j.1365-2400.2006.00515.x
- Hobday AJ, Hartog JR (2014) Derived Ocean Features for Dynamic Ocean Management. *Oceanography* 27:134–145. doi: 10.5670/oceanog.2014.92
- Hobday AJ, Young JW, Moeseneder C, Dambacher JM (2011) Defining dynamic pelagic habitats in oceanic waters off eastern Australia. *Deep Res II* 58:734–745. doi: 10.1016/j.dsr2.2010.10.006

- Howell E a., Hoover A, Benson SR, et al (2015) Enhancing the TurtleWatch product for leatherback sea turtles, a dynamic habitat model for ecosystem-based management. *Fish Oceanogr* 24:57–68. doi: 10.1111/fog.12092
- Jennings S (2005) Size-based analyses of aquatic food webs. In: *Aquatic Food Webs : An ecosystem approach*. Oxford University Press, 2017, pp 1–23
- Jennings S, Collingridge K (2015) Predicting consumer biomass, size-structure, production, catch potential, responses to fishing and associated uncertainties in the world's marine ecosystems. *PLoS One* 10:1–29. doi: 10.1371/journal.pone.0133794
- Jennings S, Mackinson S (2003) Abundance-body mass relationships in size-structured food webs. *Ecol Lett* 6:971–974. doi: 10.1046/j.1461-0248.2003.00529.x
- Jennings S, Maxwell TAD, Schratzberger M, Milligan SP (2008) Body-size dependent temporal variations in nitrogen stable isotope ratios in food webs. *Mar Ecol Prog Ser* 370:199–206. doi: 10.3354/meps07653
- Jennings S, Warr KJ (2003) Smaller predator-prey body size ratios in longer food chains. *Proc Biol Sci* 270:1413–1417. doi: 10.1098/rspb.2003.2392
- Johnson CR, Banks SC, Barrett NS, et al (2011) Climate change cascades : Shifts in oceanography, species' ranges and subtidal marine community dynamics in eastern Tasmania. *J Exp Mar Bio Ecol* 400:17–32. doi: 10.1016/j.jembe.2011.02.032
- Johnson WS, Allen DM (2005) *Zooplankton of the Atlantic and Gulf Coasts: A guide to their identification and ecology*. The John Hopkins University Press, Maryland
- Kavanaugh MT, Oliver MJ, Chavez FP, et al (2016) Seascapes as a new vernacular for pelagic ocean monitoring, management and conservation. *ICES J Mar Sci* 73:1839–1850. doi: 10.1093/icesjms/fsw086
- Kerr SR, Dickie LM (2001) *The biomass spectrum: a predator-prey theory of aquatic production*. Columbia University Press, New York
- Kiørboe T, Hirst AG (2008) Optimal development time in pelagic copepods. *Mar Ecol Prog Ser* 367:15–22. doi: 10.3354/meps07572
- Kiyashko SI, Kharlamenko VI, Sanamyan K, et al (2014) Trophic structure of the abyssal benthic community in the Sea of Japan inferred from stable isotope and fatty acid analyses. *Mar Ecol Prog Ser* 500:121–137. doi: 10.3354/meps10663
- Krupica KL (2006) Evaluating size-based indices to monitor variations in Scotian Shelf zooplankton assemblages. University of Toronto

Krupica KL, Sprules WG, Herman AW (2012) The utility of body size indices derived from optical plankton counter data for the characterization of marine zooplankton assemblages. *Cont Shelf Res* 36:29–40. doi: 10.1016/j.csr.2012.01.008

Labat JP, Gasparini S, Mousseau L, et al (2009) Mesoscale distribution of zooplankton biomass in the northeast Atlantic Ocean determined with an Optical Plankton Counter: Relationships with environmental structures. *Deep Sea Res Part I Oceanogr Res Pap* 56:1742–1756. doi: 10.1016/j.dsr.2009.05.013

Marcolin CR, Lopes RM, Jackson GA (2015) Estimating zooplankton vertical distribution from combined LOPC and ZooScan observations on the Brazilian Coast. *Mar Biol* 162:2171–2186. doi: 10.1007/s00227-015-2753-2

Marcolin R, Schultes S, Jackson GA, Lopes RM (2013) Plankton and seston size spectra estimated by the LOPC and ZooScan in the Abrolhos Bank ecosystem (SE Atlantic). *Cont Shelf Res* 70:74–87. doi: 10.1016/j.csr.2013.09.022

Marineregions.org (2016) Marine Regions · Australian part of the Coral Sea (Marine Region). <http://www.marineregions.org/gazetteer.php?p=details&id=25477>. Accessed 13 Mar 2018

Maxwell SM, Hazen EL, Lewison RL, et al (2015) Dynamic ocean management: Defining and conceptualizing real-time management of the ocean. *Mar Policy* 58:42–50. doi: 10.1016/j.marpol.2015.03.014

Moore SK, Suthers IM (2006) Evaluation and correction of subresolved particles by the optical plankton counter in three Australian estuaries with pristine to highly modified catchments. *J Geophys Res Ocean* 111:1–14. doi: 10.1029/2005JC002920

Mullaney TJ, Suthers IM (2013) Entrainment and retention of the coastal larval fish assemblage by a short-lived, submesoscale, frontal eddy of the East Australian Current. *Limnol Oceanogr* 58:1546–1556. doi: 10.4319/lo.2013.58.5.1546

Owens NJP, Hosie GW, Batten SD, et al (2013) All plankton sampling systems underestimate abundance: Response to “Continuous plankton recorder underestimates zooplankton abundance” by J.W. Dippner and M. Krause. *J Mar Syst* 128:240–242. doi: 10.1016/j.jmarsys.2013.05.003

Payet R (2006) Decision processes for large marine ecosystems management and policy. *Ocean Coast Manag* 49:110–132. doi: 10.1016/j.ocecoaman.2006.02.001

Petrik CM, Jackson GA, Checkley DM (2013) Aggregates and their distributions determined from LOPC observations made using an autonomous profiling float. *Deep Res Part I Oceanogr Res Pap* 74:64–81. doi: 10.1016/j.dsr.2012.12.009

Pilo GS, Oke PR, Rykova T, et al (2015) Do East Australian Current anticyclonic eddies leave the Tasman Sea? *J Geophys Res Ocean* 120:8099–8114. doi: 10.1002/2015JC011026

Piontkovski S, Williams R, Melnik T (1995) Spatial heterogeneity, biomass and size structure of plankton of the Indian Ocean: some general trends. *Mar Ecol Prog Ser* 117:219–227. doi: 10.3354/meps117219

Platt T, Denman K (1977) Organisation in the pelagic ecosystem. *Helgoländer Wissenschaftliche Meeresuntersuchungen* 30:575–581. doi: 10.1007/BF02207862

Pretorius M, Huggett JA, Gibbons MJ (2016) Summer and winter differences in zooplankton biomass, distribution and size composition in the KwaZulu-Natal Bight, South Africa. *African J Mar Sci* 38:S155–S168. doi: 10.2989/1814232X.2016.1144650

R Core Team (2017) R: A language and environment for statistical computing.

Ridgway KR, Dunn JR (2003) Mesoscale structure of the mean East Australian Current System and its relationship with topography. *Prog Oceanogr* 56:189–222. doi: 10.1016/S0079-6611(03)00004-1

Rissik D, Suthers IM, Taggart CT (1997) Enhanced zooplankton abundance in the lee of an isolated reef in the south Coral Sea: the role of flow disturbance. *J Plankton Res* 19:1347–1368

Ritz D, Swadling K, Hosie G, Cazassus F (2003) Guide to the Zooplankton of south eastern Australia, 10th edn. Fauna of Tasmania Committee, University of Tasmania

Roemmich D, McGowan J (1995) Climatic Warming and the Decline of Zooplankton in the California Current. *Science* (80-) 267:1324–1326. doi: 10.1126/science.39.1002.398

Roughan M, Middleton JH (2002) A comparison of observed upwelling mechanisms off the east coast of Australia. *Cont Shelf Res* 22:2551–2572. doi: 10.1016/S0278-4343(02)00101-2

Roughan M, Middleton JH (2004) On the East Australian Current: Variability, encroachment, and upwelling. *J Geophys Res Ocean* 109:1–16. doi: 10.1029/2003JC001833

Rykova T, Oke PR (2015) Recent freshening of the East Australian Current and its eddies. *Geophys Res Lett* 42:9369–9378. doi: 10.1002/2015GL066050

- San Martin E, Harris RP, Irigoien X (2006) Latitudinal variation in plankton size spectra in the Atlantic Ocean. Deep Res Part II Top Stud Oceanogr 53:1560–1572. doi: 10.1016/j.dsr2.2006.05.006
- Sato K, Matsuno K, Arima D, et al (2015) Spatial and temporal changes in zooplankton abundance , biovolume , and size spectra in the neighboring waters of Japan : analyses using an optical plankton counter. doi: 10.1186/s40555-014-0098-z
- Savage VM, Gillooly JF, Brown JH, et al (2004) Effects of Body Size and Temperature on Population Growth. Am Nat 163:429–441. doi: 10.1086/381872
- Schaeffer A, Roughan M, Morris BD (2013) Cross-Shelf Dynamics in a Western Boundary Current Regime: Implications for Upwelling. J Phys Oceanogr 43:1042–1059. doi: 10.1175/JPO-D-12-0177.1
- Schlutes S, Lopes RM (2009) Laser Optical Plankton Counter and Zooscan intercomparison in tropical and subtropical marine ecosystems. Limnol Oceanogr Methods 7:771–784
- Schwinghamer P (1981) Characteristic Size Distributions of Integral Benthic Communities. Can J Fish Aquat Sci 38:1255–1263. doi: 10.1139/f81-167
- Sheldon RW, Prakash A, Sutcliffe WH (1972) The size distribution of particles in the ocean. Limnol Oceanogr 17:327–340
- Sherman K, O'Reilly J, Belkin IM, et al (2011) The application of satellite remote sensing for assessing productivity in relation to fisheries yields of the world's large marine ecosystems. ICES J. Mar. Sci. 68:667–676
- Silvert W, Platt T (1978) Energy flux in the pelagic ecosystem: A time-dependant equation. Limnol Oceanogr 23:813–816
- Skarðhamar J, Slagstad D, Edvardsen A (2007) Plankton distributions related to hydrography and circulation dynamics on a narrow continental shelf off Northern Norway. Estuar Coast Shelf Sci 75:381–392. doi: 10.1016/j.ecss.2007.05.044
- Slotwinski A, Coman F, Richardson A (2014) Introductory Guide to Zooplankton Identification. Brisbane
- Sprules WG, Barth LE (2016) Surfing the biomass size spectrum: some remarks on history, theory, and application. Can J Fish Aquat Sci 73:477–495. doi: 10.1139/cjfas-2015-0115
- Sprules WG, Munawar M (1986) Plankton Size Spectra in Relation to Ecosystem Productivity, Size, and Perturbation. Can J Fish Aquat Sci 43:1789–1794. doi: 10.1139/f86-222

- Stephens K, Sheldon RW, Parsons TR (1967) Seasonal Variations in the Availability of Food for Benthos in a Coastal Environment. *Ecology* 48:852–855
- Stock CA, John JG, Rykaczewski RR, et al (2017) Reconciling fisheries catch and ocean productivity. *Proc Natl Acad Sci* 114:1–9. doi: 10.1073/pnas.1610238114
- Suthers IM, Taggart CT, Rissik D, Baird ME (2006) Day and night ichthyoplankton assemblages and zooplankton biomass size spectrum in a deep ocean island wake. *Mar Ecol Prog Ser* 322:225–238. doi: 10.3354/meps322225
- Suthers IM, Young JW, Baird ME, et al (2011) The strengthening East Australian Current, its eddies and biological effects - an introduction and overview. *Deep Res Part II Top Stud Oceanogr* 58:538–546. doi: 10.1016/j.dsr2.2010.09.029
- Thompson PA, Baird ME, Ingleton T, Doblin MA (2009) Long-term changes in temperate Australian coastal waters: implications for phytoplankton. *Mar Ecol Prog Ser* 394:1–19. doi: 10.3354/meps08297
- Thompson PA, Bonham PI, Swadling KM (2008) Phytoplankton blooms in the Huon Estuary, Tasmania: top-down or bottom-up control? *J Plankton Res* 30:735–753. doi: 10.1093/plankt/fbn044
- Tranter DJ, Carpenter DJ, Leech GS (1986) The coastal enrichment effect of the East Australian Current eddy field. *Deep Sea Res Part A Oceanogr Res Pap* 33:1705–1728
- Trudnowska E, Basedow SL, Blachowiak-Samolyk K (2014) Mid-summer mesozooplankton biomass, its size distribution, and estimated production within a glacial Arctic fjord (Hornsund, Svalbard). *J Mar Syst* 137:55–66. doi: 10.1016/j.jmarsys.2014.04.010
- Turner JT, Borkman DG, Scott Libby P (2011) Zooplankton trends in Massachusetts Bay, USA: 1998–2008. *J Plankton Res* 33:1066–1080. doi: 10.1093/plankt/fbq168
- Valdes L, Lopez-Urrutia A, Cabal J, et al (2007) A decade of sampling in the Bay of Biscay : What are the zooplankton time series telling us? *Prog Oceanogr* 74:98–114. doi: 10.1016/j.pocean.2007.04.016
- Vandromme P, Nogueira E, Huret M, et al (2014) Springtime zooplankton size structure over the continental shelf of the Bay of Biscay. *Ocean Sci* 10:821–835. doi: 10.5194/os-10-821-2014
- Vidal J (1980) Physioecology of zooplankton. I. Effects of phytoplankton concentration, temperature, and body size on the growth rate of *Calanus pacificus* and *Pseudocalanus* sp. *Mar Biol* 56:111–134. doi: 10.1007/BF00397129

Warner AJ, Hays GC (1994) Sampling by the Continuous Plankton Recorder survey. *Prog Oceanogr* 34:237–256. doi: 10.1016/0079-6611(94)90011-6

Wood JE (2014) The circulation on the continental shelf of south-eastern Australia from 2009 to 2013. University of New South Wales

Woodd-Walker RS, Kingston KS, Gallienne CP (2001) Using neural networks to predict surface zooplankton biomass along a 50°N to 50°S transect of the Atlantic. *J Plankton Res* 23:875–888. doi: 10.1093/plankt/23.8.875

Woodworth-Jefcoats PA, Polovina JJ, Dunne JP, Blanchard JL (2013) Ecosystem size structure response to 21st century climate projection: large fish abundance decreases in the central North Pacific and increases in the California Current. *Glob Chang Biol* 19:724–733. doi: 10.1111/gcb.12076

Wu L, Cai W, Zhang L, et al (2012) Enhanced warming over the global subtropical western boundary currents. *Nat Clim Chang* 2:161–166. doi: 10.1038/nclimate1353

Young JW, Bradford R, Lamb TD, et al (2001) Yellowfin tuna (*Thunnus albacares*) aggregations along the shelf break off south-eastern Australia: Links between inshore and offshore processes. *Mar Freshw Res* 52:463–474

Young JW, Bradford RW, Lamb TD, Lyne VD (1996) Biomass of zooplankton and micronekton in the southern bluefin tuna fishing grounds off eastern Tasmania, Australia. *Mar Ecol Prog Ser* 138:1–14. doi: 10.3354/meps138001

Zhou M (2006) What determines the slope of a plankton biomass spectrum? *J Plankton Res* 28:437–448. doi: 10.1093/plankt/fbi119

Zhou M, Carlotti F, Zhu Y (2010) A size-spectrum zooplankton closure model for ecosystem modelling. *J Plankton Res* 32:1147–1165. doi: 10.1093/plankt/fbq054

Zhou M, Tande KS, Zhu Y, Basedow S (2009) Productivity, trophic levels and size spectra of zooplankton in northern Norwegian shelf regions. *Deep Res Part II Top Stud Oceanogr* 56:1934–1944. doi: 10.1016/j.dsr2.2008.11.018

Appendix A

Table 1 Watermass characteristics of zooplankton \log_{10} Abundance

Water Mass	Range	Mean	SE	SD	CV of SD
Shelf-North	2.848-4.327	3.642	0.0159	0.328	8.99
Shelf-South	3.170-4.748	3.763	0.0332	0.412	10.94
EAC	2.801-3.958	3.460	0.00964	0.197	5.70
Mixed	2.257-4.271	3.513	0.0142	0.316	8.99
Tasman	2.817-4.544	3.790	0.0168	0.296	7.81

Table 2 Watermass characteristics of zooplankton \log_{10} Biomass

Water Mass	Range	Mean	SE	SD	CV of SD
Shelf-North	1.19 – 3.84	2.439	0.0215	0.441	18.1
Shelf-South	1.73 – 4.42	3.024	0.0592	0.735	24.3
EAC	1.34 – 3.62	2.387	0.0204	0.417	17.5
Mixed	0.754 – 4.02	2.537	0.0207	0.462	18.2
Tasman	1.35 – 4.58	3.120	0.0421	0.740	23.7

Table 3 Watermass characteristics of zooplankton Geometric Mean Size

Water Mass	Range	Mean	SE	SD	CV of SD
Shelf-North	390 – 540	438	1.31	26.9	6.13
Shelf-South	388 – 638	486	4.46	55.3	11.4
EAC	393 – 566	441	1.05	21.5	4.88
Mixed	391 – 640	464	1.48	33.0	7.11
Tasman	410 – 717	525	4.69	82.5	15.7

Table 4 Watermass characteristics of zooplankton NBSS_{slope}

Water Mass	Range	Mean	SE	SD	CV of SD
Shelf-North	-1.587 - -0.628	-1.05	0.0090	0.185	-17.6
Shelf-South	-1.389 - -0.451	-0.800	0.0193	0.239	-30.1
EAC	-1.578 - -0.394	-0.985	0.00980	0.200	-20.3
Mixed	-1.568 - -0.425	-0.916	0.00951	0.212	-23.2
Tasman	-1.424 - -0.365	-0.774	0.0133	0.233	-30.1

Table 5 Watermass characteristics of zooplankton NBSS_{intercept}

Water Mass	Range	Mean	SE	SD	CV of SD
Shelf-North	0.0522 – 2.50	1.39	0.0208	0.426	30.6
Shelf-South	0.589 – 3.05	1.90	0.0499	0.619	32.6
EAC	0.182 – 2.03	1.30	0.0177	0.361	27.7
Mixed	-0.300 – 2.49	1.48	0.0190	0.425	28.7
Tasman	0.449 – 3.16	2.00	0.0323	0.568	28.5

Linear Regression with SST_{sat}

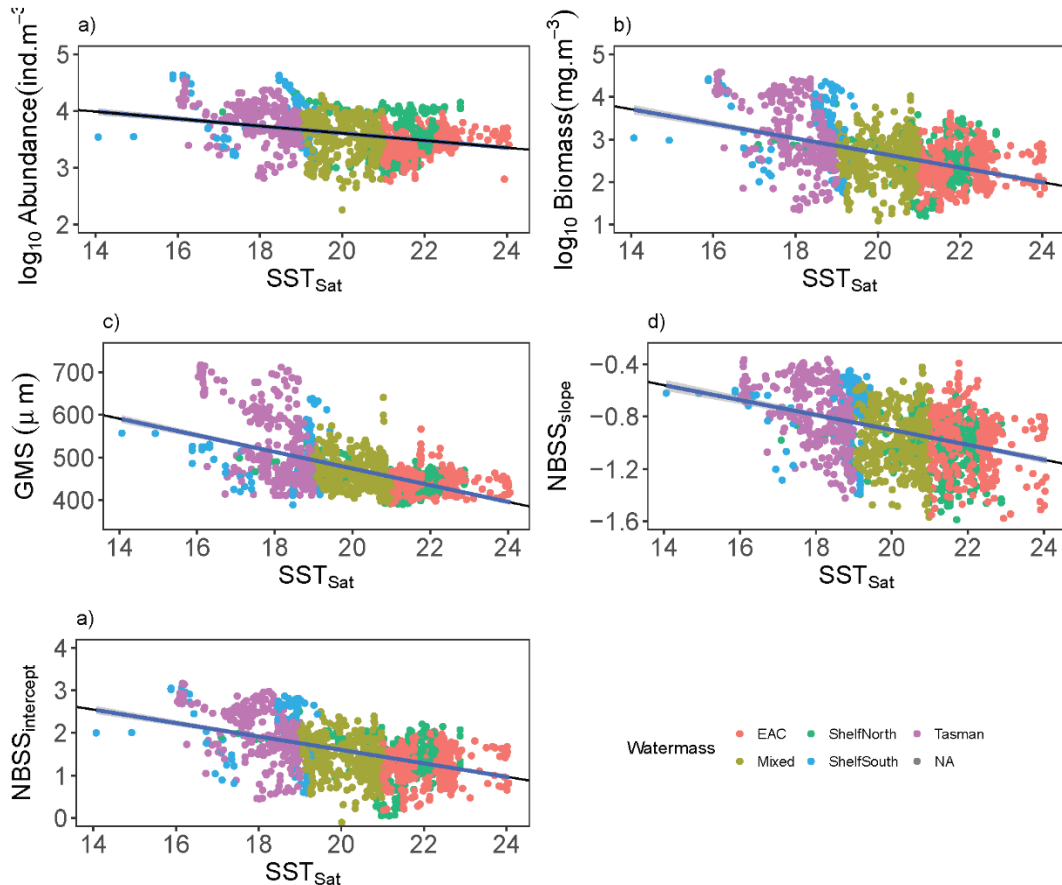


Figure 1 Linear regressions with shaded 95% confidence intervals, of Satellite Temperature (SST_{sat}) regressed against a) log₁₀Abundance, b)log₁₀Biomass, c) GMS (Geometric Mean Equivalent Spherical Diameter), (d) NBSS_{slope}, and e) NBSS_{intercept}. Points coloured by Watermass.

Table 6 Model output of linear regressions against SST_{sat}.

	Intercept	SSTsat	r ²	St Error	p-value
Log ₁₀ Abundance	4.88	-0.0640	0.10	0.31	0
Log ₁₀ Biomass	6.11	-0.171	0.21	0.55	0
GMS	865	-19.5	0.35	44.7	0
NBSS _{slope}	0.237	-0.057	0.17	0.211	0
NBSS _{intercept}	4.75	-0.158	0.24	0.465	0

Linear Regressions against Chl_{sat}

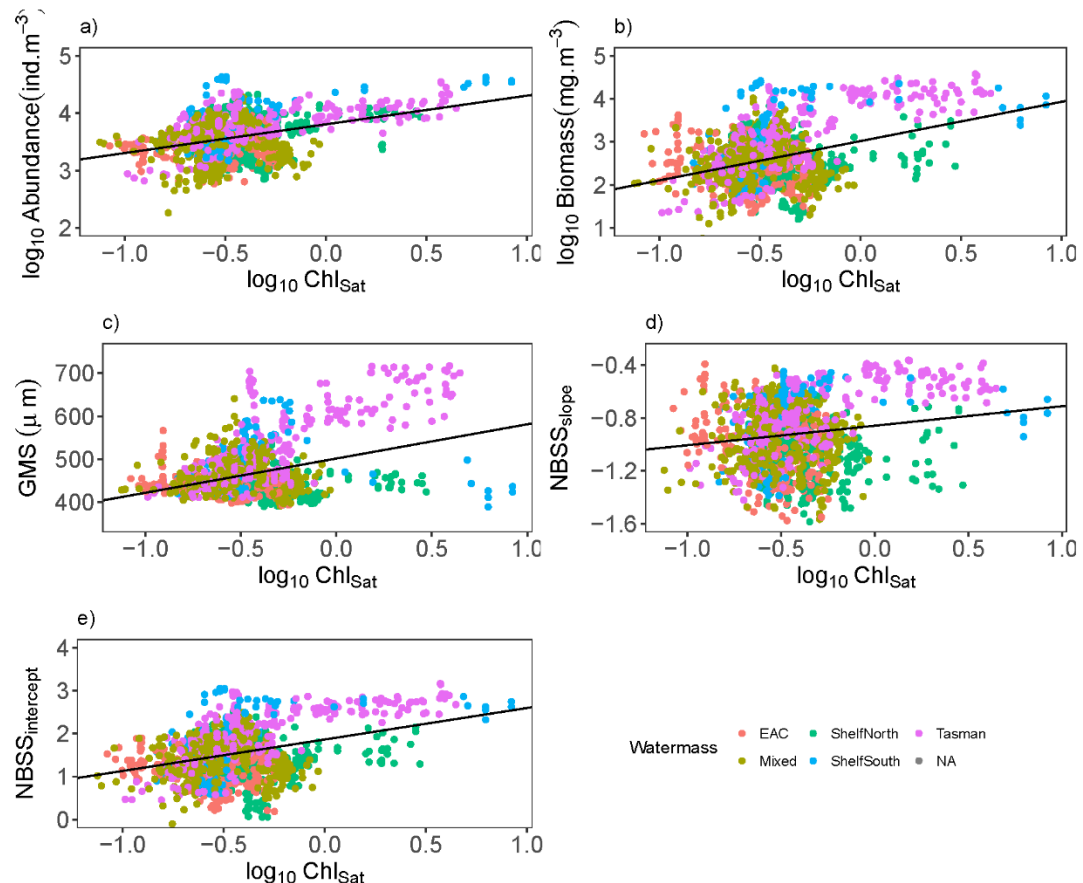


Figure 2 Linear regressions of \log_{10} satellite chlorophyll ($\log_{10}\text{Chl}_{\text{sat}}$) regressed against a) $\log_{10}\text{Abundance}$, b) $\log_{10}\text{Biomass}$, c) GMS (Geometric Mean Equivalent Spherical Diameter), d) NBSS_{slope}, and e) NBSS_{intercept}. Points coloured by watermass.

Table 7 Model outputs of linear regressions against $\log_{10}\text{Chl}_{\text{sat}}$

	Intercept	$\log_{10}\text{Chl}_{\text{sat}}$	r2	St Error	p-value
Log ₁₀ Abundance	3.80	0.50	0.14	0.31	0
Log ₁₀ Biomass	3.02	0.914	0.14	0.57	0
GMS	0.501	79.7	0.13	51.5	0
NBSS _{slope}	0.859	0.147	0.03	0.229	<0.001
NBSS _{intercept}	1.86	1.73	0.12	0.50	0

Linear model outputs

Table 8 Log₁₀Abundance linear model output

	Estimate	St. Error	t-value	p-value	r ²	Standardised Coefficient Value
Log₁₀Abundance ~ Sat_SST + Sat_SLA + WaterDepth + Salinity + LogSat_ChI						
(Intercept)	5.08	0.085	59.76	<0.001	0.29	
Sat_SST	-0.0612	0.00420	-14.56	<0.001		-0.308
Sat_SLA	-0.686	0.0469	-14.64	<0.001		-0.336
WaterDepth	-2.63x10 ⁻⁵	4.12x10 ⁻⁶	-6.396	2.05x10 ⁻¹⁰		-0.146
LogSat_ChI	0.439	0.028	15.71	<0.001		0.330

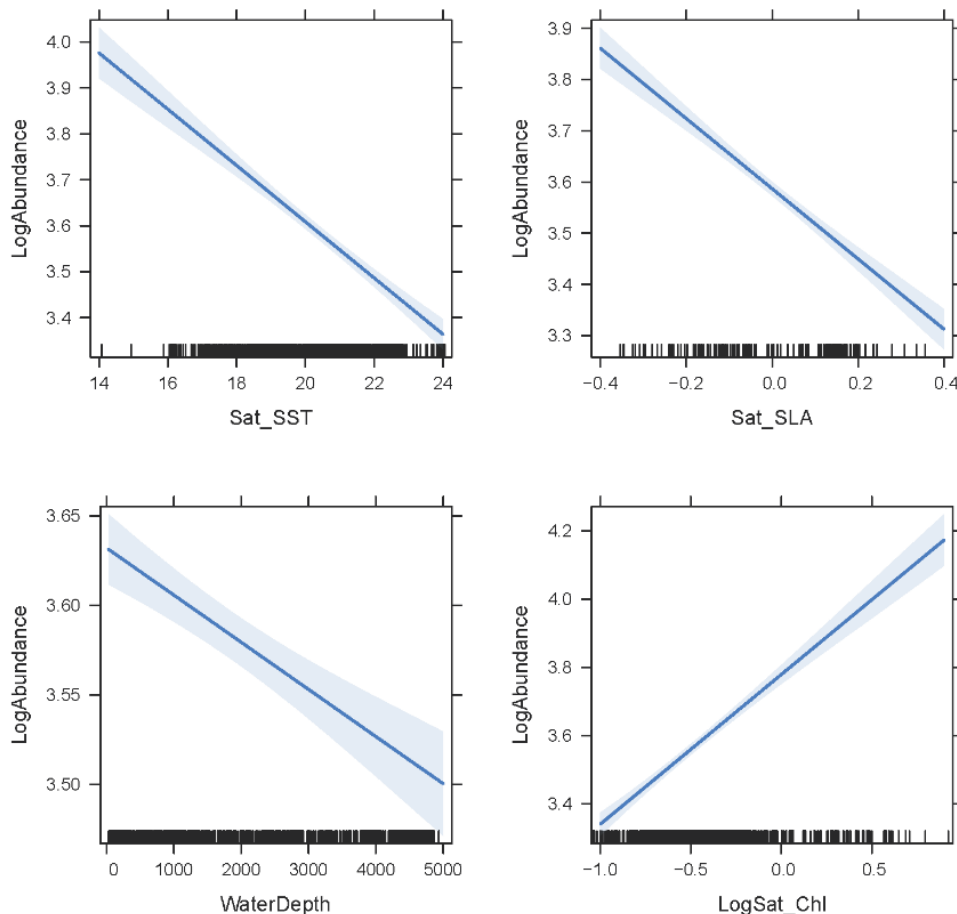


Figure 3 Log₁₀Abundance model output Effects plots, showing the contribution of the retained variables to log₁₀Abundance. 95% confidence intervals shaded in blue.

Table 9 $\text{Log}_{10}\text{Biomass}$ linear model output

	Estimate	St. Error	t-value	p-value	r^2	Standardised Coefficient
						Value
$\text{Log}_{10}\text{Biomass} \sim \text{Sat_SST} + \text{Sat_SLA} + \text{LogSat_Chl}$						
(Intercept)	6.301	0.152	41.52	<0.001	0.34	
Sat_SST	-0.166	0.008	-21.93	<0.001		-0.448
Sat_SLA	-0.866	0.076	-11.35	<0.001		-0.227
LogSat_Chil	0.684	0.050	13.76	<0.001		0.276

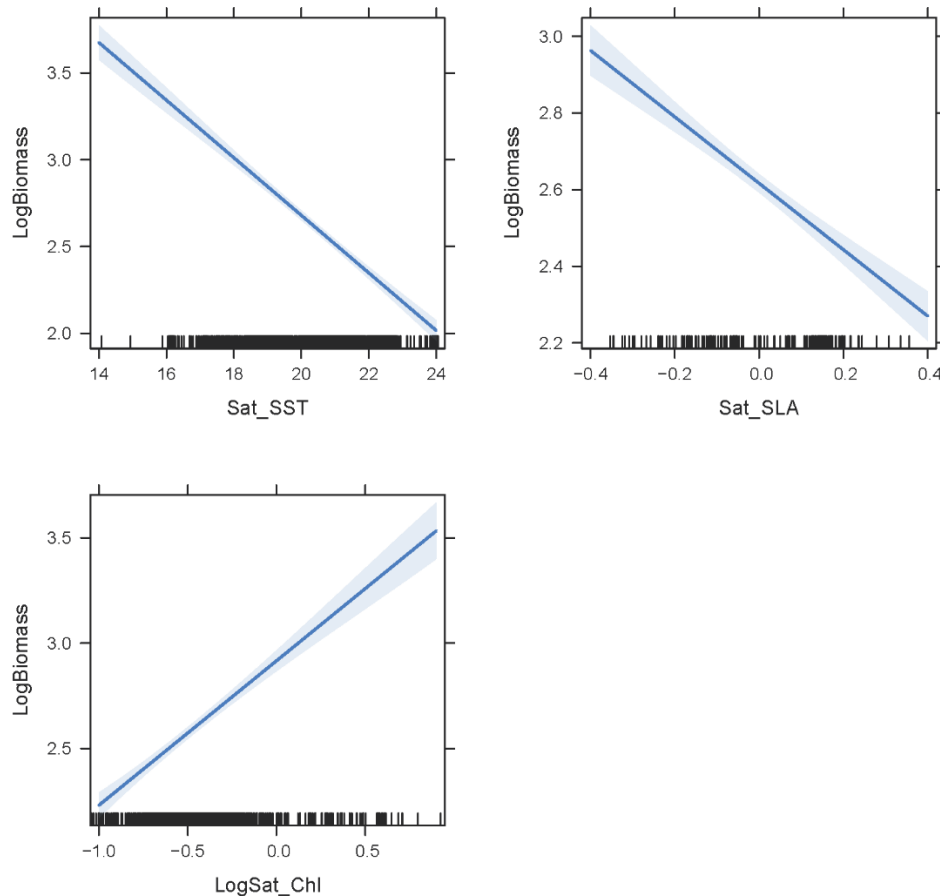


Figure 4 $\text{Log}_{10}\text{Biomass}$ model output Effects plots, blue shaded area around line represents the 95% confidence interval.

Table 10 GMS linear model output

	Estimate	St. Error	t-value	p-value	r^2	Standardised Coefficient Value
GMS ~ Sat_SST + Sat_SLA + WaterDepth + LogSat_ChI						
(Intercept)	0.089	12.39	70.25	<0.001	0.46	
Sat_SST	-19.12	0.613	-31.19	<0.001		-0.575
Sat_SLA	-50.48	6.836	-7.384	2.39×10^{-13}		-0.147
WaterDepth	0.004	6.01×10^{-4}	7.305	4.26×10^{-13}		0.145
LogSat_ChI	49.49	4.073	12.15	<0.001		0.222

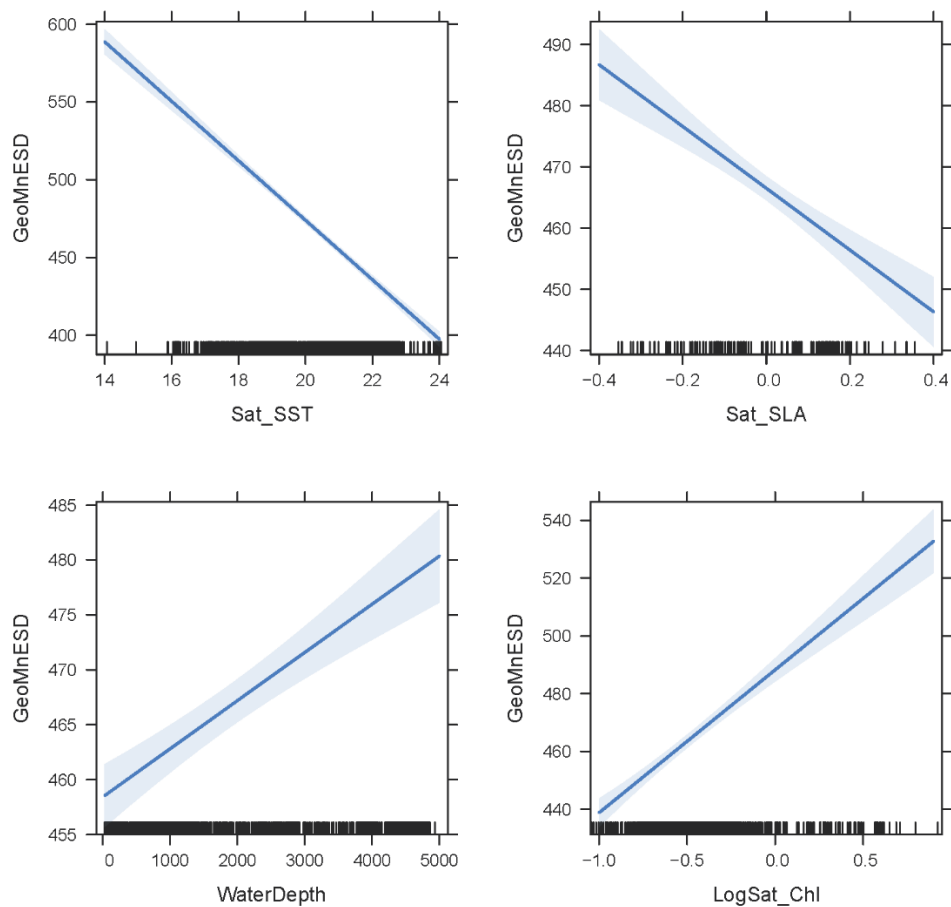


Figure 5 GMS model output Effects plots with shaded 95% confidence intervals.

Table 11 NBSS_{slope} linear model output

	Estimate	St. Error	t-value	p-value	r^2	Standardised Coefficient Value
NBSS_Slope ~ Sat_SST + Sat_SLA + Salinity + LogSat_ChI						
(Intercept)	0.280	0.064	4.394	<0.001	0.18	
Sat_SST	-0.058	0.003	-18.10	<0.001		-0.413
Sat_SLA	-0.151	0.032	-4.73	<0.001		-0.106
LogSat_ChI	0.070	0.021	3.342	<0.001		0.0751

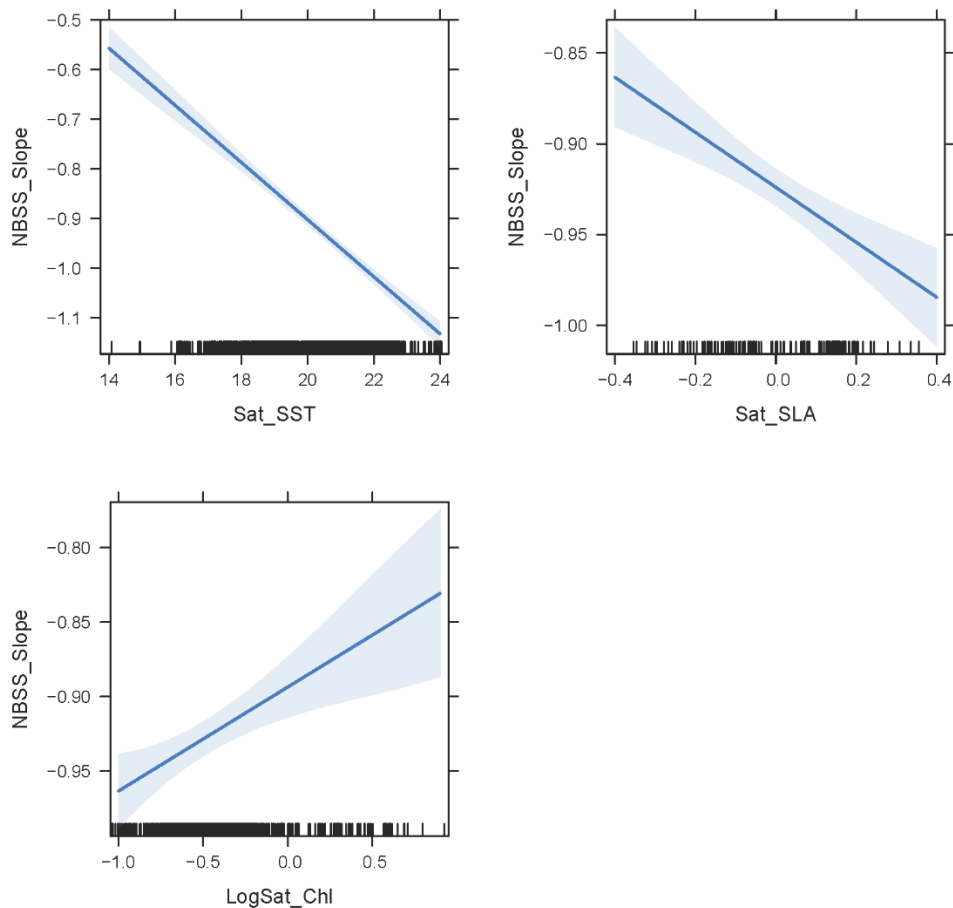


Figure 6 NBSSslope Model output Effects plots. Shaded 95% confidence intervals.

Table 12 NBSS_{intercept} linear model output

	Estimate	St. Error	t-value	p-value	r^2	Standardised Coefficient Value
NBSS_Intercept~ Sat_SST + Sat_SLA + WaterDepth + LogSat_ChI						
(Intercept)	5.043	0.130	38.94	<0.001	0.38	
Sat_SST	-0.158	0.006	-24.64	<0.001		-0.492
Sat_SLA	-0.997	0.071	-13.95	<0.001		-0.302
WaterDepth	-2.48x10 ⁻⁵	6.29x10 ⁻⁶	-3.95	8.27x10 ⁻⁵		-0.0849
LogSat_ChI	0.539	0.043	12.68	<0.001		0.251

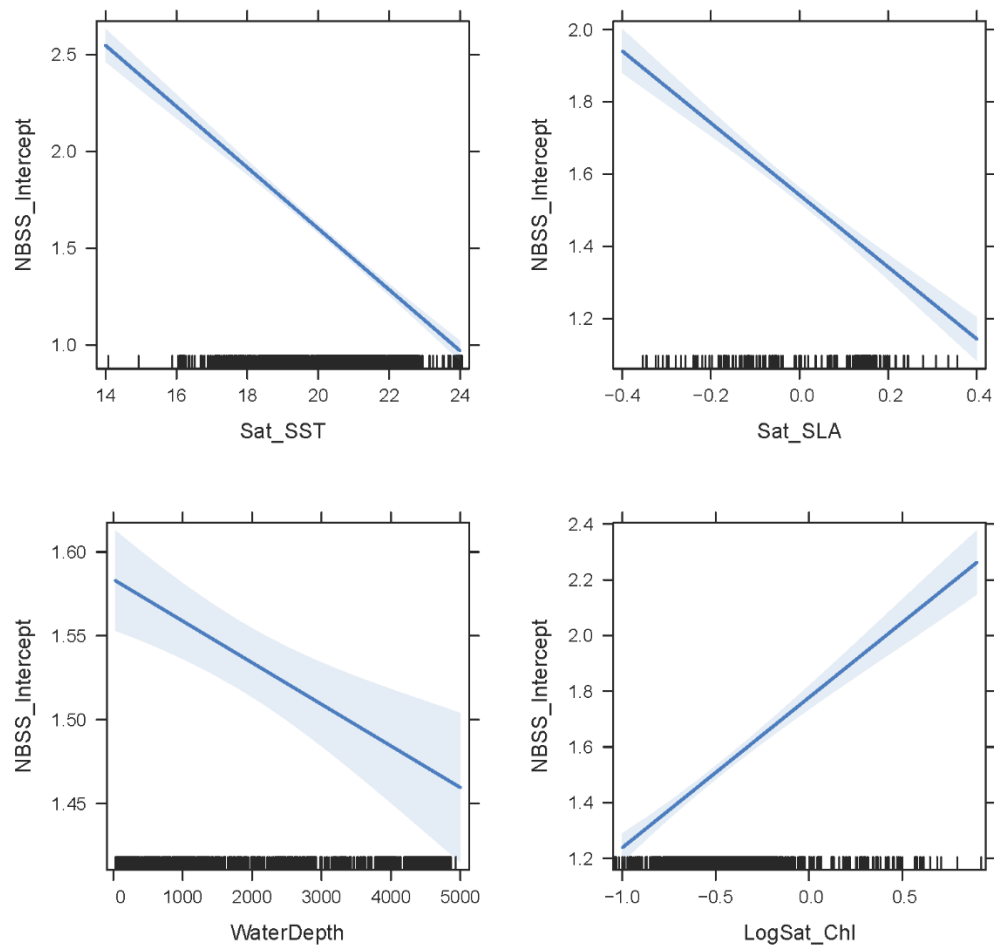


Figure 7 NBSS_{intercept} Model output Effect plots with shaded 95% confidence intervals.

Appendix B

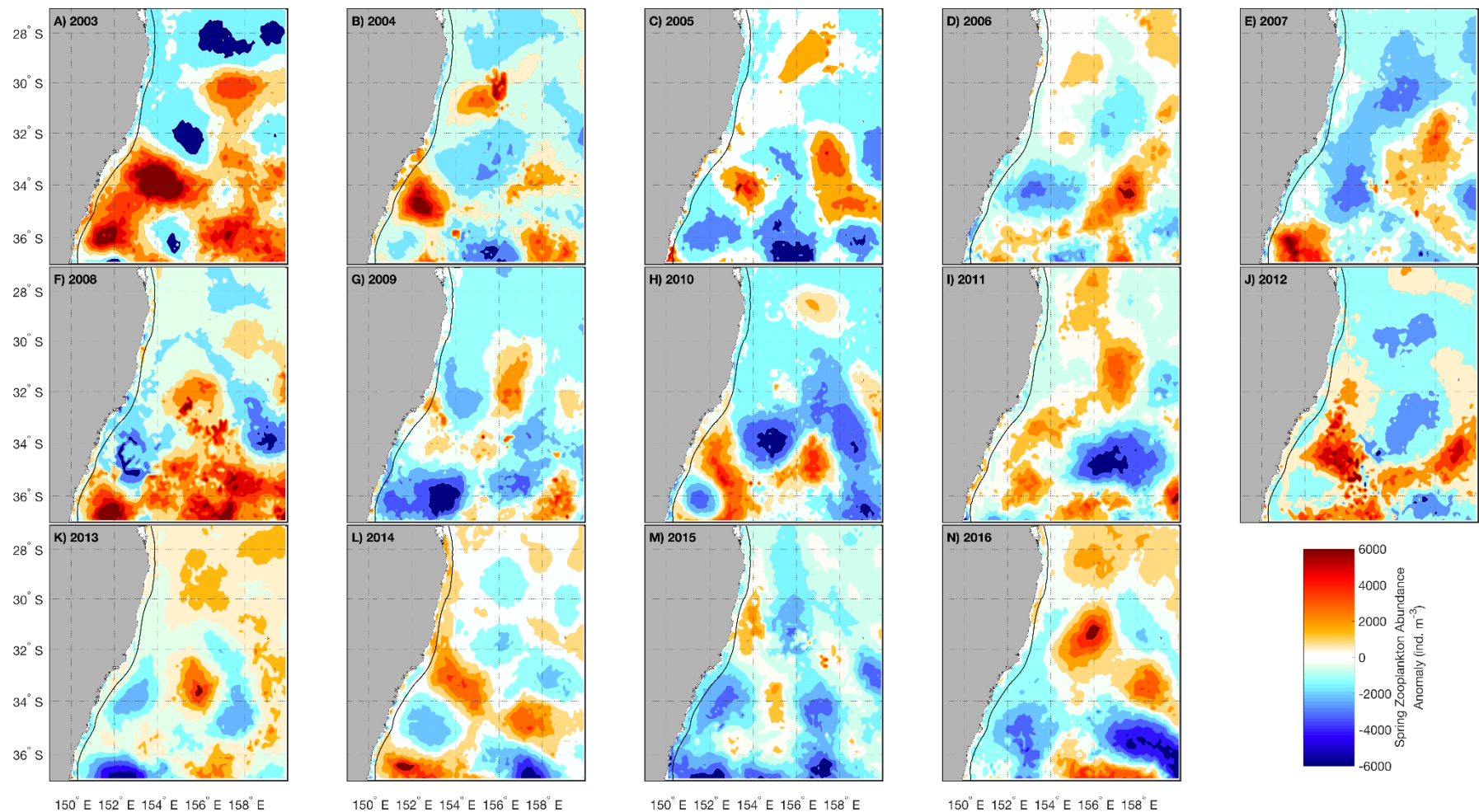


Figure 1 Springtime zooplankton Abundance (ind. m^{-3}) anomalies from 2003 to 2016.

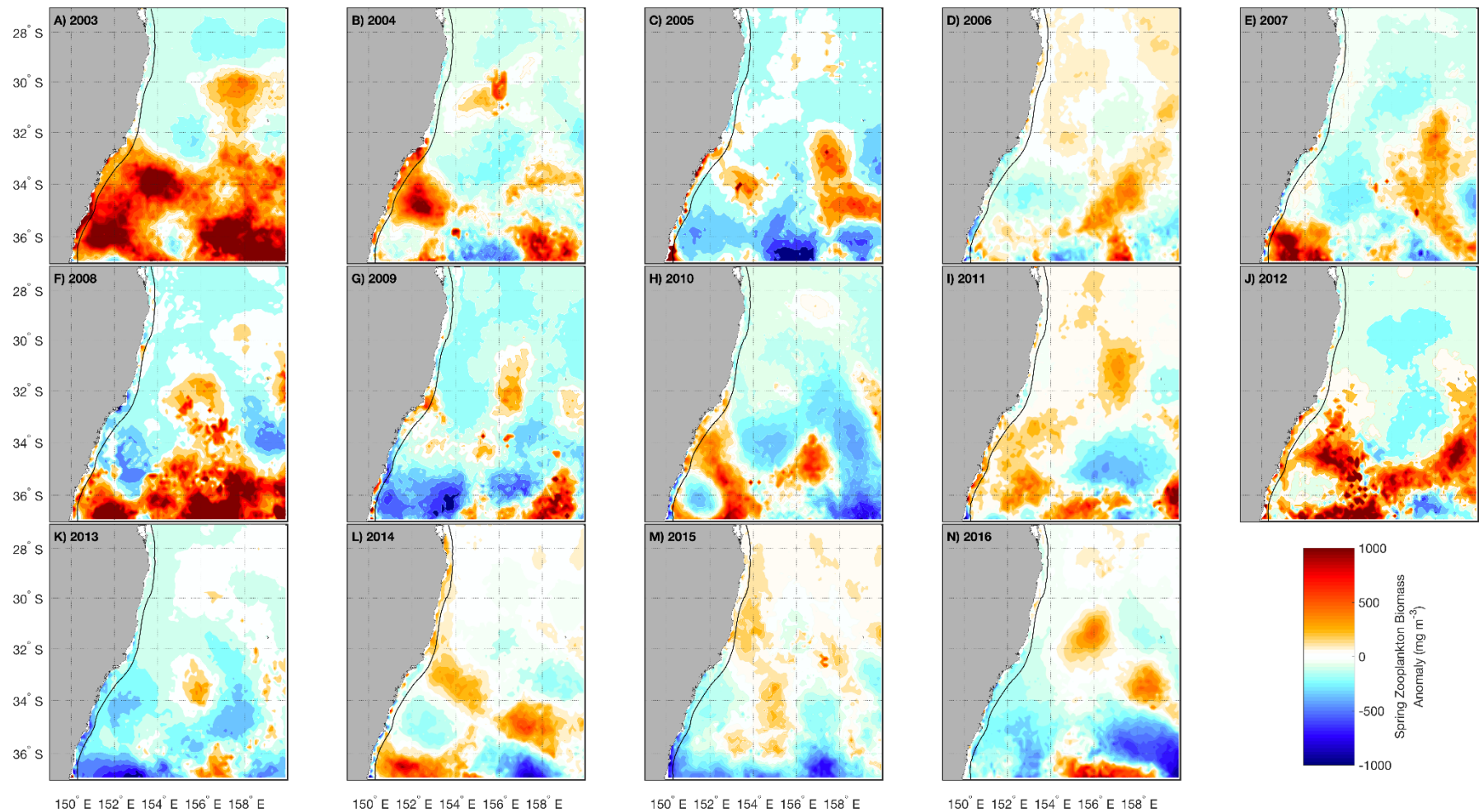


Figure 2 Springtime zooplankton Biomass ($\log_{10}(\text{mg m}^{-3})$) anomalies from 2003 to 2016.

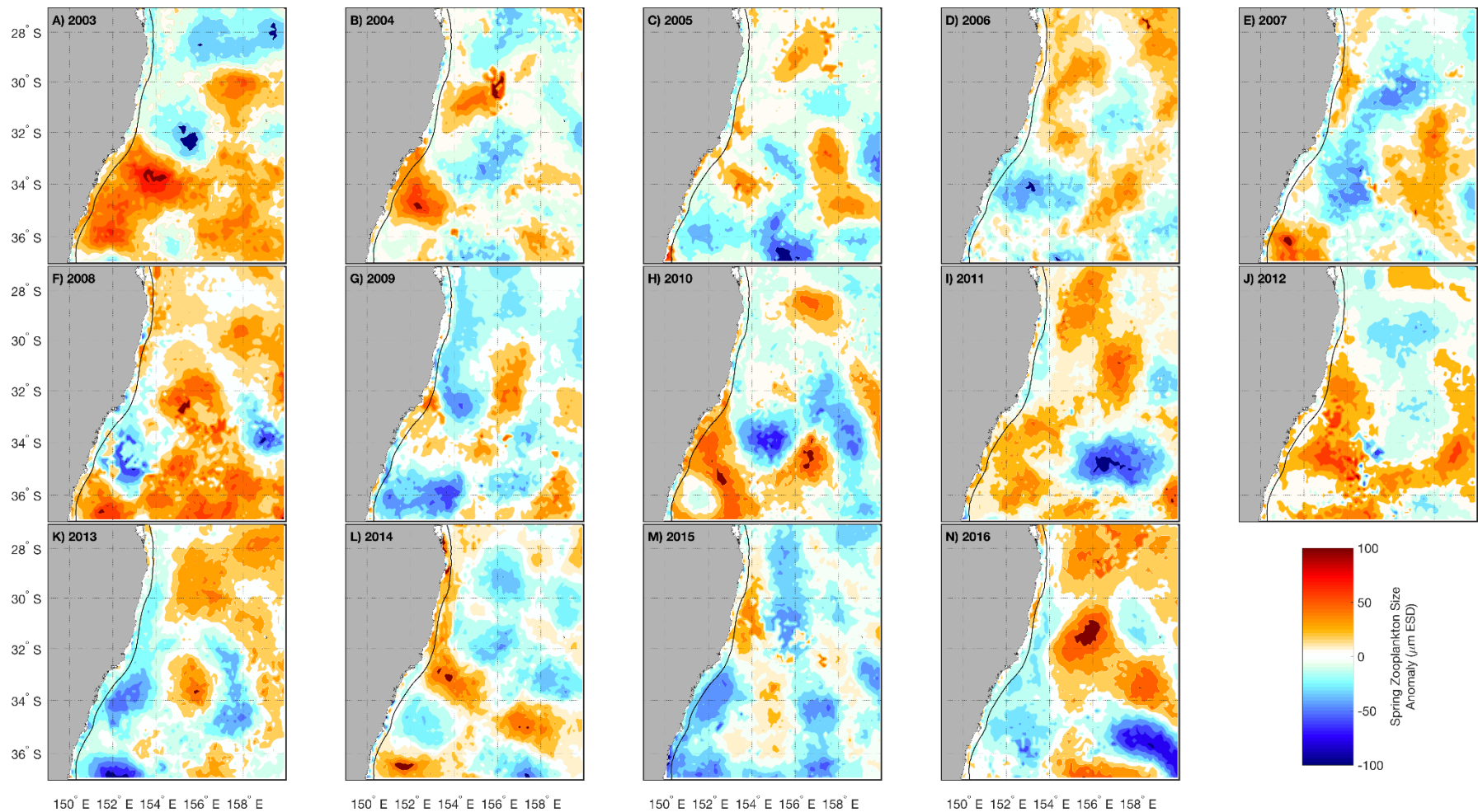


Figure 3 Springtime zooplankton GMS (μm) anomalies from 2003 to 2016.

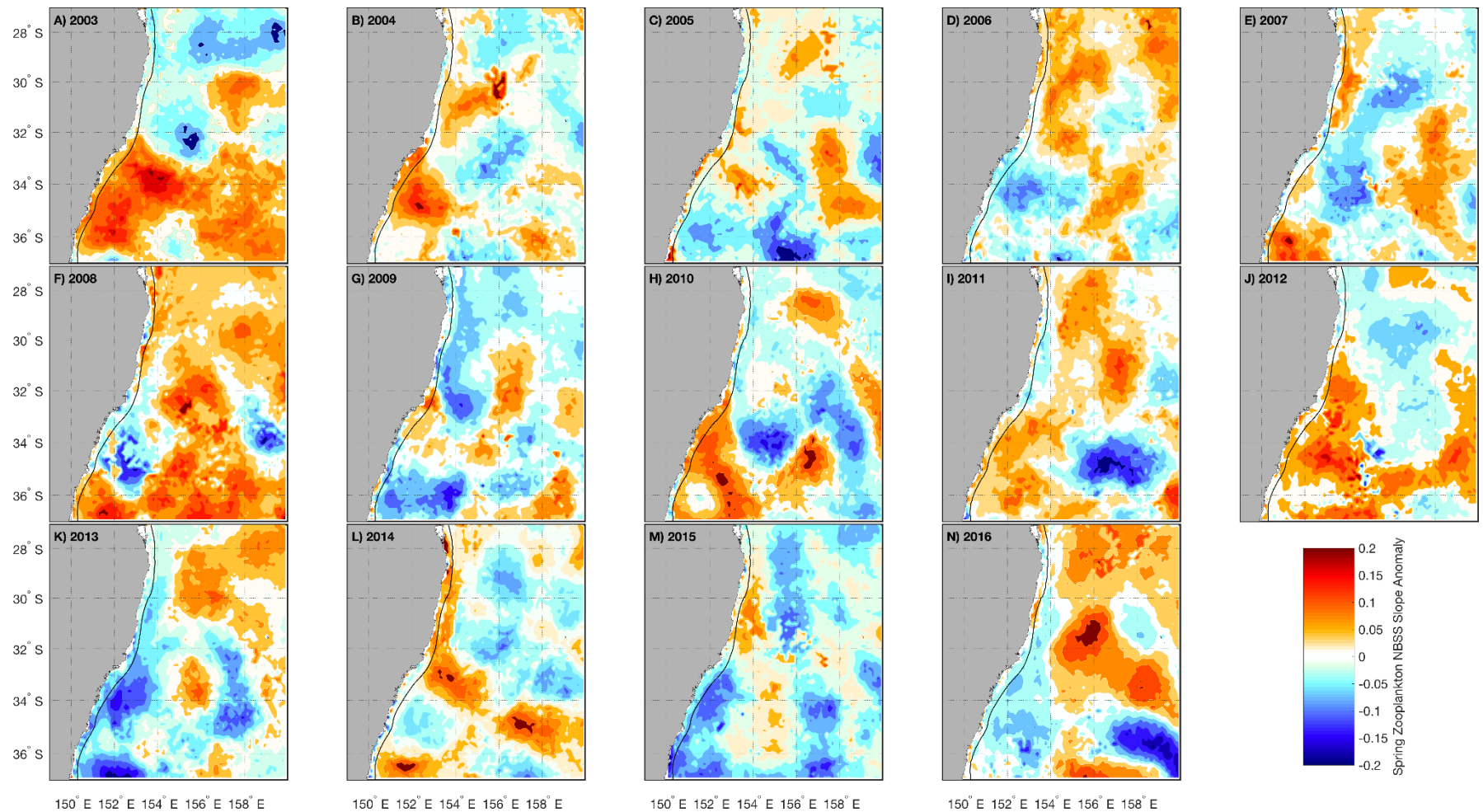


Figure 4 Springtime zooplankton NBSS_{slope} anomalies from 2003 to 2016.

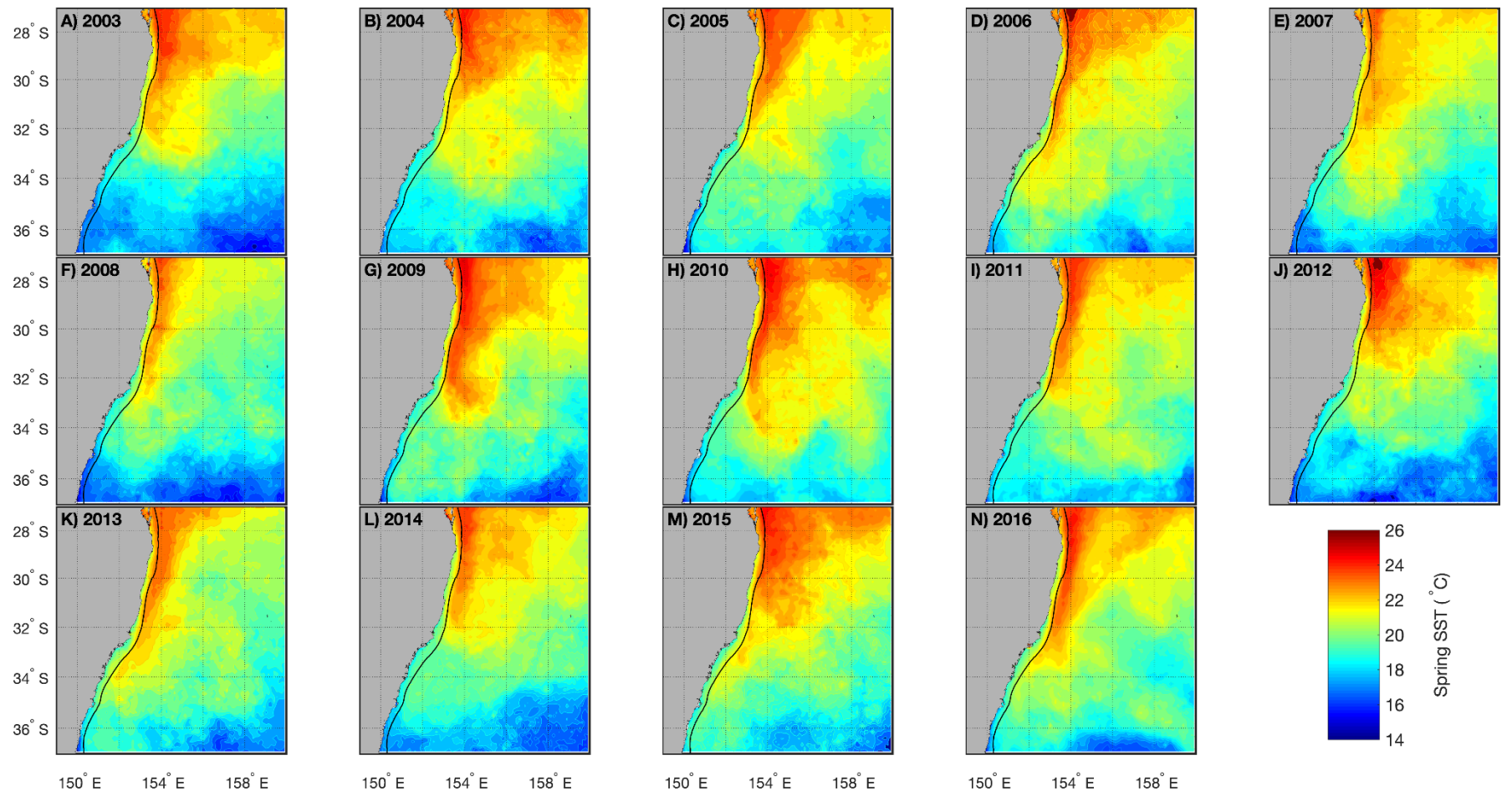


Figure 5 Springtime SST_{sat} from 2003 to 2016.

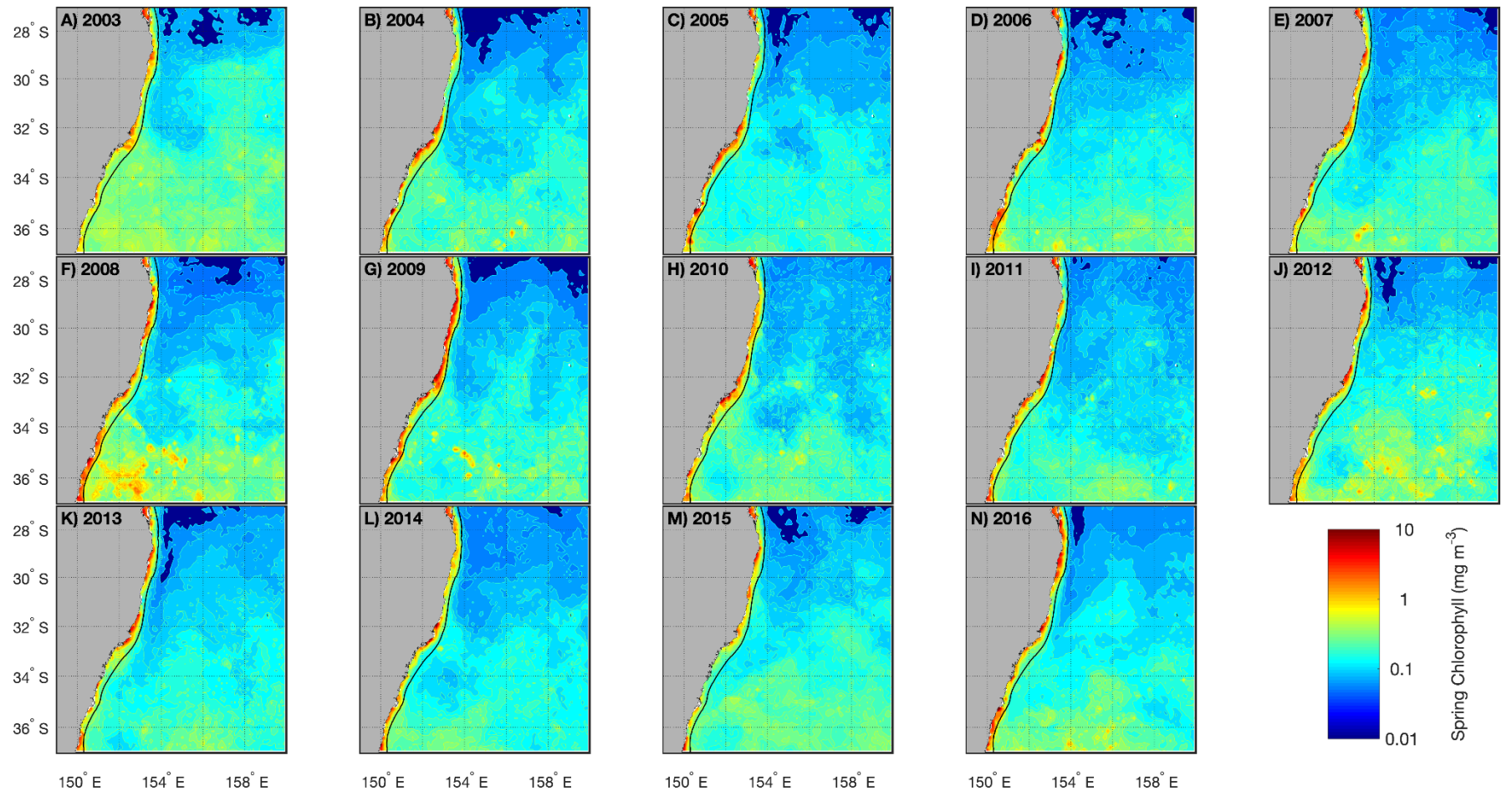


Figure 6 Springtime Chl_{sat} from 2003 to 2016

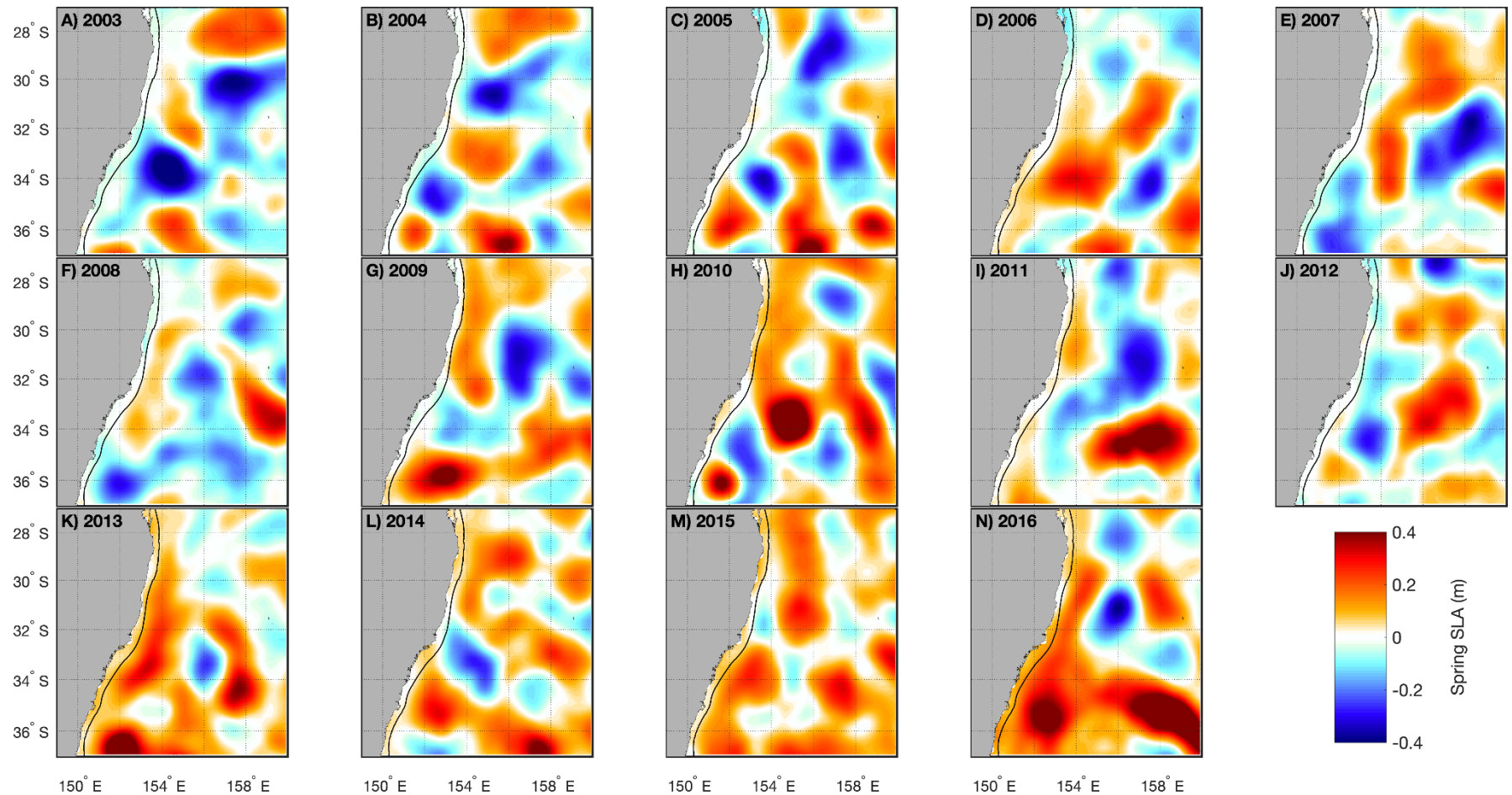


Figure 7 Springtime SLA_{sat} from 2003 to 2016

Table 1 Analysis of variance results for yearly significant differences in Abundance, Biomass, GMS and NBSS_{slope}.

	Df	Sum Sq	Mean Sq	F Value	Pr(>F)
1. AoV(Abundance ~Time)					
Year	13	1209	93.00	2908	<2 * 10 ⁻¹⁶
Residuals	620626	19846	0.03		
2. AoV(Biomass ~Time)					
Year	13	4234	325.7	2574	<2 * 10 ⁻¹⁶
Residuals	627712	79413	0.1		
3. AoV(GMS ~Time)					
Year	13	0.0000427	3.286 * 10 ⁻⁶	2439	<2 * 10 ⁻¹⁶
Residuals	627712	0.0008457	1 * 10 ⁻⁹		
4. AoV(NBSS_{slope} ~Time)					
Year	13	291	22.396	2420	<2 * 10 ⁻¹⁶
Residuals	627712	5810	0.009		

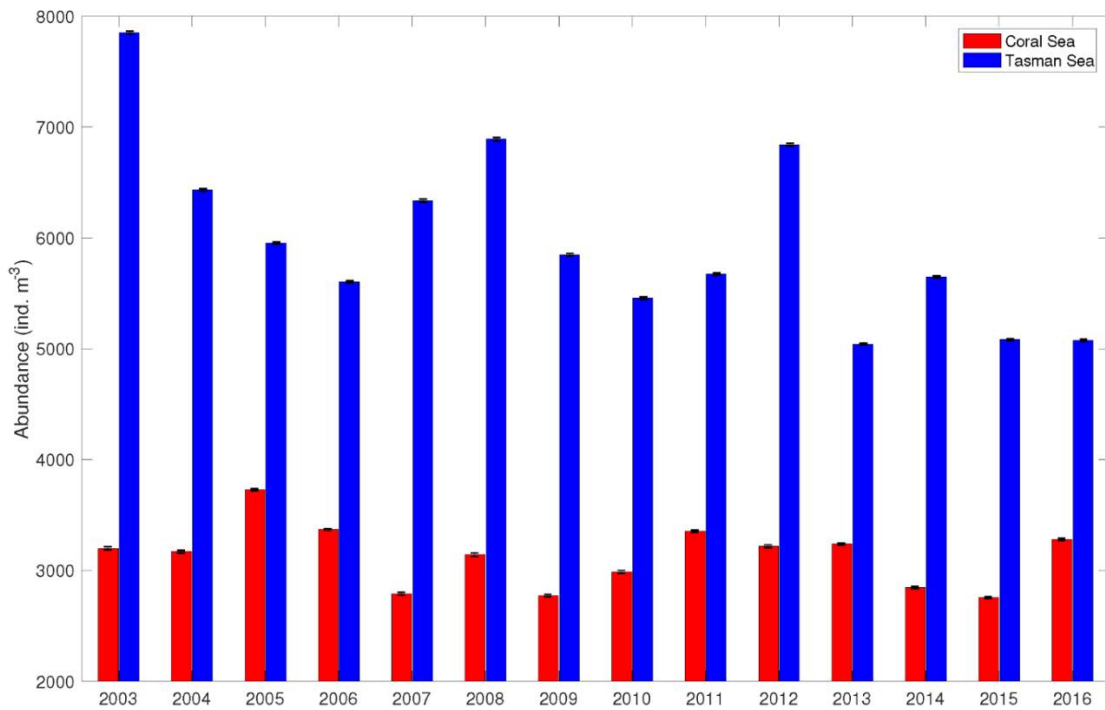


Figure 5 Mean Abundance ($ind \cdot m^{-3}$) values for the Tasman and Coral Sea areas.

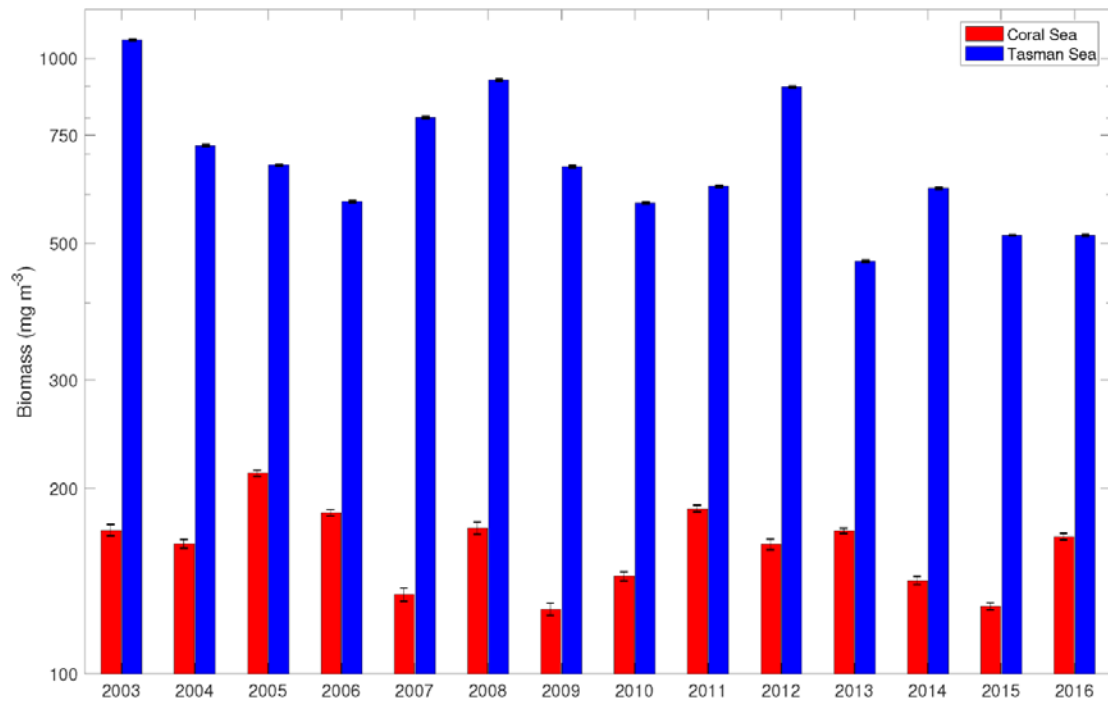


Figure 6 Mean Biomass ($mg \cdot m^{-3}$) values for the Tasman and Coral Sea areas.

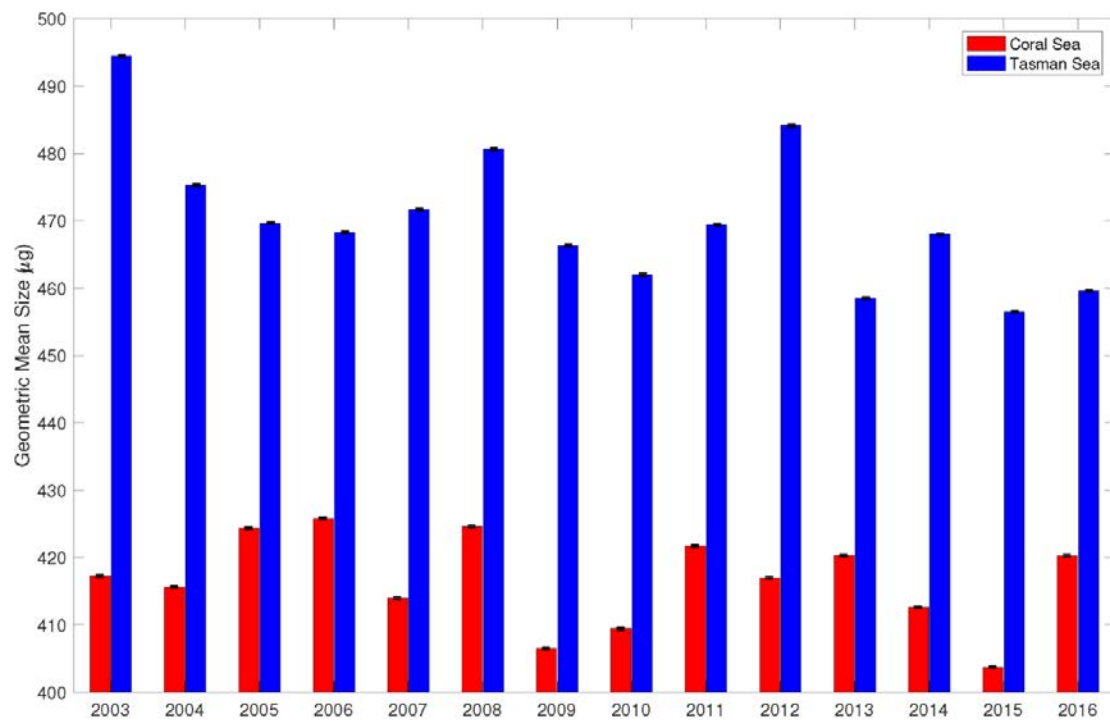


Figure 7 Mean Geometric Mean Size (GMS) (μm) values for the Tasman Sea and Coral Sea areas.

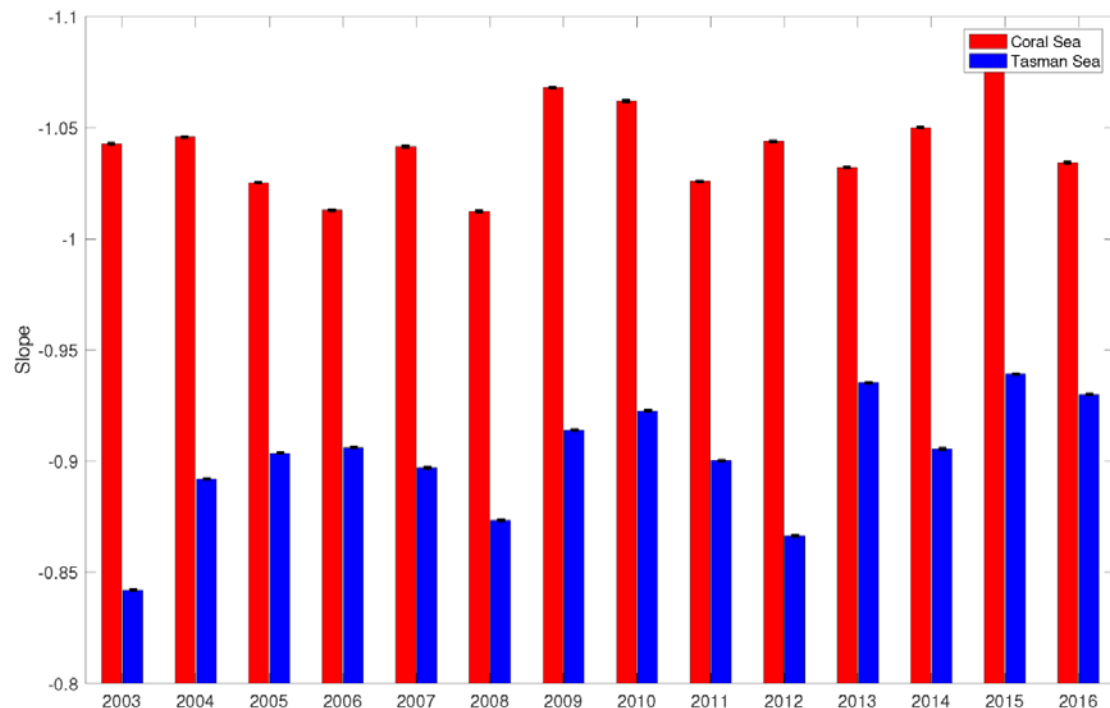


Figure 8 Mean NBSS_{slope} values for the Tasman and Coral Sea areas.

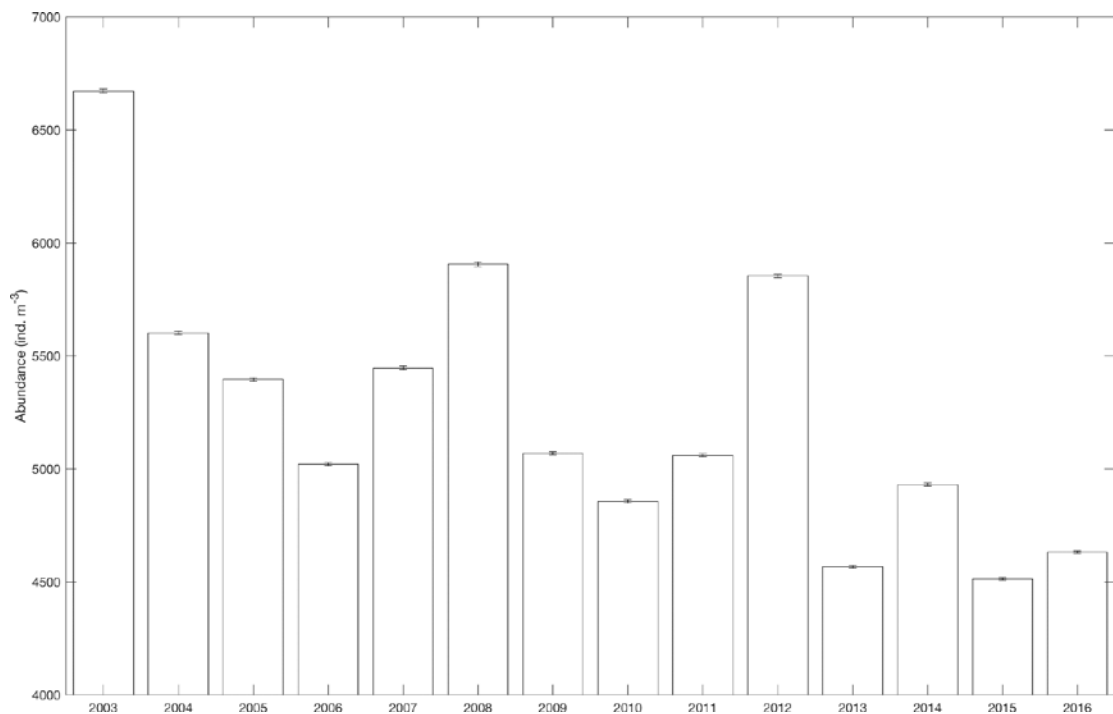


Figure 9 Mean Abundance (ind- m^{-3}) of overall study region.

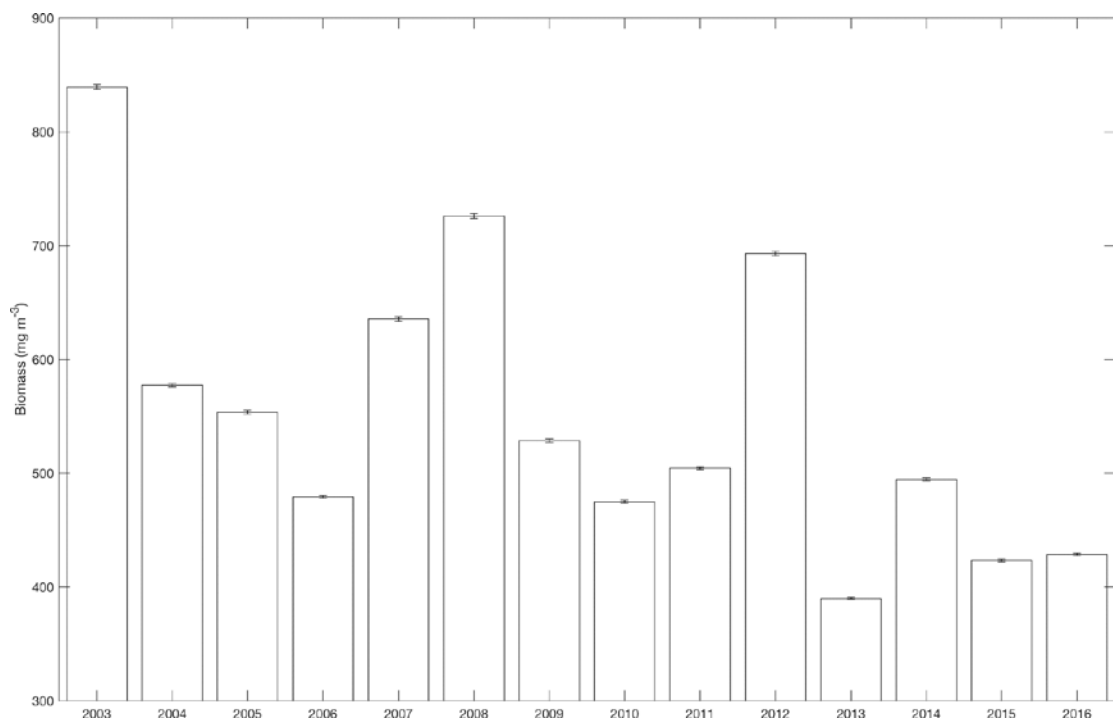


Figure 10 Mean Biomass (mg m^{-3}) of entire study region.

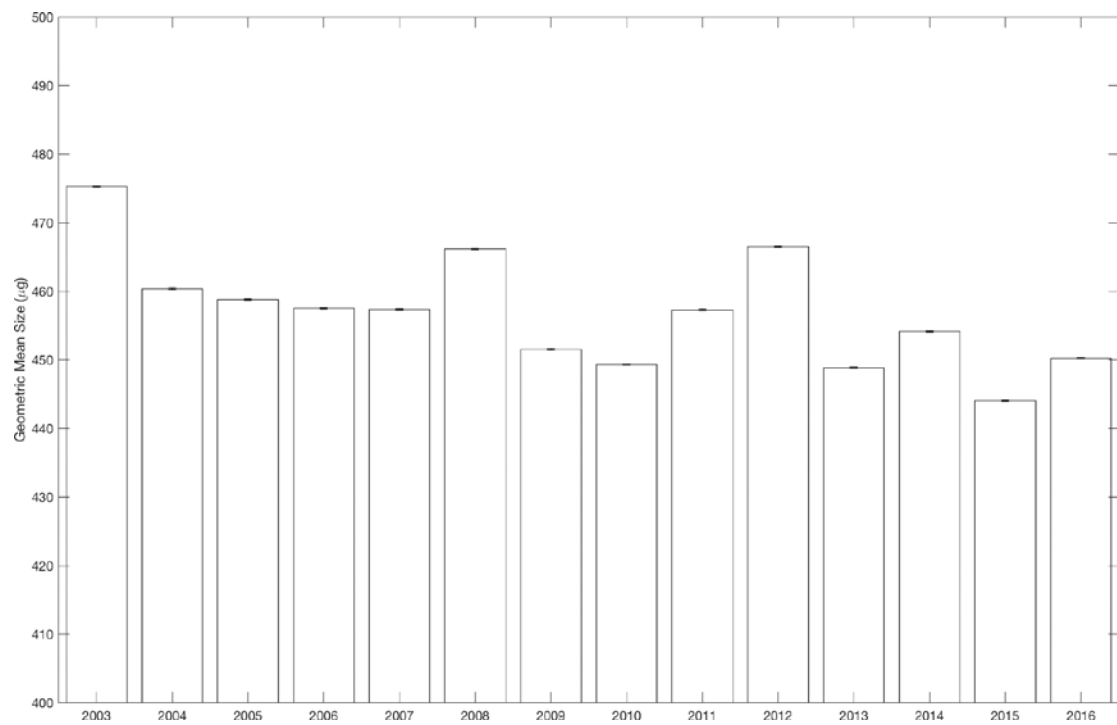


Figure 11 Mean Geometric Mean Size (GMS) (μm) of entire study region.

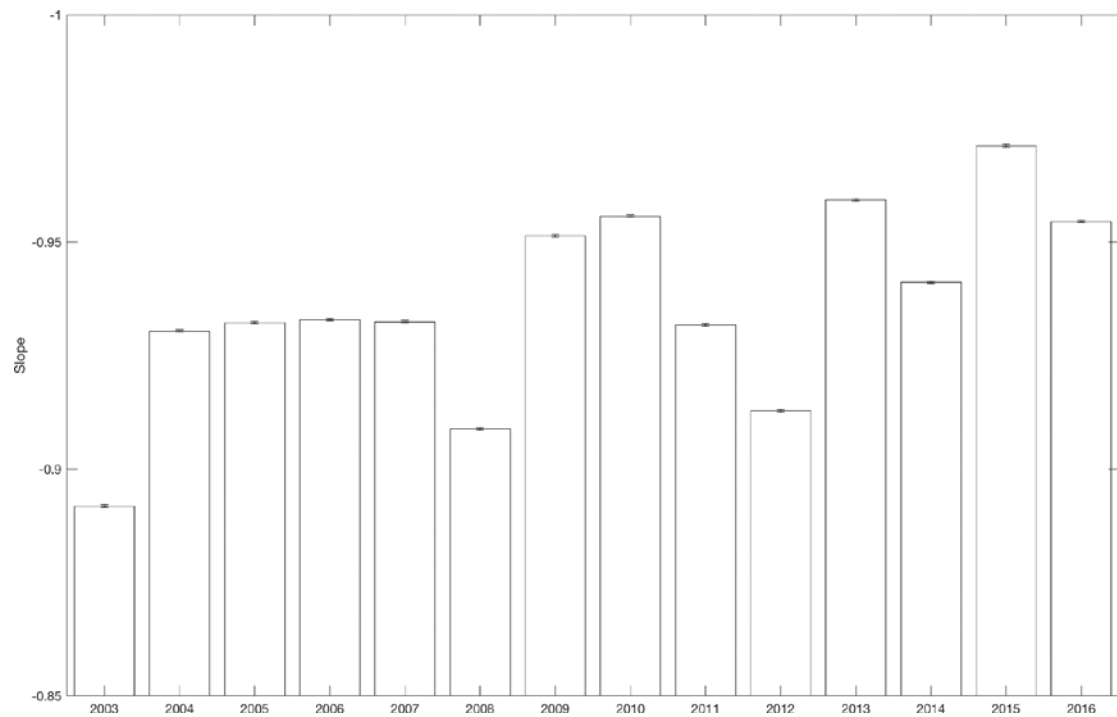


Figure 12 Mean NBSS_{slope} of entire study region.

